BEDFORM SEDIMENTOLOGY AND MORPHOMETRICS OF THE SHOREFACE-ATTACHED SAND RIDGES ON SABLE ISLAND BANK, SCOTIAN SHELF

Andrew W. Campbell

Submitted in Partial Fulfilment of the Requirements
For the Degree of Bachelor of Science, Honours
Department of Earth Sciences
Dalhousie University, Halifax, Nova Scotia
March 2001

Dalhousie University

Department of Earth Sciences
Halifax, Nova Scotia
Canada B3H 3J5
(902) 494-2358
FAX (902) 494-6889

DATE April 30/2001

AUTHOR Andrew W. Campbell

TITLE Bedform Sedimentology and Morphometrics of the Shoreface-Attached Sand Ridges on Sable Island Bank, Scotian Shelf.

Degree BSc Honours Convocation May 22 Year 2001

Permission is herewith granted to Dalhousie University to circulate and to have copied for non-commercial purposes, at its discretion, the above title upon the request of individuals or institutions.

Abstract

The series of shoreface-connected sand ridges occuring on Sable Island Bank adjacent to Sable Island are best developed to its south and southwest and extend as far as 23 km south of the island in water depths up to 45m. The question of whether or not the sand ridges and superimposed bedforms present on the bank show signs of short-term mobility is of importance for hydrocarbon development seabed installations. In an effort to obtain a better understanding of the morphological and sedimentological dynamics of the ridge field, a database of new and existing seismic data (from the Geological Survey of Canada, Atlantic) and regional bathymetric data (from the Canadian Hydrographic Service) was compiled to analyse the wavelength, height and crestline-normal symmetry of the sand ridges. The database will also serve as a means of comparison between bathymetric seismic data types.

To address the hierarchy of reactivation events within individual sand ridges, seven vibrocores were collected during B.I.O Cruise Hudson-2000-030A in July 2000 and 997, and 5873 bedforms were measured from the Bathymetric and seismic data respectively. The average wavelength of the measured bedforms was 620 m (max: 33896m, min: 28m), and the average height was found to be 1.04 m (max: 32m, min: 0.10). Through comparing the size of the measured bedforms with the classification scheme defined by Amos and King (1984), the bedforms are almost exclusively within the sand ridge/sand ribbon size zone. This implies a flow-parallel genesis. The measured symmetry of the sand ridges shows a wide range in asymmetry with no readily discernable geographic trends. Vibrocores from the ridges have thick units of the parallel laminae bound by a basal lag and fining upward sequences at the base, and angled laminae, cross bedding and bioturbated deformation near the top. This sequence are associated with storm generated winnowing, sheet flow and waning conditions.

The traditional understanding of the shoreface-attached sand ridges on Sable Island Bank is that they are migrating in an eastward direction by means of transverse sediment flow. The results from this study have found that the majority of the measured bedforms (sand ridges and sand ribbons), and internal structures from the cores, (thick units of parallel laminae associated with sheet flow) are similar to those formed under longitudinal flow conditions. Transverse bedform migration appears to be more of a secondary process. Multibeam bathymetry images south of Sable Island show a complex network of sand ribbons coming away from Sable Island and into the sand ridges that could be the pathways for longitudinally transported sediments.

Table of Contents

Abstract..... i
Table of Contents..... ii
Table of Figures..... iv
Table of Tables..... x
Acknowledgements..... xi

Chapter 1: Introduction
1.1 General Setting..... 1
1.2 Objectives and Scope of Thesis..... 5
1.3 Organization..... 6

Chapter 2: Background
2.1 Geology..... 7
2.2 Glaciation, Sea Level and Depositional History..... 12
2.3 Sand Ridge Morphology..... 14
2.3.1 Bedform Classification..... 14
2.3.2 Ridge Characteristics..... 16
2.3.3 Sediment Migration..... 25
2.3.4 Ridge Generation..... 27
2.4 Morphological Comparisons..... 29
2.5 Parallel Studies..... 33

Chapter 3: Data Collection and Processing

3.1 CHS Bathymetric and GSCA Seismic Data for Bedform metric Analysis... 36
3.1.1 CHS Data..... 36
3.1.2 Seismic Data..... 45
3.1.3 Multibeam Bathymetry..... 48
3.2 GIS Database..... 48
3.3 Vibrocore Data..... 49
3.3.1 Collection, location and handling..... 49
3.3.2 Core Analysis Techniques..... 58

Chapter 4: Results
4.1 Morphometrics Database..... 60
4.1.1 CHS Bathymetry Data..... 60
4.1.2 Seismic Data..... 64
4.1.3 Summary Comparison of Results..... 68
4.1.4 Geographic Summary..... 71
4.2 Vibrocore Analysis..... 74
4.2.1 Core Descriptions and Initial Interpretation..... 74
4.2.2 Summary..... 89

Chapter 5: Discussion and Conclusions
5.1 Introduction..... **90**
5.2 Discussion of Results..... **90**
5.2.1 Symmetry..... **90**
5.2.3 Internal Structures..... **91**
5.3 Longitudinal Flow..... **93**
5.3.1 Schematic Model..... **93**
5.3.2 Supporting Evidence..... **96**
5.3.2.1 Paleo-lagoonal deposit..... **96**
5.3.2.2 Ridge Geometry..... **98**
5.4 Conclusions..... **99**
5.5 Recommendations for Ruther Work..... **101**

References..... **102**

Table of Figures

Figure 1.1. Location map of Sable Island Bank on the Scotian Shelf. The locations of Sable Island, Northern Spur, West Bar, East Bar, and Desbarres Spur are also shown. Natural gas is currently being produced from the Thebaud and Venture cites, and future hydrocarbon development is planned for Panuke Alma, Gleneig and N. Triumph. Production has stoped at the Cohasset cite (Modified from King 2001). **2**

Figure 1.2. Bathymetry map of Sable Island Bank (E. King 2001). **4**

Figure 2.1. Geologic profiles illustrating the stratigraphic units and their bounding surfaces from two locations on Sable Island Bank. Profile A (see inset map), from Desbarres Spur (east Sable Island Bank) is compiled from air gun and NSRF data collected during B.I.O. cruise 86-041 and is exaggerated vertically 75X. Profile B (see inset map), southwest of Sable Island is compiled from NSRF sparker data collected during B.I.O. cruise 86-035 and is exaggerated vertically 100X (E. King 2001). The unit, and horizon labels correspond those in Table 2.1. **10**

Figure 2.2. Contoured thickness of the Sable Island Sand Body (Amos and Nadeau 1988). **11**

Figure 2.3. Composite observed relative sea level (RSL) curve for Sable Island (Scott et al. 1989) **15**

Figure 2.4. Schematic illustration of the peripheral bulge at 18 ka and the present (Modified from Quinlan and Beaumont). The peripheral bulge migrates towards the ice centre with the retreat of the glacier causing subsidence of the crust at Zone D (Sable Island Bank Area). The Relative Sea level Curve (RSL) shows the response of Zone D due to isostatic re-adjustment as the weight of the ice sheet is removed. **15**

Figure 2.5. Enhanced bedform map displaying the distribution and orientation of the shoreface-attached sand ridges on Sable Island Bank (E. King 2001). The main ridge field is southwest, south and southeast of Sable Island. The second, smaller ridge field is north of Sable Island, between West Bar and East Bar. **18**

Figure 2.6. Schematic illustration of the distribution of small-scale bedforms over a shoreface-attached sand ridge on Sable Island Bank (Hoogendoorn 1989). **19**

Figure 2.7. Bathymetry map of Sable Island Bank showing the divisions of the four morphological zones of the sand ridge complex (Hoogendoorn 1989). Zone 1 is to the west of Sable Island, Zone 2 is south of Sable Island, Zone 3 is East of Sable Island (south of East Bar) and Zone 4 is north of Sable Island, between West and East Bars. Zones 2 and 3 are separated by the Harcourt-Cameron Ridge, the largest of the sand ridges on Sable Island Bank. **21**

Figure 2.8. Schematic representation of a sand ridge on Sable Island Bank showing the orientation of the Basal Reflector and Master Bedding Planes. Grain size across the ridge decreases from the stoss to the lee side (Redrawn and modified from Hoogendoorn 1989 and Dalrymple and Hoogendoorn 1997). **24**

Figure 2.9. A plot of measured bedform sizes from sand ridge fields around the world, including Atlantic Canada and Sable Island Bank. The dashed lines represent the approximate limits between each bed phase (Amos and King 1984). **32**

Figure 2.10. Ridge wavelength vs. height ratios from global sand ridges (A), and Eastern Canadian sand ridges (B). The plots show the high degree of consistency between ridges around the world, as well as the slightly lower amplitudes of the sand waves on Canada's East coast (Amos and King 1984). The black line represents the boundary between the sand ridge and sand wave size fields. **34**

Figure 3.1. Geographic coverage of the CHS bathymetry data used in this study. The data was collected using a 200m spaced grid close to Sable Island, and a 400m spaced grid over the surrounding area (Sankarelli 1988, Unpublished Msc Thesis). **37**

Figure 3.2. The geographic coverage of the seismic data used in this study. **38**

Figure 3.3. Surface relief map of eastern Sable Island Bank showing medium to large-scale bedforms. The image was generated using CHS data (King unpublished). **40**

Figure 3.4 The division of zones created for the CHS database across eastern Sable Island Bank, southern Middle Bank, and southwestern Banqureau. The profiles lines (dark, thin) are oriented approximately perpendicular to the most dominant sand ridge crest lines. Sable Island is located in the small space between the South Sable shoreface (directly south of the island) and North Sable shoreface (directly north of the island) zones, in the middle of the page (King unpublished). **41**

Figure 3.5. Example profile line created using the CHS bathymetry data (line five, Copan, west of Sable Island). The sand ridge is drawn in purple, the red base was drawn as a guideline for drawing the wave heights (vertical green) and the wavelengths (horizontal green). The profile line is vertically exaggerated 200X **42**

Figure 3.6. Schematic example as to how bedform symmetry was calculated. Symmetry was measured as a ratio of the distance from the ridge crest to the lee trough (A), and the distance from the ridge crest to the stoss tough (B). A ratio less than one means the bedform is skewed west (asymmetric east) and a ratio greater than one means the bedform is skewed east (asymmetric west). A symmetric bedform will have a ratio of 1. The smaller, or larger the ratio is (relative to one), the more asymmetric the bedform is. The example bedform drawn above would have a ratio less than one, as it is skewed left (west), and asymmetric to the right (east). **44**

Figure 3.7. Example profile line created using the seismic data (profile line 31, from cruise 85-037). The sand ridge heights (vertical line) are displayed in green, and their wavelengths (horizontal line) are displayed with brown colored lines. The blue lines are guidelines used to help determine the boundary of the different order sand ridges. The vertical scale is exaggerated 200X. This profile also illustrates the basal reflector and master bedding planes disscused in Chapter 2.3.1 (illustrated in Figure 2.7). **46**

Figure 3.8. The positions across Sable Island Bank where vibracore samples were collected during B.I.O. cruise HUD-2000-30A. The geographical position (Latitude and Longitude), water depth, and length of each core are given in Table 3.1 (modified from King unpublished). **50**

Figure 3.9. Multibeam bathymetric map where the vibracore sample locations for the Copan transects were chosen. The data was collected during B.I.O. Cruises Creed 96-501, Creed 97-090 and Creed 98-100 (Hudson 2000-30a unpublished cruise report). **52**

Figure 3.10. Multibeam bathmetric map showing where the vibracore sample locations for the South Sable transect were chosen. The data was collected during B.I.O. Cruises Creed 96-501, Creed 97-090 and Creed 98-100 (Hudson 2000-30a unpublished cruise report). **53**

Figure 3.11. Positioning of the three vibracore samples taken over the CoPan-1 sand ridge transect. The sand ridge profile was generated using multibeam data collected on the 1996, 1997 and 1998 Creed cruises. The vertical scale is exaggerated 100X. **54**

Figure 3.12. Positioning of the two successful (96 and 97) and the two unsuccessful (99 and 98) vibracore samples taken over the CoPan-2 sand ridge transect. The sand ridge profile was generated using seismic data collected during B.I.O. cruise HUD-2000-30A.. The vertical scale is exaggerated 100X. **56**

Figure 3.13. Positioning of the two vibracore samples taken over the South Sable sand ridge transect. The sand ridge profile was generated using multibeam bathimetric data collected during B.I.O. cruise HUD-2000-30A. The vertical scale is exaggerated 100X. **57**

Figure 4.1. Geographic locations of the measured bedforms from the CHS Bathymetry data. Each point on the map identifies the location of a ridge crest. **61**

Figure 4.2. Plot of the wavelength distribution of the measured bedforms. The most common bedform sizes are between 1000 and 1750 m long. **62**

Figure 4.3. Plot of the height distribution of the measured bedforms. The most common bedform height is close to one meter high. **62**

Figure 4.4. Bedform wavelength vs. height from the CHS data. Using the bedform zone boundaries defined by Amos and King (1984), almost all of the bedforms measured fall into the sand ridge field. Although ridge heights less than 0.20 m were measured, it is unlikely that bedforms of that size were resolved by CHS bathymetry. Any heights less than 0.20 m were therefore considered to be artefacts created during the data processing, and were omitted from the database. The sharp cut off of data points at < 0.20 m is caused by the removal of these values. **63**

Figure 4.5. Bedform symmetry measurements from the CHS database. A bedform with a symmetry less than one is positively skewed (asymmetric to the east), where as a symmetry greater than one is negatively skewed (asymmetric to the west). The inset (top right) is a schematic illustration of a bedform that has a symmetry value of 0.5, and is therefore asymmetric east. **65**

Figure 4.6. Geographic locations of the measured bedforms from the seismic data. Each point on the map identifies the location of a ridge crest. **66**

Figure 4.7. Plot of the wavelength distribution of the measured bedforms. The most bedforms are close to 500 m long. **67**

Figure 4.8. Plot of the height distribution of the measured bedforms. Most of the bedforms are between 0.5 - 1.0 m high. **67**

Figure 4.9. Bedform wavelength vs. height from the seismic data. Using the bedform zone boundaries defined by Amos and King (1984), almost all of the bedforms measured fall into the sand ridge field. Although ridge heights less than 0.10 m were measured, it is unlikley that bedforms of that size were resolved by seismics. Any heights less than 0.10 m were therefore considered to be artifacts created during the data processing, and were omitted from the database. The sharp cut off of data points at < 0.10m is caused by the removal of these values. **69**

Figure 4.10. Bedform symmetry measurements from the seismic data. A bedform with a symmetry less than one is positively skewed (asymmetric to the east), where as a symmetry greater than one is negatively skewed (asymmetric to the west). The inset (top right) is a schematic illustration of a bedform that has a symmetry value of 0.5, and is therefore asymmetric east **70**

Figure 4.11. Comparison plot (wavelengths and heights) of seismic (blue) and CHS bathymetry (red) data. **72**

Figure 4.12. Vibracore 2000-30A-61. Cored from the bottom, stoss side of the Copan-1 transect sand ridge. The column on the left side is a sketch of the core, illustrating the lithology and dominant features. The plots in the center are grain size results for the corresponding depths. The two columns on the right side of the page are photographs of the core (left) and the resin peel (right). The white patches in the resin peel photographs are where sub-samples were extracted for the grain size anaysis. The core depths are of the far left side of the figure. Figures 4-13 to 4-18 follow the same layout. **75**

Figure 4.13. Vibracore 2000-30A-62. Cored from the middle, stoss side of the Copan-1 transect sand ridge. **78**

Figure 4.14. Vibracore 2000-30A-63. Cored from the middle, lee side of the Copan-1 transect sand ridge. **80**

Figure 4.15. Vibracore 2000-30A-63. Cored from the bottom, lee side of the Copan-2 transect sand ridge. **81**

Figure 4.16. Vibracore 2000-30A-97. Cored from the top of the Copan-2 transect sand ridge. **84**

Figure 4.17. Vibracore 2000-30A-165, Cored from the top of the South Sable transect sand ridge. **85**

Figure 4.18. Vibracore 2000-30A-166, Cored from thebottom, lee side of the South Sable transect sand ridge. **87**

Figure 5.1. Schematic interpretation showing the proposed migration direction of longitudinally transported sediments. Sediment is transported via sand ribbons over the ridge crests and into the trough. From the trough it is transported farther away for Sable Island. (Modified from Hudson 2000-30A unpublished cruise report). **94**

Figure 5.2. Schematic illustration of the paleo-lagoon horizon south of Sable Island, and its positions relative to the sand ridge crest and trough **97**

Table of Tables

Table 2.1. Provisional Seismo-stratigraphy of Sable Island Bank (E. King 2001). **9**

Table 2.2. Morphological characteristics of the shoreface-attached ridges on Sable Island Bank as defined by Hoogendoorn (1989). **22**

Table 2.3. Morphological characteristics of the shoreface-attached ridges found off the coast of Maryland (Swift and Field 1981), Argentina (Parker et al. 1982), Virginia (Swift et al. 1972) and Brazil (Figueiredo et al. 1982). **30**

Table 3.1. Geographic position, location, water depth, and length of each vibracore sample taken during B.I.O. cruise HUD-2000-30A. **51**

Table 4.1. Summary table of bedform height, wavelength and water depth results from the CHS bathymetry database. **66**

Table 4.2. Summary table of bedform height, wavelength and water depth results from the Seismic database. **64**

Acknowledgements

First and foremost, I would like to thank my supervisor, Dr. Edward King, not only for giving me the opportunity to take part in such a multi-dimensional project, in which I learned more than I ever though I would, but also for the seemingly endless amount of time and patience he gave me. I would also like to thank Dr. Martin Gibling, for his patience, suggestions and support throughout the year.

Support also came from Sable Offshore Energy Inc. (SOE), and the federal Panel on Energy Research and Development (PERD) program who support the Sable Island studies of the Geological Survey of Canada (Atlantic).

Finally I would like to thank my friends at Dalhousie, who helped make the past year a lot easier than it could have been.

Chapter 1: Introduction

1.1 General Setting

The Scotian Shelf off Canada's east coast is floored by lower to mid Paleozoic granitic bodies and meta-sedimentary rocks on the inner shelf overlain by Mesozoic and Cenozoic sandstones, mudstones and carbonates which built out the bulk of the shelf in a progradational pattern on the middle and outer shelf. The geomorphology of the seabed depicts a series of basins and topographically isolated banks (King 1970, King et al. 1974) that have evolved through modification by a combination of fluvial and glacial processes. The largest bank on the Scotian Shelf is Sable Island Bank, which is 255 km long (northeast to southwest), 115 km wide (northwest to southeast) and has an average depth of 40m below sea level (bsl). (Mobil Oil Canada Ltd 1983, Hoogendoorn 1989), (Fig. 1.1). It is the only bank on the Scotian Shelf that extends above sea level.

Sable Island, a relict glacial end moraine, was formed as a result of a glacial re-advance across the northern part of Sable Island Bank ca. 15 ka (King 2001). With continued transgression these sands were highly reworked by marine processes forming locally thick progradational sand bodies (Northern Spur, DesBarres Spur and East and West Bars) (Fig 1.1).

First discovered between 1497 and 1505 by either John Cabot or an unnamed Portuguese fisherman (Patterson 1894), Sable Island is located on the northeast side of Sable Island Bank at 43° 57′ N; 59° 55′ W. It is 50 km long from tip to tip (parallel to its crescent shaped shoreline), 2 km wide at its widest point near the center of the Island, and has a maximum elevation of 26m above mean sea level (Cameron 1965, Mobil Oil Canada Ltd 1983). The island extends subaqueously at both ends as the West and East

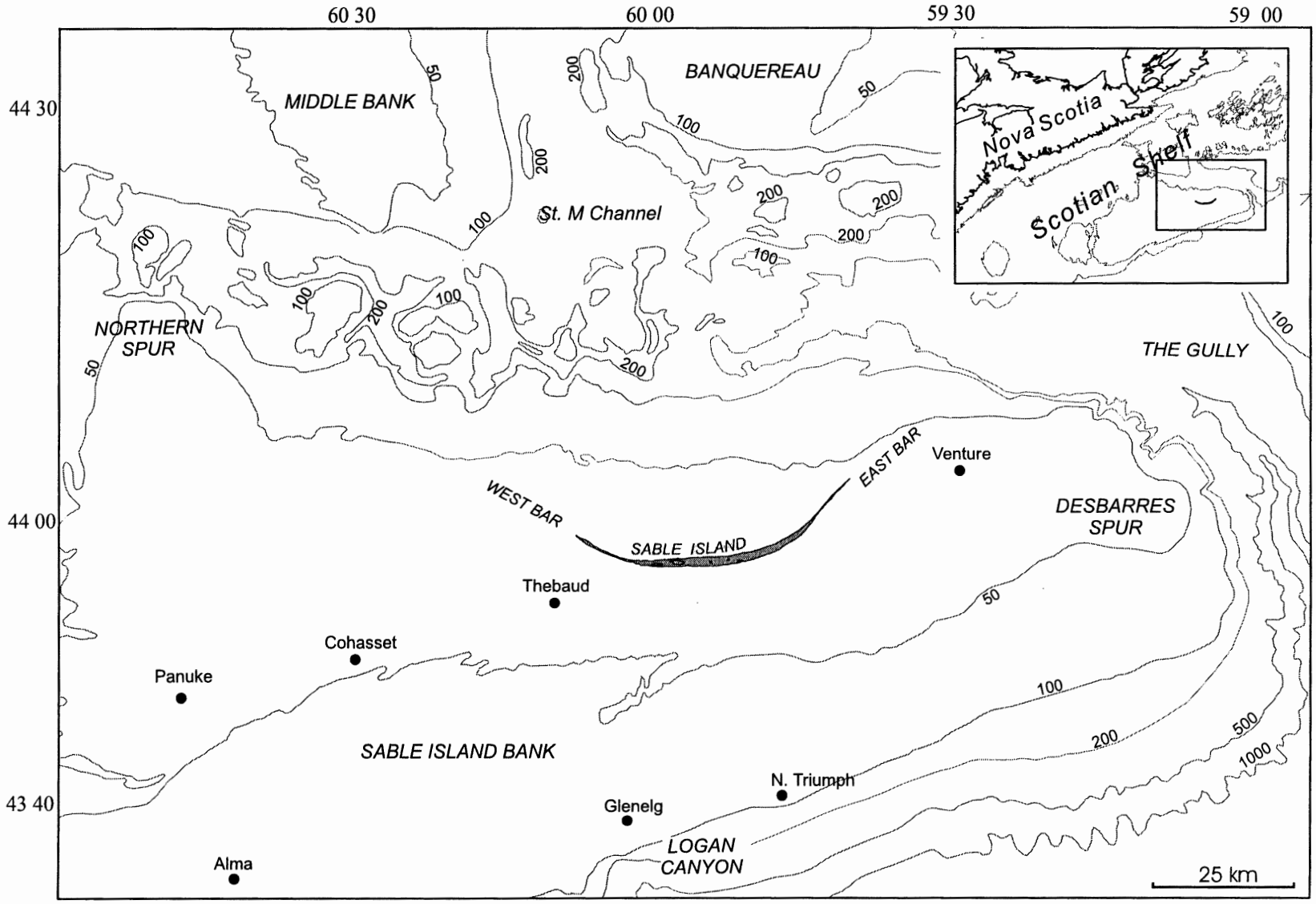

Figure 1.1. Location map of Sable Island Bank on the Scotian Shelf. The locations of Sable Island, Northern Spur, West Bar, East Bar, and Desbarres Spur are also shown. Natural gas is currently being produced from the Thebaud and Venture sites, and future hydrocarbon development is planned for Panuke, Alma, Gleneig and N. Triumph. Production has stoped at the Cohasset site (Modified from King 2001).

Bars. West Bar extends 32 km from the island's western point, and ranges from 9-12 km wide. East Bar extends about 18 km from the island's eastern point and ranges in width from 4-5 km. Both West and East Bars can be approximately delineated by the 20 m isobath (Fig.1.2).

A series of shoreface connected sand ridges occur adjacent to Sable Island, best developed to its south and southwest and extends as far as 23 km south of the island in water depths up to 45m (Hoogendoorn and Dalrymple 1986, Dalrymple and Hoogendoorn 1997). These authors recognized a geographic zonation and a general eastward migration pattern in ridges of varying sizes. Seismic data demonstrate the historically dynamic nature of the ridges and the ridge system since their inception (Hoogendoorn and Dalrymple 1986).

Sable Island Bank's position along the outer edge of the continental shelf leaves it open to wind and wave influences from a variety of directions (Hoogendoorn 1989). The tides on the bank are micro-tidal, semidiurnal in nature (two high and low tides per lunar day), (Forrester 1983, Davies 1964), with a mean tidal range of 1.04m (maximum of 1.46m and minimum of 0.45m). The wave climate varies seasonally, where the winter storms bring the highest significant wave heights of 6 to 8 meters with the longest periods of 10 to 13 seconds (Anonymous 1984). The majority of winter waves and winds associated with the major storms approach the bank from the west and northwest (Evans-Hamilton Inc. 1977, Atmospheric Dynamics Corporation 1979, Anonymous 1984). The summer months rarely bring waves higher than two meters, when the wave and current direction is influenced by the occasional storm and local tidal effects (Neu 1982).

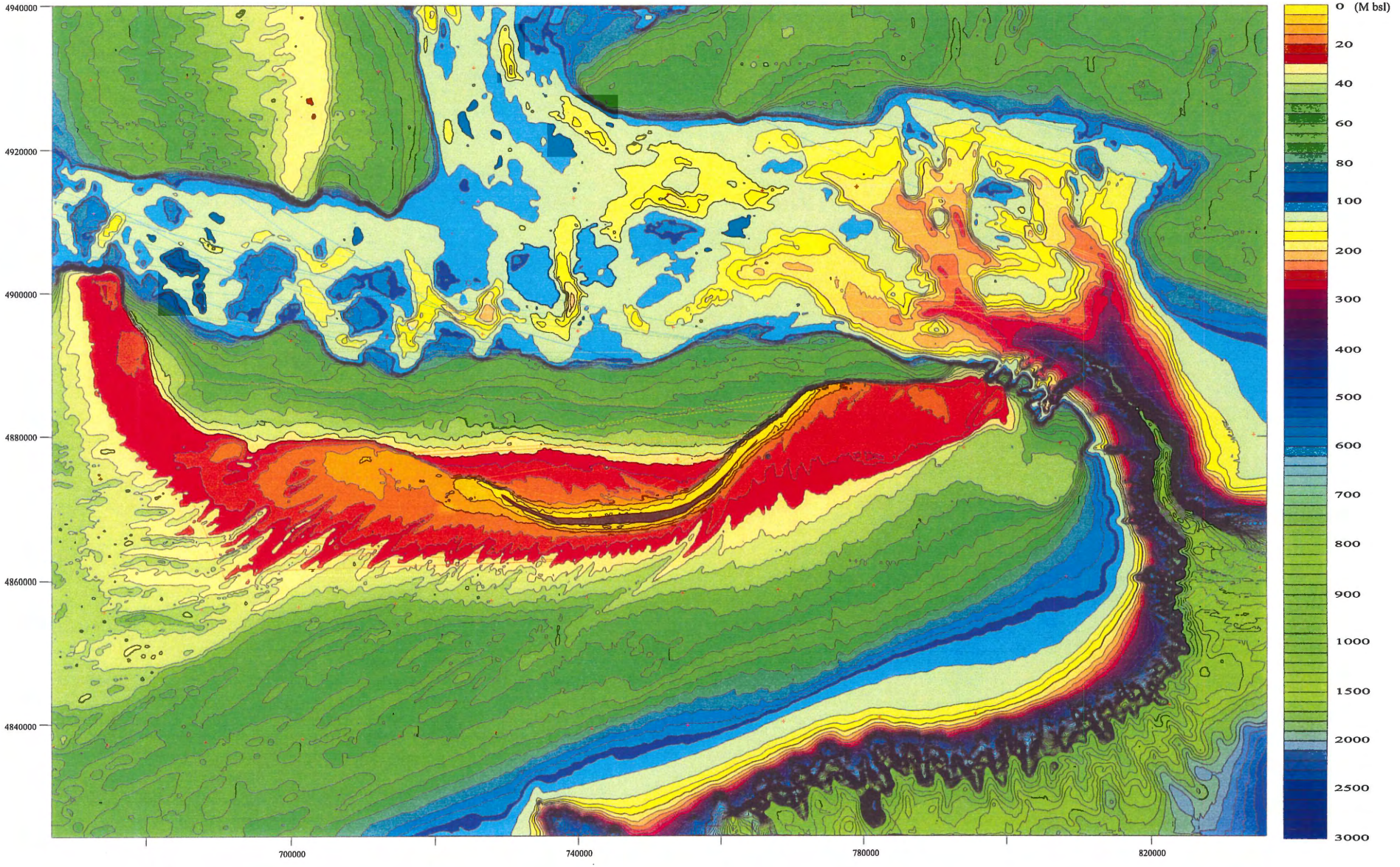

Figure 1.2. Bathymetry map of Sable Island Bank generated form gridded data. (E. King 2001). Note the varying contour interval on the color bar.

Shallow stratigraphic, sedimentologic and environmental studies on Sable Island Bank have increased significantly over the past 40 years, largely spawned by hydrocarbon development. Natural gas is currently produced at two sites and accelerated exploration and further production development is underway (Fig 1.1). This, together with extensive new gas finds in the area, underscores the requirement for further understanding of shallow, and surficial geologic conditions. The stability of the sand ridges is of importance to the hydrocarbon industry concerning pipelines and other seabed installations. If the sand ridges are moving, buried pipelines may become exposed over time creating free-spans and possible overstress conditions (Ingersoll and Ryan 1997). The rate and magnitude of seabed sand migration and its connection with extreme climatic events remains uncertain.

1.2 Objectives and Scope of Thesis

From July 13 to 21, 2000, BIO cruise HUDSON-2000-030A was conducted with two main objectives. i) To better understand the morphological and sedimentological dynamics of the large sand ridge field south and southwest of Sable Island and to investigate the geological properties along future pipeline transects associated with Sable Offshore Energy Inc (SOE) tier II development. ii) To target key areas for improving the understanding of the glacial and sea level history of the region (Li et. al. 2001). To achieve these goals, van Veen grabs, IKU grabs, vibracores and bottom photography were taken. Sidescan sonar and seismic data were also collected. The purpose of this paper is to conduct a sedimentological analysis on the vibracores collected during this cruise to address the hierarchy of reactivation events within individual sand ridges, and to

use the new and existing seismic data and regional bathymetric data (from Canadian Hydrographic Service) to compile a database of wavelength, height and symmetry of the sand ridges and superimposed bedforms to find local and regional trends in the ridge and wave formations. Through integration of the sedimentological analysis with the morphometric analysis, inferences can be made on the stability of the sand bedforms at various locations within the study area. The study should also serve to provide the local setting for planned dating of the bedforms with an aim to better quantifying the processes and rates of bedform migration

1.3 Organization

There has already been a large amount of research done on the Scotian Shelf and Sable Island Bank. Chapter 2 presents the general geology, glaciation and depositional history of the area, discusses the nature and morphology of the shoreface-connected sand ridges, and briefly compares them to similar sand ridge complexes found around the world. Chapter 2 also outlines parallel studies being conducted at the same time as this study. The means by which the data were collected, processed and analyzed is described in Chapter 3. The results from the seismic database and the core analysis are presented in Chapter 4. Finally, an attempt to place the finding in the context of the objectives and in a regional sense is presented in the discussion (Chapter 5).

Chapter 2: Background

2.1 Geology

Sable Island Bank consists of at least three stacked packages of Tertiary and Quaternary, unconsolidated sandstones and mudstones deposited in a regular, seaward prograding pattern, overlain by the Pleistocene Sable Island Sand and Gravel formation (King et al 1974, McLaren 1988). The sequence has been studied a number of times and different interpretations have been suggested, leading to a fair amount of debate and confusion. The stratigraphy is currently under review by King (2001).

King (1970) first mapped the surficial geology on the Scotian Shelf identifying eight regional unconformities throughout the entire sequence. On the bank, the uppermost unit, the Sable Island Sand and Gravel Formation was separated into two main groups, a sand and a gravel dominated facies. Amos and Miller (1990) divided the entire Quaternary sequence on Sable Island Bank into four units based on four distinct acoustic reflectors (R1-R4) interpreted to be major breaks in sedimentation. The conformable Tertiary – Quaternary boundary separating the Banquereau and Laurentian Formations (R4) was identified at 220 m bsl from a borehole on Sable Island by Boyd et al. (1988). After projecting the 0.5 ^{o} seaward-dipping boundary to the shelf edge, the Quaternary deposits were found to be at least 500m thick (Boyd et al. 1988). R3 is present at depths from 50-120m below the sea floor (bsf) and separates the Laurentian Formation from the Emerald Silt Formation and its four members, which lie between R1 and R3. The upper unit on the bank is the Sable Island Sand and Gravel Formation, which they divided into three members, lies above R1 (Amos and Miller 1990). McLaren (1989), referring to the Sable Island Sand and Gravel Formation as the Sable Island Sand Body (SISB),

recognized an additional transgressive unconformity (R0) separating the mobile surface layer from the underlying sediments. Most recently, King (2001) recognized eight regional unconformities throughout the mid. to upper Quaternary sequence and subdivided the SISB into seven stratigraphic units and facies (Table 2.1). The top two unconformities (U-1 and U-2) correspond respectively to McLaren's R0 and R1. King also recognized the equivalents of Amos and Miller's R2 and R3 (U-6 and U-7 respectively) but questioned their relatively young age assignment. Figure 2.1 shows two geologic profiles interpreted from outer bank seismic lines, demonstrating the present understanding of the stratigraphic and geometric relationships.

The surficial SISB contains up to 50m of sediment and covers an area of ca. 12,000 km^2 (Fig 2.2). It lies above the Late Wisconsinan (early post-glacial) marine transgression horizon and comprises mainly gravel lag and some organics (U-2 or R1). The SISB is composed of a series of individual glacially deposited and reworked sand bodies with overlying progradational sand sheets and ridges (McLaren 1988, King 2001). The lower sequence consists of a core of a morainal bank with distal flat-lying deposits as a shallow marine ice apron and relatively small but complex channel cut-and-fill feature. Buried tunnel valleys dominate the northern, proximal (up-ice) side (Boyd et al. 1988, King 2001). The upper sequence is a discontinuous sheet-like cover ranging in thickness from 10m over most of the bank, to as thick as 15-30m over Sable Island, East Bar and West Bar. The unit consists of progradational sand sheets and coastal deposits overlain by the shoreface-connected sand ridges (McLaren 1988, Amos and Miller 1990, King 2001).

Fm.	Setting	Member or Facies	Interpretation	Event & Age comment
Sable Island Sand and Gravel Formation	Sable Island Sand Body (SISB) — Marine reworked sands	1(SR)	reworked/remobilized sand ridges	extreme storm events?
		U-1a	reactivation horizons	
		2(SR)	shoreface-connected sand ridges, eastward transport	time transgressive with Holocene sea-level rise
		U-1b	reorganization of current regime	
		3(SS)	progradational sand sheets and coastal deposits	since early post-glacial; <14ka?
		U-1	renewed transgression and continued wavebase-generated lag ("R-0" of McLaren, 1988)	
	Moraine and associated facies	4(TV)	buried tunnel valleys on proximal side of moraine	
		U-2a	sub-glacial meltwater channel erosion	
		4(CS)	shallow and coastal sands ("Cross-bedded Sand" of Amos & Miller, 1990)	
		4(MB) 4(DA)	4(MB) - core of morainal bank; in part sub-aerial 4(DA) - shallow marine ice distal apron; horiz. bedding	late Late Wisconsinan glacial re-advance between 16 and 14 ka?
		U-2	bank-top planation with transgression ("R-1" of Amos &Miller, 1990 and McLaren, 1988)	
Laurentian Formation	Marine/ glacimarine	5(SM) 5(DM)	5(SM) - ridge/bar/channel sands on outer bank 5(DM) - deeper marine/glacimarine equivalents	synchronous with ice retreat?
	Partial or complete ice cover	6(GL) 6(PG)	glacigenic blanket (pro- and sub-glacial?)	Late Wisconsinan ice maximum; >18 ka?
		U-3	erosion, marine and sub-glacial?	
	Ice cover	Undiff.	undifferentiated multi-generational tunnel valleys along northern bank margin	Mid-Late Pleistocene
		U	sub-glacial erosion, multiple stratigraphic depths	
	Periodic partial or complete ice cover and/or associated low-stands. poorly resolved	7(GL)	glacigenic blanket?	Mid-Late Pleistocene
		U-4	erosional on bank-top	
		8(GL)	glacigenic blanket?	
		CH	conformable horizon, possibly locally erosional	
		9(GL)	glacigenic blanket?	
		Undiff.	unmapped or undifferentiated glacigenic blanket(s)	
		U-5	erosion, marine and sub-glacial?	
		10(GL)	thick progradational blanket; glacial?	
		U-6	sub-aerial channelization and shelf-break canyon equivalent to R-2 (Amos & Miller, 1990)	
		U-7	equivalent to R-3 (Amos & Miller, 1990)	Early-Mid Pleistocene
		11	largely unresolved, undulating horizon	
		U-8		
Banquereau		Plio.-Pleist.	Pliocene-Pleistocene boundary (Boyd et al., 1988)	Tertiary
		12(PG)	seaward prograding; shelf construction	

across-shelf correlations unconfirmed

Table 2.1. Provisional Seismo-stratigraphy of Sable Island Bank (King 2001).

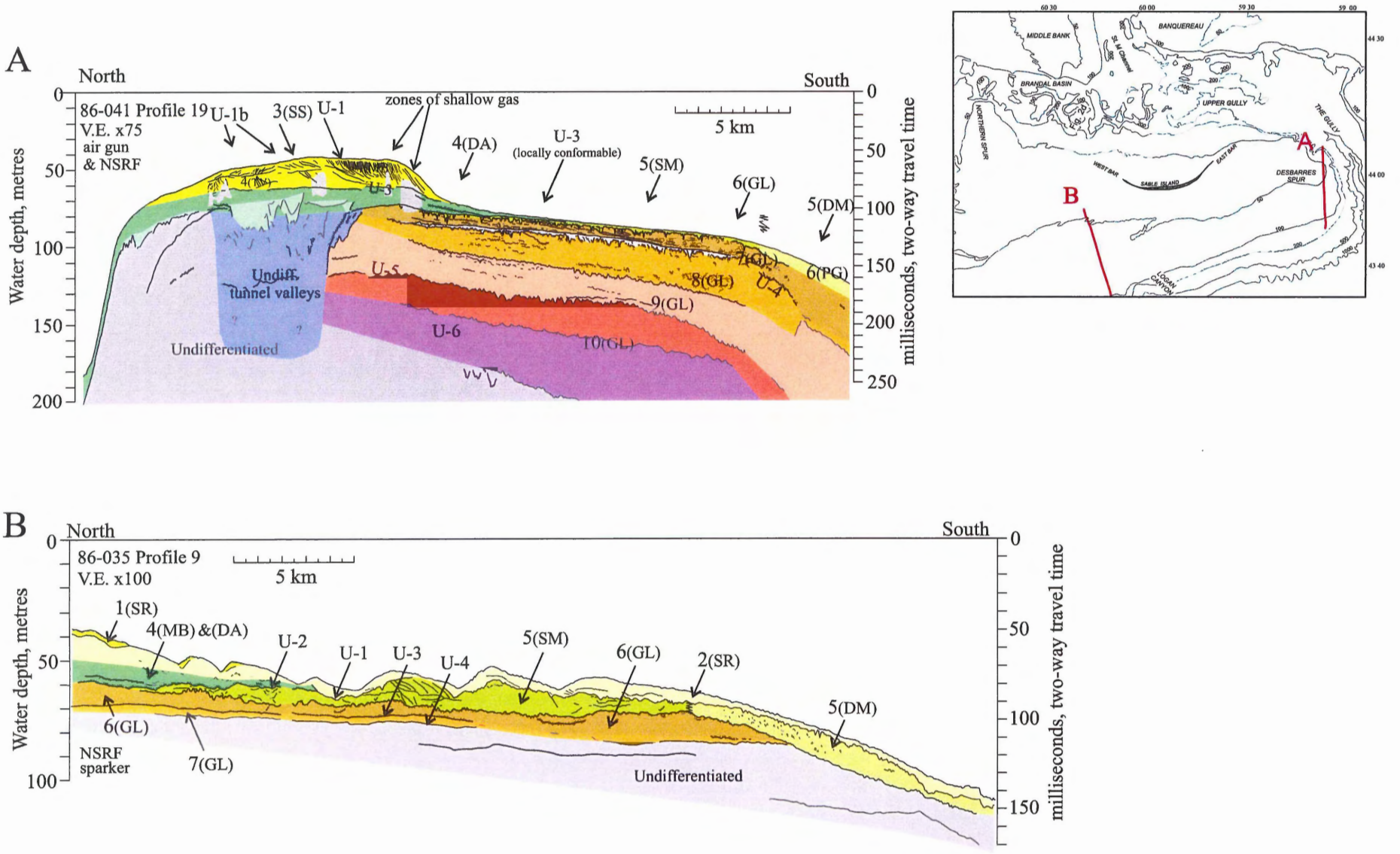

Figure 2.1. Geologic profiles illustrating the stratigraphic units and their bounding surfaces from two locations on Sable Island Bank. Profile A (see inset map), from Desbarres Spur (east Sable Island Bank) is compiled from air gun and NSRF data collected during B.I.O. cruise 86-041 and is exaggerated vertically 75X. Profile B (see inset map), southwest of Sable Island is compiled from NSRF sparker data collected during B.I.O. cruise 86-035 and is exaggerated vertically 100X (King 2001). The unit, and horizon labels correspond those in Table 2.1.

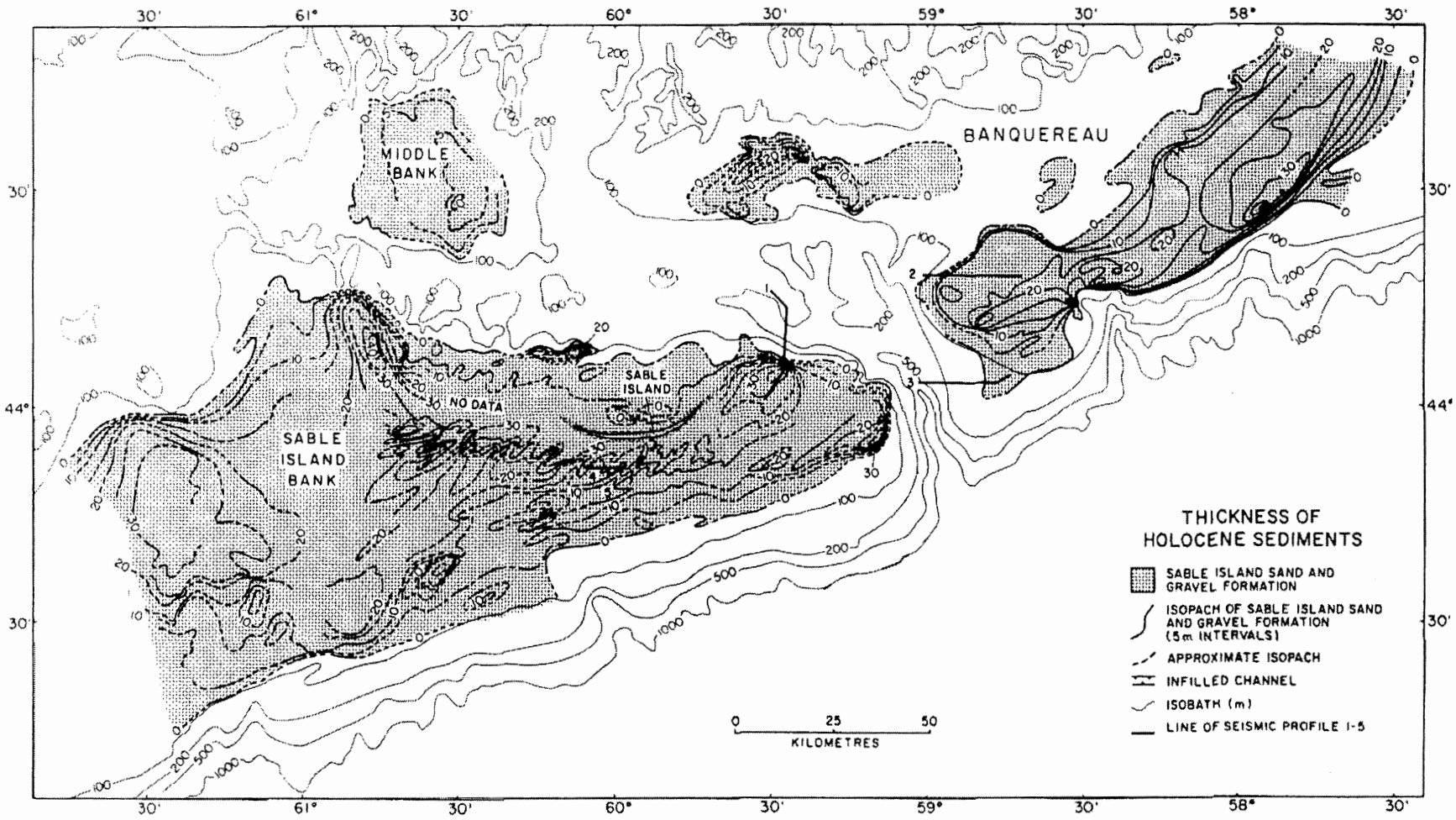

Figure 2.2. Contoured thickness of the Sable Island Sand Body (Amos and Nadeau 1988).

The texture of surface sediments across the bank is highly variable and grain sizes range from very fine to coarse sand (Amos and Nadeau 1988). On the extreme western part of the bank, patches of coarse to very coarse sand occur with gravel, and the sand fractions decrease in size eastward, becoming medium, fine, and ultimately very fine on the eastern side of the largest shoreface-connected ridge (the Harcourt Cameron Ridge). Medium sand covers most of the western, northern and northeastern parts of the bank including Sable Island, and its distribution is bounded by the 100 m isobath. Fine sand is found throughout most of the south-central bank and upper slope, and a zone of very fine sand is present at the center of this region, southeast of Sable Island. This is the only location on the bank where very fine sand exists above the 100m isobath (Amos and Nadeau 1988).

2.2 Glaciation, Sea Level and Depositional History

The shallow, complex structures on Sable Island Bank were formed during periods of ice influence and associated low stands of sea level and reworked during ice-free periods and sea level rise throughout the Wisconsinan and early Holocene (Amos and Miller 1990). It is clear that ice sheets covered large portions of the Scotian Shelf but the number, extent and timing remains uncertain (Amos and Miller 1990, King 1996, Stea et al. 1998, King 2001). This is especially true for the eastern Scotian Shelf. Amos and Miller (1990) postulated a number of advances from early to late Wisconsinan time, including a strong Younger Dryas (ca 10.5 ka) influence. King (1996) inferred Late Wisconsinan ice cover to the shelf break until after 20 ka and a slow subsequent retreat from the eastern shelf. In recognizing numerous Pleistocene glacigenic blankets with

intervening glacial, marine, and sub-aerial erosion surfaces, King (2001) suggested an older age for some of the advances assigned Wisconsinan age by Amos and Miller. He suggested at least six advances since the early Pleistocene, including a two-step Late Wisconsin advance, the latter responsible for the core of the SISB sometime between 16 and 14 ka.

Following a major low stand of ca. 150 m below sea level, a series of at least five glacigenic sheets was deposited and interpreted as representing multiple glacial ice extensions. The late Wisconsinan ice maximum extended locally to the shelf break and modified the bank through planar erosion, depositing a pro-glacial, prograding blanket with a channelized, iceberg scoured top as well as a hummocky proximal, or subglacial blanket (King 2001). Shallow marine reworking, and transport of sands forming bars, ridges and channels resulted from the ice retreat as the bank was exposed to marine and coastal forces, planing it nearly flat. A southward re-advance of the glacier's margin between 16-14.5 ka moved across the northern bank and deposited the SISB core as its end moraine, forming ancestral Sable Island. With the final ice retreat, transgression was renewed, modifying and redistributing the sediments into the bars, sand ridges and sand sheets that are present today (King 2001).

Sea level on Sable Island Bank has been rising continuously since the ice margin retreat. Scott et al. (1984) retrieved a 7,000 year record of continuous relative sea level (RSL) rise using microfossil data from core sediment. Scott et al. (1989) updated their sea level curve when they obtained sea level points from –48.8m (11 ka bp) and –35.3 m (8.1 ka bp) and combined them with previously colleted data. By extrapolating the sea level change back to 15,000, a new curve was created giving a –78m low stand in the late

Wisconsinan (Scott et al. 1989) (Fig 2.3). The new RSL curve correlates with Quinlan and Beaumont's (1981) theoretical curve based on their peripheral bulge model. Their model is based on the weight of the ice sheet on the shelf, which creates a peripheral bulge of mantle material towards the ice margin. As the ice retreated, the peripheral bulge migrated towards the center of the ice sheet (landward, away from Sable Island Bank), parallel to the ice margin (Fig. 2.4). Sable Island Bank is in zone D of the model, on the leeward side of the bulge crest. As the bulge migrates landward with the retreating ice sheet, RSL rises (the crust is actually sinking) as isostatic rebound restores the crust to its equilibrium position. The rate of RSL change was greatest soon after ice retreat as ecstatic sea level rose. The late Wisconsinan ice re-advance postulated by King (2001) further complicated sea level rise, but is previous to the RSL curve gathered by Scott et al. 1989. Sea level on Sable Island Bank continues to rise at a rate of 3 mm/year, as isostasy has not yet reached its resting point.

2.3 Sand Ridge Morphology

2.3.1 Bedform Classification

There are a number of different bedforms that play a significant role in the morphology of sand ridge fields. Specific bedforms are characterized by specific styles of migration. This section defines the characteristic bedforms that form under two types of sediment flow, Transverse flow, where bedforms are formed, and migrate with their crests perpendicular to the flow direction, and Longitudinal flow, where bedforms are formed and migrate with their crests parallel to the flow direction (Amos and King 1984).

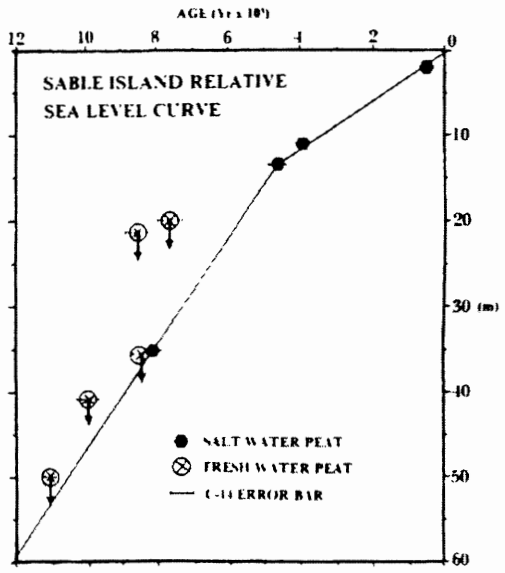

Figure 2.3. Composite observed relative sea level (RSL) curve for Sable Island (Scott et al. 1989)

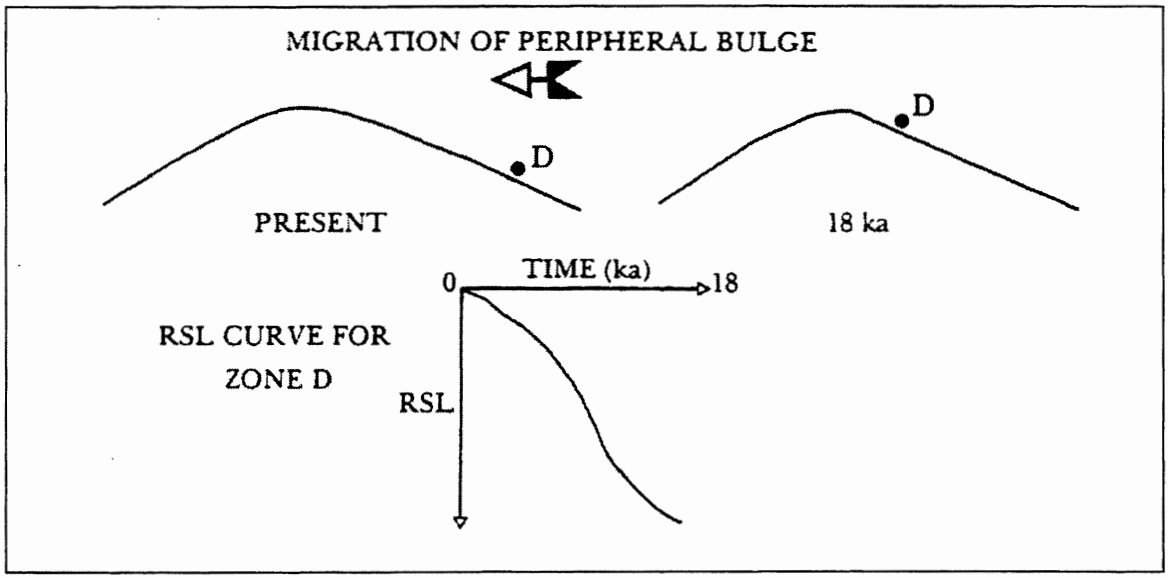

Figure 2.4. Schematic illustration of the peripheral bulge at 18 ka and the present (Modified from Quinlan and Beaumont). The peripheral bulge migrates towards the ice centre with the retreat of the glacier causing subsidence of the crust at Zone D (Sable Island Bank Area). The Relative Sea level Curve (RSL) shows the response of Zone D due to isostatic re-adjustment as the weight of the ice sheet is removed.

Sand waves are constructive features characteristic of transverses flow, formed in medium to coarse sand or gravel, and are transported by the superposition and migration of megaripples.

2-D megaripples are straight, sharp-crested, flow transverse, discrete bedforms composed of medium to coarse sand. They are usually single-crested and are often found with ripples superimposed on their flanks

3-D megaripples are short-crested, flow transverse, discrete bedforms composed of medium to coarse sand and may have ripples superimposed on their flanks.

Sand ridges are composite, flow parallel, linear accumulations of sand formed by the superposition and migration of sand wave or megaripple fields. They are often featureless and round crested and are symmetrical or only slightly asymmetrical.

Sand ribbons are current parallel 'streaks' of sand with no measurable relief, demarcated laterally by shallow depressions formed by current scouring

2.3.1 Ridge Characteristics

Shoreface-attached ridges are linear to slightly curved shoreline-oblique sand bodies that lie directly seaward of the shoreface and are outlined by seaward deflections of coast-parallel, shoreface isobaths. Globally they are characteristic features of a transgressive coastline. Using bathymetric maps and seismic limited seismic data, Hoogendoorn (1989) identified two fields of shoreface-attached ridges off Sable Island. He recognized a main ridge field and counted 79 ridges extending 110 km along the south side of the island and its extensions. The second field is much smaller, where he counted only six ridges, located to the north of the island (Hoogendoorn and Dalrymple

1986, Hoogendoorn 1989, Dalrymple and Hoogendoorn 1997). The CHS digital bathymetric compilation (Chapter 3) enables recognition and mapping of much smaller features, enabling King (2001) to enhance the bedform maps of Hoogendoorn and Dalrymple (Fig 2.5).

Two distinct sizes of sand ridges have been identified and are most notable south and southwest of the island. The larger, first order ridges are 18-22 km long, 10 m high and 5-10 km wide. The smaller, second order ridges are 5-7 km long, less than 5 m high, and 1-2 km wide. Their crests are parallel with the crests of the first order ridges, on which they are commonly superimposed. Superimposed on the first and second order ridges are smaller scale, third order bedforms including what they interpreted as sandwaves, megaripples, hummocky megaripples, wave ripples, and tidally generated current ripples. The sandwaves have wavelengths between 100 to 300 m and are 1-3 m high, oriented with their crests parallel to the ridge crestlines (Fig 2.6). Both first and second order ridges are straight to gently curved, and strike SW-NE (Fig. 2.5). The angle in which they converge with the shoreface of Sable Island (closing angle) is typically 50°, and occasionally as high as 75°, which is unusually high in comparison to other shoreface-attached ridge complexes (Hoogendoorn 1989). The ridges all exhibit rounded crests and V-shaped troughs, and were thought to be mostly asymmetrically skewed to the east, with the eastern lee side steeper than the western stoss side.

This study makes an alternative interpretation as to the genesis and relationship between the first, second, and superimposed bedforms and also addresses the level of asymmetry with in the ridges, which is discussed in chapter 5

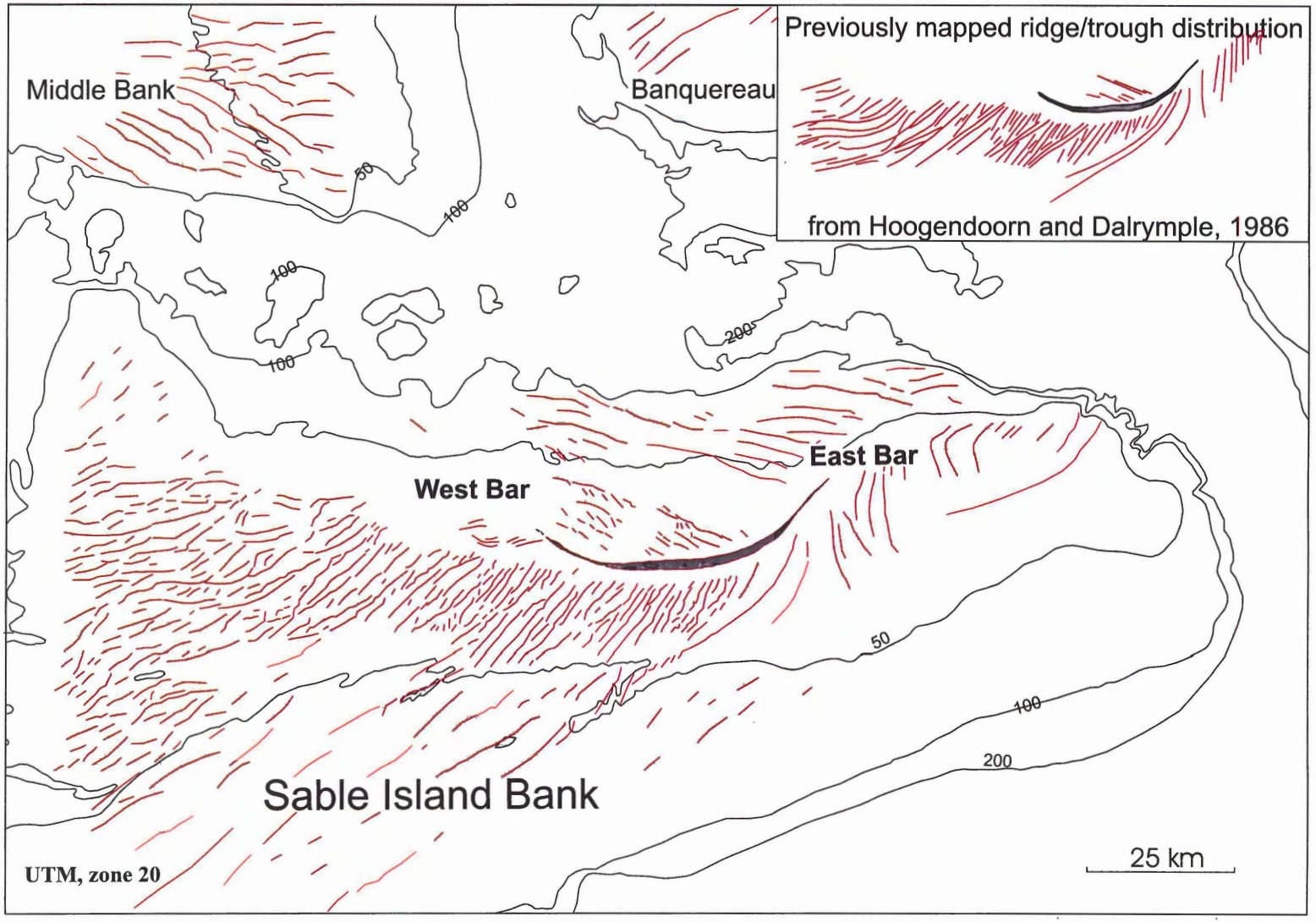

Figure 2.5. Enhanced bedform map displaying the distribution and orientation of the shoreface-attached sand ridges on Sable Island Bank (King 2001). The main ridge field is southwest, south and southeast of Sable Island. The second, smaller ridge field is north of Sable Island, between West Bar and East Bar.

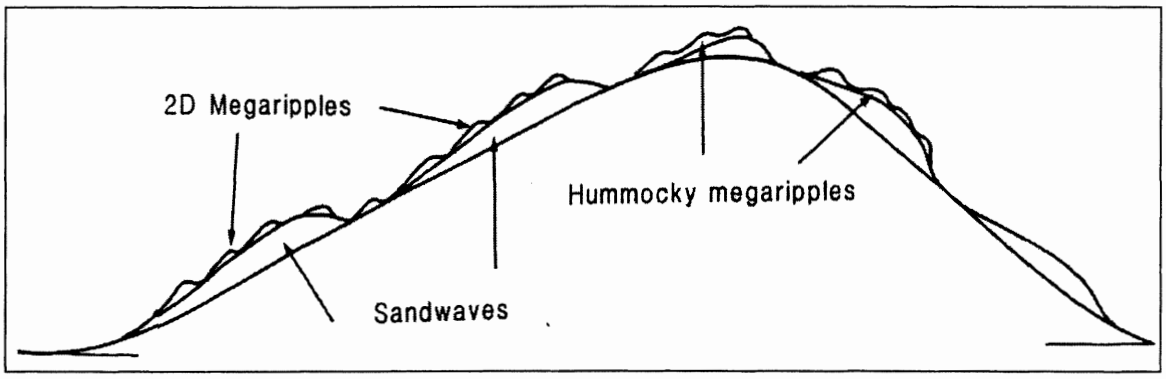

Figure 2.6. Schematic illustration of the distribution of small-scale bedforms over a shoreface-attached sand ridge on Sable Island Bank (Hoogendoorn 1989).

Hoogendoorn (1989) divided the ridge fields into four zones based on their systematically changing morphological characteristics. Zones 1, 2 and 3 are subdivisions of the main ridge field on the southwest, south, and southeast side of Sable Island, respectively, and zone 4 consists of the ridge field north of the Island (Fig 2.7). The size, slope, closing angles, water depth and dynamism of the ridges decrease to the east along the southern side of Sable Island, placing the largest ridges with the most superimposed bedforms in zone 1, and the smallest ridges with the least superimposed bedforms in zone 3. The ridges in zone 4 are smaller than those in zone 3, having smaller closing angles and, found in shallower water depths (Table 2.2). Grain size of the sand throughout the ridge complex also decreases slightly to the east, from an average phi of 1.56 (0.34 mm) in zone 1 to 1.84 (0.28 mm) in zone 3. The eastward decreasing trends are attributed to a regional eastward decreasing energy gradient. The gradient was thought to be controlled by the orientation of the Island and ridge complex relative to the prevailing wind and current directions. The strongest storm winds come from the west and southwest, as do most storm generated waves. Sheltering by Sable Island causes the intensity of wave action to decrease from west to east through the ridge complex. The west-northwest origin of wind and wave generated currents were also thought to have caused a net migration of the sand ridges in an easterly direction. An alternative interpretation as to the migration direction, and the process causing the migration of the sand ridge field is discussed in chapter 5.

The exception to these trends is the Harcourt-Cameron Ridge (Fig 2.7), which is distinctly different from any of the other ridges in the ridge complex, and does not appear to fit into the classification of first and second order ridges. Beginning at the shoreface of

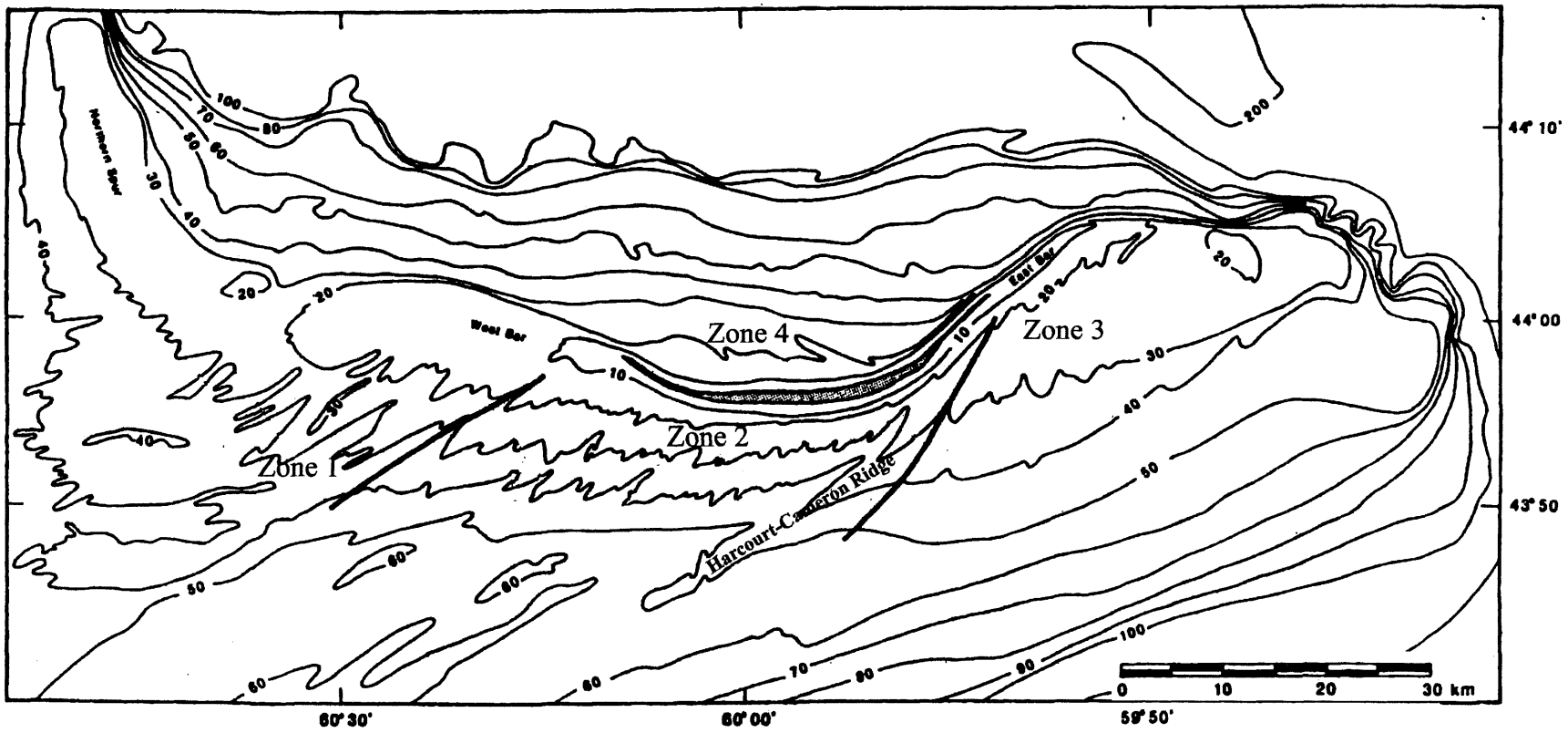

Figure 2.7. Bathymetry map of Sable Island Bank showing the divisions of the four morphological zones of the sand ridge complex (Hoogendoorn 1989). Zone 1 is to the west of Sable Island, Zone 2 is south of Sable Island, Zone 3 is East of Sable Island (south of East Bar) and Zone 4 is north of Sable Island, between West and East Bars. Zones 2 and 3 are separated by the Harcourt-Cameron Ridge, the largest of the sand ridges on Sable Island Bank.

Zone/Ridge Order	Water Depth (m) (Inner end-outer end)	Length (m) avg. (max-min)	Height (m) avg. (max-min)	Width (m) avg. (max-min)	Stoss side Slope avg. (max-min)	Closing Angle avg. (max-min)
Zone 1						
1st order	18 - 14	22500 (45000 – 6000)	9.7 (20 – 2.4)	4200 (8200 – 1700)	0.61° (2.50° – 0.15°)	56° (62° – 45°)
2nd order	18 - 45	5600 (21000 – 1400)	4.4 (14.5 – 1)	1450 (2700 – 600)	0.33° (0.91° – 0.06°)	50° (60° – 40°)
Zone 2						
1st order	20 - 40	18500 (21000 – 15000)	~ 9.0 (no data)	7200 (8300 – 5300)	no data	44° (50° – 35°)
2nd order	20 - 40	6700 (17000 – 1600)	4.4 (17 – 0.5)	1350 (3300 – 750)	0.34° (0.80° – 0.05°)	60° (75° – 40°)
Zone 3	15 - 30	8000 (11000 – 5200)	2.3 (3.2 – 0.3)	1800 (4800 – 1000)	0.13° (0.20° – 0.04°)	39° (42° – 38°)
Zone 4	10 - 25	5200 (12300 – 15000)	4.5 (7.9 – 0.5)	1350 (1900 – 900)	0.37° (1.24° – 0.09°)	28° (34° – 21°)

Table 2.2. Morphological characteristics of the shoreface-attached ridges on Sable Island Bank as defined by Hoogendoorn (1989).

East Spit in water depths of 14 – 16 m and curving gently to the southwest, the ridge is over 70 km long and continues out to depths of approximately 80 m (Hoogendoorn 1989).

An eastward reduction in grain size has also been observed within each individual sand ridge. The coarse sediments are rich in shell debris and occur low on the erosional stoss side of the ridge. From here there is a progressive eastward decrease in mean grain size over the crest and down the depositional lee side of the ridge. This pattern causes an abrupt difference in sediment size on either side of each trough axis and both first and second order ridges exhibit this pattern. This grain size contrast was determined to have formed as the ridges migrate. Coarse grains and shells that are too heavy to be transported (per-modern ridge deposits) are concentrated into a lag layer in the troughs and stoss flanks of the ridges as finer sediments (modern ridge deposits) are transported and deposited on the eastern (lee) side. As the ridge migrates, the pre-modern sediments are buried beneath the advancing modern ridge sediments. The pre-modern and modern ridge deposits are separated by an erosion surface marked by a high-amplitude reflector termed the Basal Reflector (Fig 2.8). The modern ridge sediments range in thickness from <1-10m and are characterized by the presence of laterally continuous, eastward-dipping, low-amplitude reflectors that resemble large-scale cross-stratification, which Hoogendoorn (1997) termed "master bedding planes". The master bedding planes are concordant with the present day lee faces of the ridges (Fig 2.8). The modern ridge deposits (< 10 years old) (King and Li personal communication) are also known as the mobile zone, as they have been deposited during the growth and migration of the ridges,

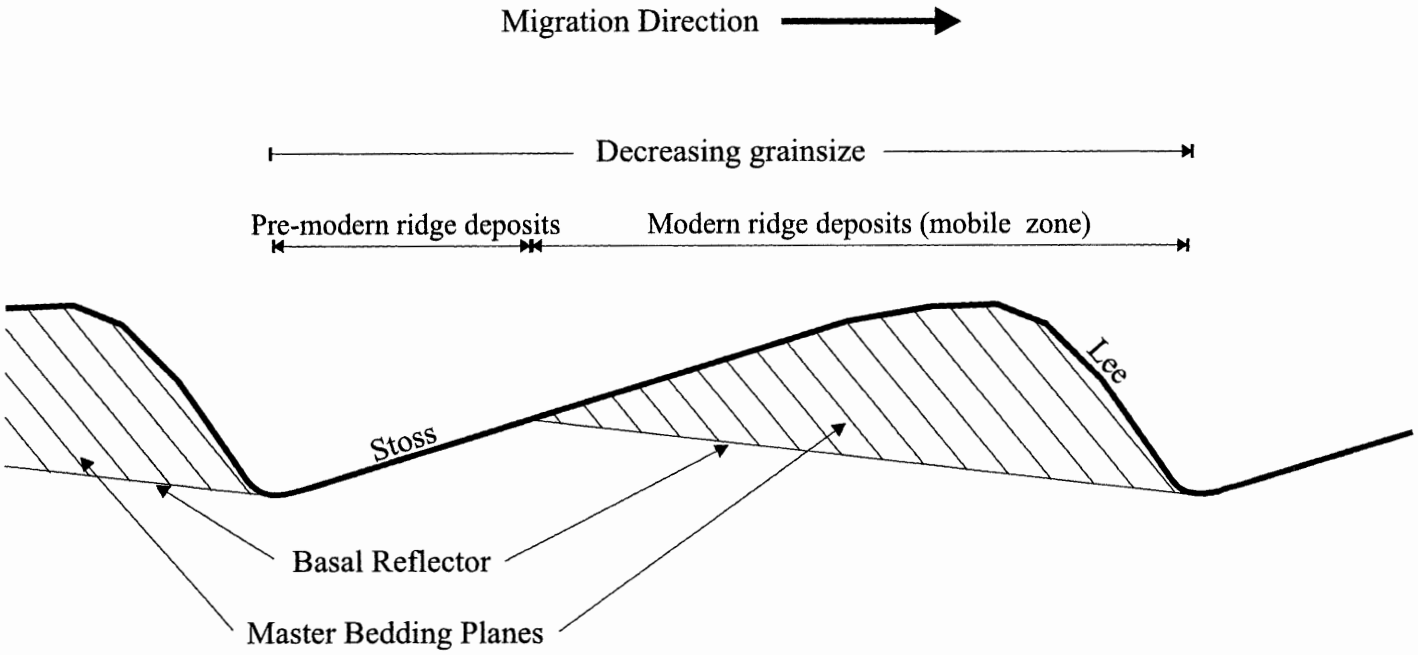

Figure 2.8. Schematic representation of a sand ridge on Sable Island Bank showing the orientation of the Basal Reflector and Master Bedding Planes. Grain size across the ridge decreases from the stoss to the lee side (Redrawn and modified from Hoogendoorn 1989 and Dalrymple and Hoogendoorn 1997).

and continue to migrate during storm events (Hoogendoorn and Dalrymple 1986, Hoogendoorn 1989, Dalrymple and Hoogendoorn 1997).

The mobile zone is the upper ca. 0-50 cm of the sand ridge. This zone exhibits a number of sedimentary features that are typical of a moving sand body that Hoogendoorn and Dalrymple (1986, 1997) and Hoogendoorn (1989) defined as wave and current ripples, transitional wave and current ripples, dunes and hummocky megaripples. The dunes are straight crested and have wavelengths of 5-300 m and heights up to 2 m. The dunes occur on both the stoss and lee side of first and second order ridges. The hummocky megaripples occur near the ridge crests and have heights of less than 1 m and spacings of 2-15 m. The hummocky megaripples and small dunes commonly occur adjacent to each other, with the dunes on the ridge stoss side passing into hummocky megaripples on the ridge crest and the upper part of the lee flank (Hoogendoorn and Dalrymple 1986, Hoogendoorn 1989, Dalrymple and Hoogendoorn 1997). Recent studies have seen megaripples only in the troughs of the sand ridges (King 2000, Li 2001). The results of these studies, as well as this one are used to make an alternative interpretation as to what the previous studies refer to as dunes, and is discussed in chapter 5).

2.3.2 Sediment Migration

The geometry of the basal reflector and the surficial bedforms within the mobile zone appears to show that the ridges are migrating eastward (an alternative interpretation is presented in chapter 5). The migration would have occur by erosion on the western, stoss side of each ridge creating the coarse-grained lag, and deposition of the finer

grained sediment on the eastern, lee flank. Obtaining migration rates of the ridge complex has been difficult. One attempt was through comparisons of existing data spanning a number of years. This was largely inconclusive due to the navigational/positional accuracy limitation of the data, particularly for the surveys performed before 1990 (Ingersoll and Ryan 1997). Direct dating of ridge migration rates has also led to inconsistent results. Hoogendoorn (1989) dated shells from lag surfaces within cores that resulted in inconsistent age distributions due to the large amount of re-worked and old shells, giving a large scatter in the ages within individual cores and over the entire ridge. Boczar-Karakiewicz et al. (1987) used mathematical models to predict ridge migration rates. Their models calculate that ridges in 40 m of water form over 890 years and have an average migration rate of 1.9 m/y. Their model of ridge formation, from shelf-break generated internal waves, is inconsistent with a number of other observations (discussed below).

Amos et al. (1988 and 1999) concentrated on seabed observatories (RALPH) and current meters to directly measure changes in seabed features (photographically and sonically) as well as sediment concentrations in the water column. They used time-lapse photography over 12 days off Sable Island's East Bar to record ripple migration and bedform transport of the surficial sand caused by wave and tidal current motion. They found that sand movement during non-storm events was principally bedload, as well-developed ripples. The combined, near-bed motions of waves and currents decreased the thresholds for sand transport and the generation of well-developed bedforms (Amos et al. 1988, 1999). Li and Amos (1999) observed ripple generation during the build up of a storm south of West Bar. At the early stages of the storm, relict wave-dominated ripples

with worm tubes and animal tracks first changed into irregular, sinuous, asymmetrical current-dominated and intermediate wave-current ripples under bedload transport. As the storm progressed, the bedforms evolved into regular, nearly straight or sinuous, asymmetrical wave-dominant ripples under strong sand suspension. At the peak of the storm, the ripples were completely washed out and upper plane bed sheet flow prevailed. Amos et al. (1997) found that the maximum, net daily transport rate of sediments was 10-15 kg/m/day under low-energy summer conditions in 1982. Those results are comparable to the results of the non-storm periods obtained by Li et al. (1997) and Li and Amos (1998), where near-bed measurements of waves, currents, seabed responses and ripple migration rates were obtained during the winter of 1992/93. Storm transport rates during this study ranged from 306-822 kg/m/day, which are consistent with rates from past studies conducted in the region during the winter months. Transport directions during non-storm periods are typically to the northwest-north-northeast, and southwest-south-southeast, which corresponds to the tidal directions. During storm events, the direction of sediment transport depends on the relative directions of the waves and currents at the storm's peak (Li et al. 1997).

2.3.3 Ridge Generation

The generation of sand ridge systems throughout the world has yet to be completely understood. A number of formation models and theories attempting to explain their formation have been proposed; however, due to the dynamic environments where ridge complexes are generated, each model has applicable and non-applicable aspects with regards to ridge formation under different conditions. It is unlikely that a single process is responsible for the formation of a ridge complex but rather they are

likely to be the product of a combination of processes, depending on the regional environment and characteristics unique to where the ridge field is situated.

Three hydrodynamic models have been proposed to address the issues of sand ridge formation with the understanding that the sediment patterns that produce the shoreface-attached ridges are a result of a regional hydrodynamic climate and changing conditions caused by rising sea level. All three have been applied to the ridge complex on Sable Island Bank with varying degrees of success. The three models also assume the ridges have grown after there initial formation through transverse flow.

1. The ebb-tidal model proposed by Swift and Field (1981), and applied to Sable Island Bank by McBride et al. (1986) suggests that the ridges developed due to tidal-inlet migration coupled with coastal transgression, producing a ridge along the ebb-tidal-delta retreat path. The ridge acts as an initial perturbation that migrates alongshore and lengthens seaward as the shoreline transgresses.

2. Boczar-Karakiewicz and Bona (1986) and Boczar-Karakiewicz et al (1987) proposed a model attempting to explain the ridge orientation on the inner shelf, ridge spacing, grain size distributions over ridges and the ridge migration direction as a function of infragravity waves (long period waves (80-120 seconds) in the frequency spectrum between gravity waves and tidal oscillations). Infragravity waves are thought to be produced by wind, large storm systems and underwater seismic activity.

3. A mathematical model developed by Huthnance (1982) originally for tidal sand ridges, involves the vertical growth and lengthening of an initial irregularity on the seabed oriented at an optimum angle to the prevailing tidal, and weather related currents.

The irregularity causes flow veering and deceleration over the crest, leading to upward growth as well as a preferred spacing.

The ebb-tidal model does predict the alongshore migration in the direction of closing angles, however, because of the absence of tidal inlets it does not appear to be applicable to Sable Island Bank. There are also too many ridges for each ridge to represent a separate inlet-ebb-tidal-delta pair given the microtidal conditions that are present on the bank. The infragravity model is able to explain the general orientation of the ridge field, as ridge crests are approximately parallel to the crests of infragravity waves arriving from the open ocean. The model also predicts the grain size distributions over the ridges; however, the model requires a clockwise curvature of the ridge crests in shallow water as well as predicting a northeast migration direction both of which are opposite to what is observed on the bank. Furthermore, it cannot explain the ridges north of Sable Island. The Huthnance model is the most reliable of the three, and is able to explain the majority of the ridge characteristics, such as the grain size distribution, the orientations of the megaripples and sandwaves, the migration direction of the ridges and their closing angles. An alternative hypothesis as for the initial formation of the sandwaves is presented in this study in chapter 5.

2.4 Morphological Comparisons

The characteristics of the ridge complex are similar to patterns in many shoreface ridges elsewhere in the world. The second order ridges on Sable Island Bank have height, width, and slope measurement that are similar in magnitude to the ridges on the U.S. East Coast, the Brazilian Coast, and the Argentinian Coast (Table 2.3) (Swift and

	Maryland	Argentina	False Cape (Virgina)	Brazil
Water Depth (m)	3 - 40	4 - 40	3 - 21	8 - 24
Length (m)	4000 - 20000	Up to 25000	> 4	Up to 22000
Height (m)	3 - 12	4.7	6.2	4 - 10
Width (km)	1 - 3	1 – 4.5	1 - 2	2 - 6
Slope	0.2° – 2.5°	< 1.9°	< 2.0°	0.30°
Closing Angle	1° – 35°	20 - 35°	20 - 35°	35°

Table 2.3. Morphological characteristics of the shoreface-attached ridges found off the coast of Maryland (Swift and Field 1981), Argentina (Parker et al. 1982), Virginia (Swift et al. 1972) and Brazil (Figueiredo et al. 1982).

Field 1981, Figueiredo et al. 1982, Parker et al. 1982, Hoogendoorn 1989). The first order ridges on Sable Island Bank are however, generally broader than any of the other known ridge complexes in the world. The Sable Island Bank ridge complex is also a continuous field of bedforms separated by relatively narrow troughs, which is similar to those of the shoreface ridges along the coasts of Brazil and Argentina (Figueiredo et al. 1982, Parker et al. 1982). The Ridges in the U.S. Mid-Atlantic Bight, on the other hand are relatively isolated and separated by wide, flat troughs (Duane et al. 1972, Swift and Field 1981). The magnitudes of some of the morphological parameters of the Sable Island Bank ridge complex differ from shoreface-attached ridges in other parts of the world. The heights and closing angles of the ridges in the Mid-Atlantic Bight, the Argentine coast and the Brazilian coast (Duane et al. 1972, Parker et al. 1982, Swift and Field 1981, Figueiredo et al. 1982,) are typically smaller than the first-order ridges on Sable Island Bank (Hoogendoorn 1989). The slopes of the ridges are all of similar degree, and the side slopes decrease seaward along the length of individual ridges in all of the ridges (Table 2.3) (Duane et al. 1972, Parker et al. 1982, Swift and Field 1981, Figueiredo et al. 1982, Hoogendoorn 1989).

Amos and King (1984) compiled published and unpublished data pertaining to sand ridges from eastern Canada and 18 ridge fields worldwide. The sand ridges fields from around the world all contained a variety of bedforms (megaripples, sand waves, sand ribbons, sand ridges). The bedforms measured on the Atlantic coast fall almost entirely in the sand wave and sand ridge fields and those measured on Sable Island Bank fall almost exclusively in the sand ridge size field (Fig. 2.9). Amos and King (1984) also found that width/height ratios for sand ridges around the world have a high degree of

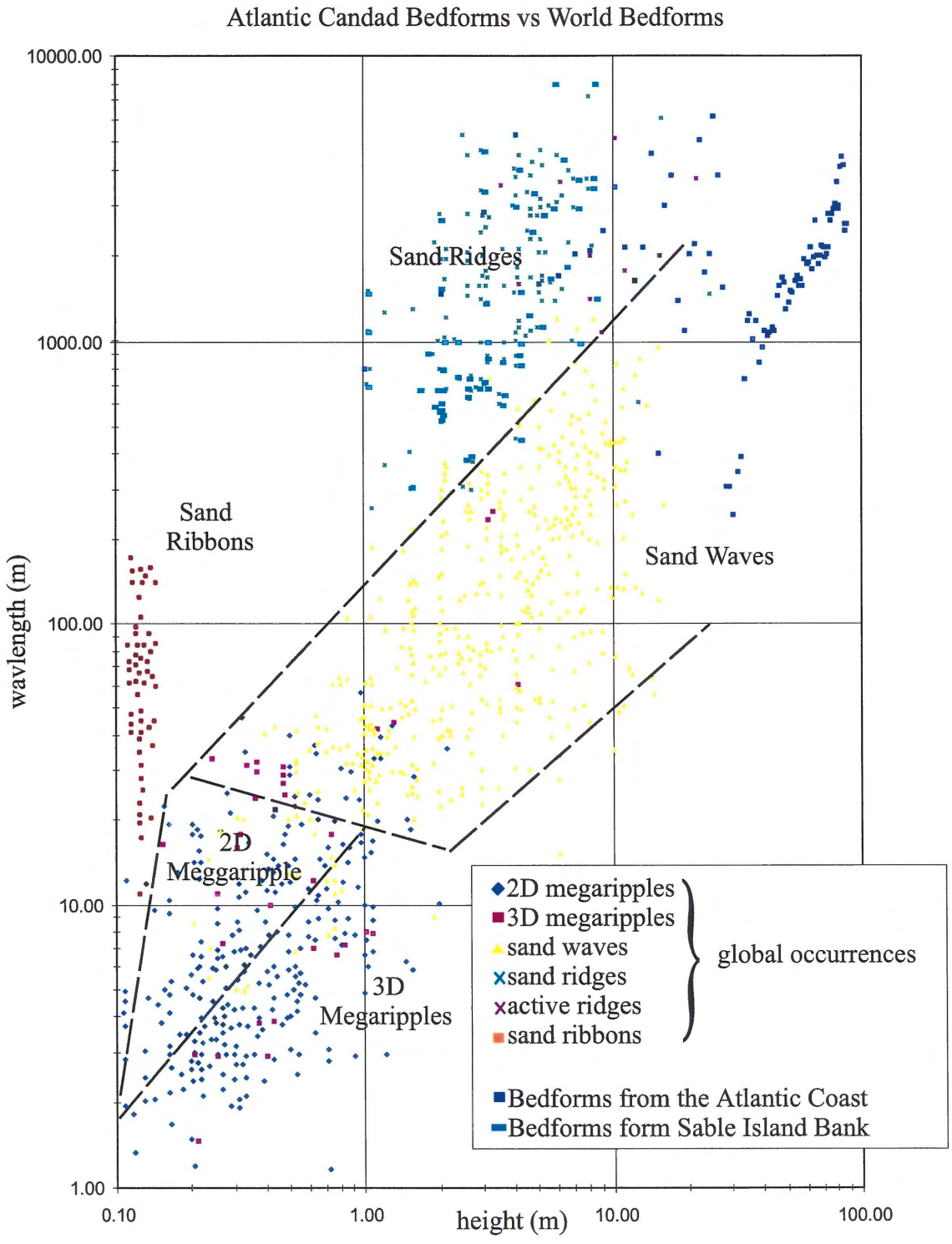

Figure 2.9. A plot of measured bedform sizes from sand ridge fields around the world, including Atlantic Canada and Sable Island Bank. The dashed lines represent the approximate limits between each bed phase (Amos and King 1984).

coherence despite the different location, water depth and environments in which they were formed (Fig 2.10). Sand ridges from Canada's east coast, however, are of lower amplitude than those worldwide (Fig 2.10). The majority of these ridges have been described as 'moribund', or intermittently active whereas the ridges from around the world are mostly derived from tidally dominated regions. Degradation of moribund ridges reduces their height, but not necessarily their width, thus accounting for the differences.

2.5 Parallel studies

Current research at GSCA by King on migration of the sand ridges includes constructing a database that will provide the basis for compilation of a lithologic, geotechnical, and geohazard zonation and a suite of maps depicting unit thickness distribution, unconformities as well as surficial bedforms and buried channels. Studies aimed at addressing seabed mobility under the present hydraulic regime (tidal, current and storm) over a several year span are being carried out by Michael Li through annual/biannual deployment of the seabed observatory RALPH and S-4 current meters on south Sable ridge crests and troughs under normal and storm conditions. These studies are supported by Sable Offshore Energy Inc. (SOE) and Panel on Energy Research and Development (PERD).

Sediment migration conditions on the bank are also the subject of this study, where the vibracore samples collected on the recent Hudson cruise are being analyzed using Optical Stimulated Luminescence (OSL) techniques by Dorothy Godfrey- Smith, and are also the subject of a Dalhousie University undergraduate thesis by Mark Rabin

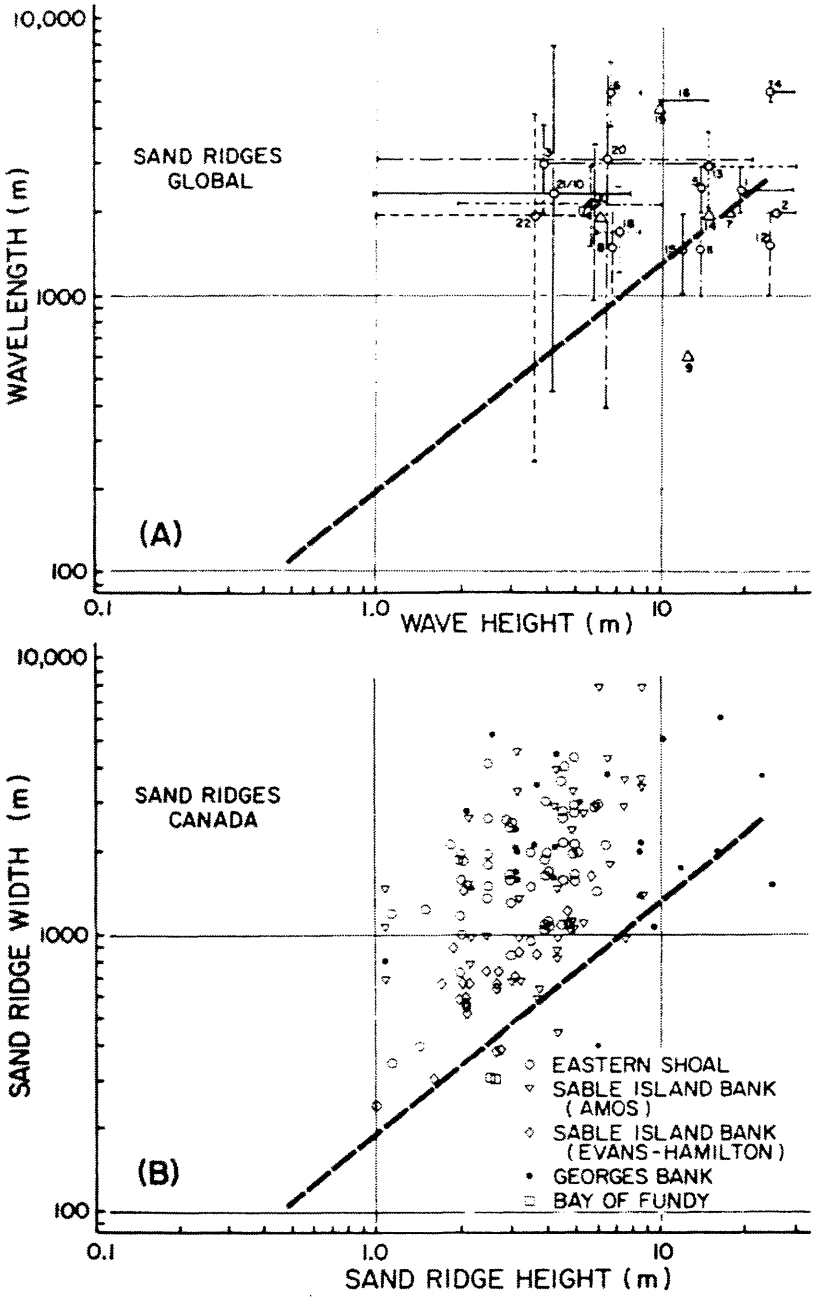

Figure 2.10. Ridge wavelength vs. height ratios from global sand ridges (A), and Eastern Canadian sand ridges (B). The plots show the high degree of consistency between ridges around the world, as well as the slightly lower amplitudes of the sand waves on Canada's East coast (Amos and King 1984). The black line represents the boundary between the sand ridge and sand wave size fields.

which include an evaluation of the present day zeroing (light exposure) of the quartz grains in the shallow Sable Island Bank environment. Three samples were taken from both vibracore 165 and 166, and are presently being dated. A brief technical report (King and Godfrey-Smith, 2001) will present these dating results.

King is also revising the confusing seismo-stratigraphy of Sable Island Bank after digitally compiling all relevant GSC seismic data and collecting new seismic data from BIO Cruise HUD-2000-30A. This is part of a multifaceted study at the GSC, that is also funded in part by the hydrocarbon industry supported Panel on Energy Research and Development (PERD), the GSC, and Sable Offshore Energy Inc. (SOEI) whom are responsible for the construction and reliable operation of existing and new pipelines.

Chapter 3: Data Collection and Analysis

3.1 CHS Bathymetric and GSCA Seismic Data for Bedform Morphometric Analysis

Until now, most of the bedform analyses conducted on the Sable Island Bank sand ridges have been conducted from maps using bathymetric data from the Canadian Hydrographical Service (CHS) or seismic data of limited coverage. The database created in this study combines seismic data collected over a number of years, and uses the existing CHS data to outline the geographic and vertical range and variability of bedforms as an initial step in better understanding the sediment dynamics. By comparing the results from the seismic data with those of the CHS data, the accuracy of the past research using only the CHS data can be assessed.

The CHS data, in the format they were available (profiles interpolated from original gridded data), have a lower spatial resolution than profiles generated from seismic profiles (discussed below), but the full-coverage of the CHS data set (Fig. 3.1) shows the magnitude and extent of these bedforms in a continuous sense. In practice, the CHS data delineate sand ridges and large sand wave-scale bedforms (2 to 15 m relief) while the seismic data preserve depth information on a sub-metre scale. The geographic coverage of the seismic data used in this study is shown in Figure. 3.2. Although over 8500 km of seismic profiles are available for bedform metrics analysis, this data set lacks the continuity of the CHS set. Thus both data sets were used in the analysis.

3.1.1 CHS Database

Digital compilations of bathymetric postings derived from CHS surveys from the mid to late 1980's and the geographic/depth postings compiled for the eastern Scotian

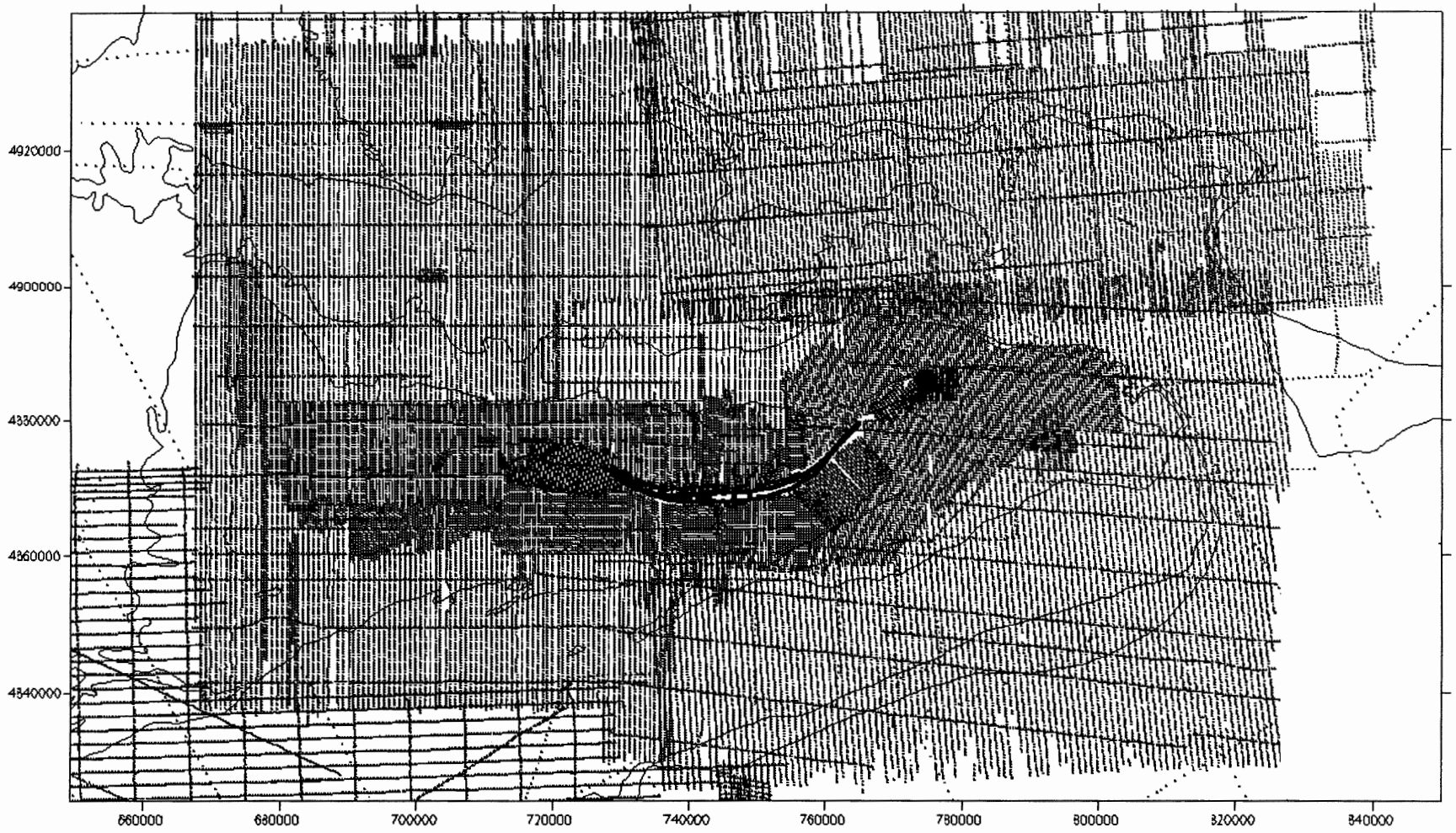

Figure 3.1. Geographic coverage of the CHS bathymetry data used in this study. The data was collected using a 200m spaced grid close to Sable Island, and a 400m spaced grid over the surrounding area (Sankarelli 1988, Unpublished Msc Thesis).

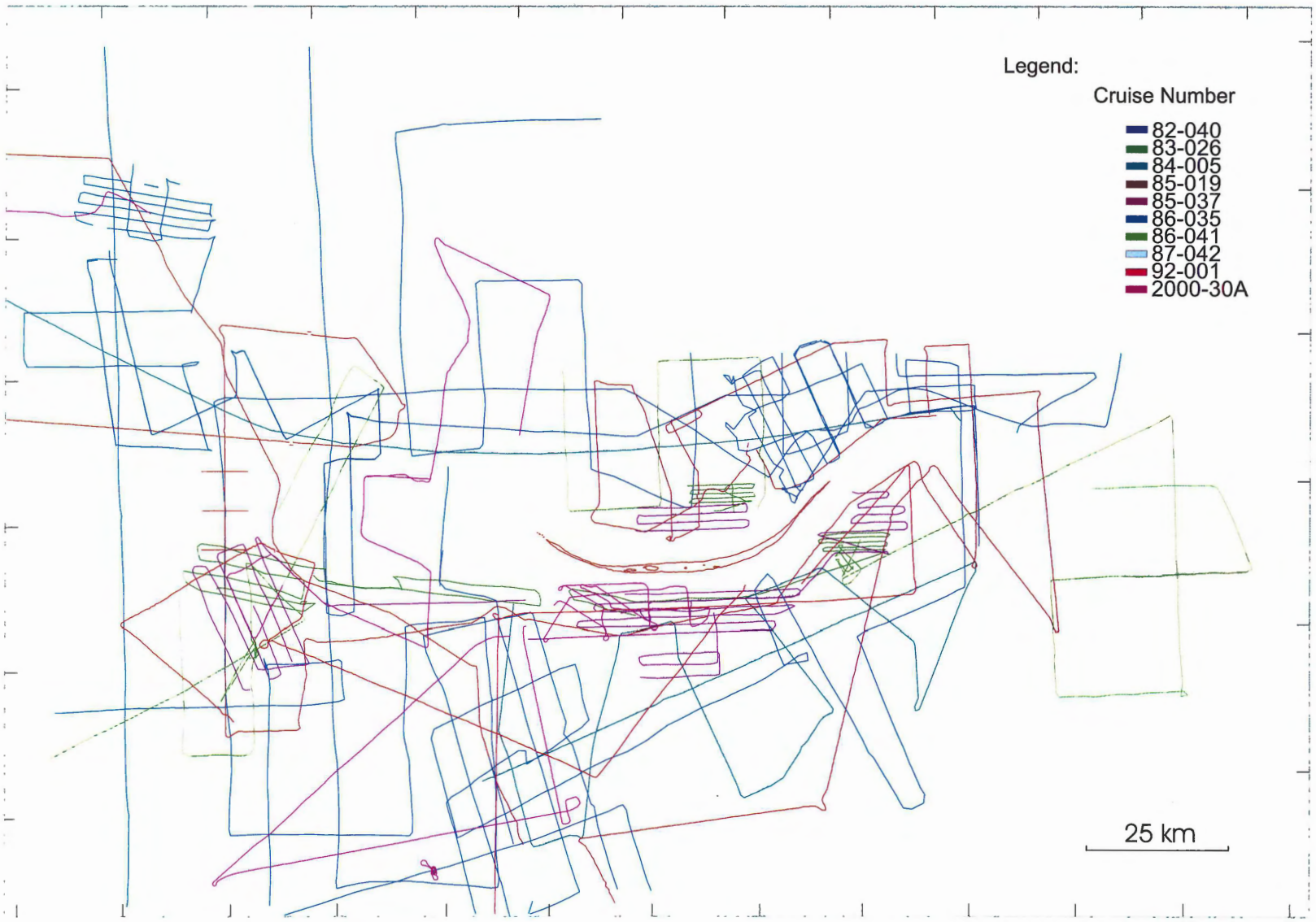

Figure 3.2. The geographic coverage of the seismic data used in this study.

Shelf were used (Sankarelli, 1998). The portion that covers the Sable Island Bank sedimentary bedforms was reprocessed (filtered and gridded) by King, into surface relief maps. From this, a bank-wide map of medium to large-scale bedforms was generated (Fig. 3.3). This was an enhancement of the work of Hoogendoorn and Dalrymple (1986), Hoogendoorn (1989), and Dalrymple and Hoogendoorn (1997). The digital analysis also presented the possibility for further analysis of the relief of these bedforms, carried out in is study.

For purposes of bedform measurement analysis, the CHS bathymetry data were divided into eight different zones across Sable Island Bank, southern Middle Bank and western Banquereau, and named after their geographic location (Middle Bank, Banquereau, CoPan, South Sable Offshore, South Sable Shoreface, North Sable Shoreface, North Sable Deep Shoreface, and Venture & East Bar). This was done such that each zone contained transects oriented approximately perpendicular to the most dominant crest lines of the sand ridges (Fig. 3.4). Along each of these transects a bathymetric profile was generated from the gridded seabed surface. The purpose of this was to obtain width/wavelength measurements with a minimal error due to crestline-oblique profiles. Such errors cannot be avoided in measurements from the seismic profiles (discussed below), which were rarely oriented perpendicular to bedforms. A morphometric database was constructed by measuring the height (trough to crest) and wavelength (trough to trough) of surficial bedforms in these profiles (Fig 3.5). The process of bedform measurement involves a visual identification of bedforms from the bathymetric profile and then drawing of vertical and horizontal lines representing the observed height and wavelength respectively, of each bedform. The profiles are

Figure 3.3. Surface relief map of eastern Sable Island Bank showing medium to large-scale bedforms. The image was generated using CHS data (King unpublished)

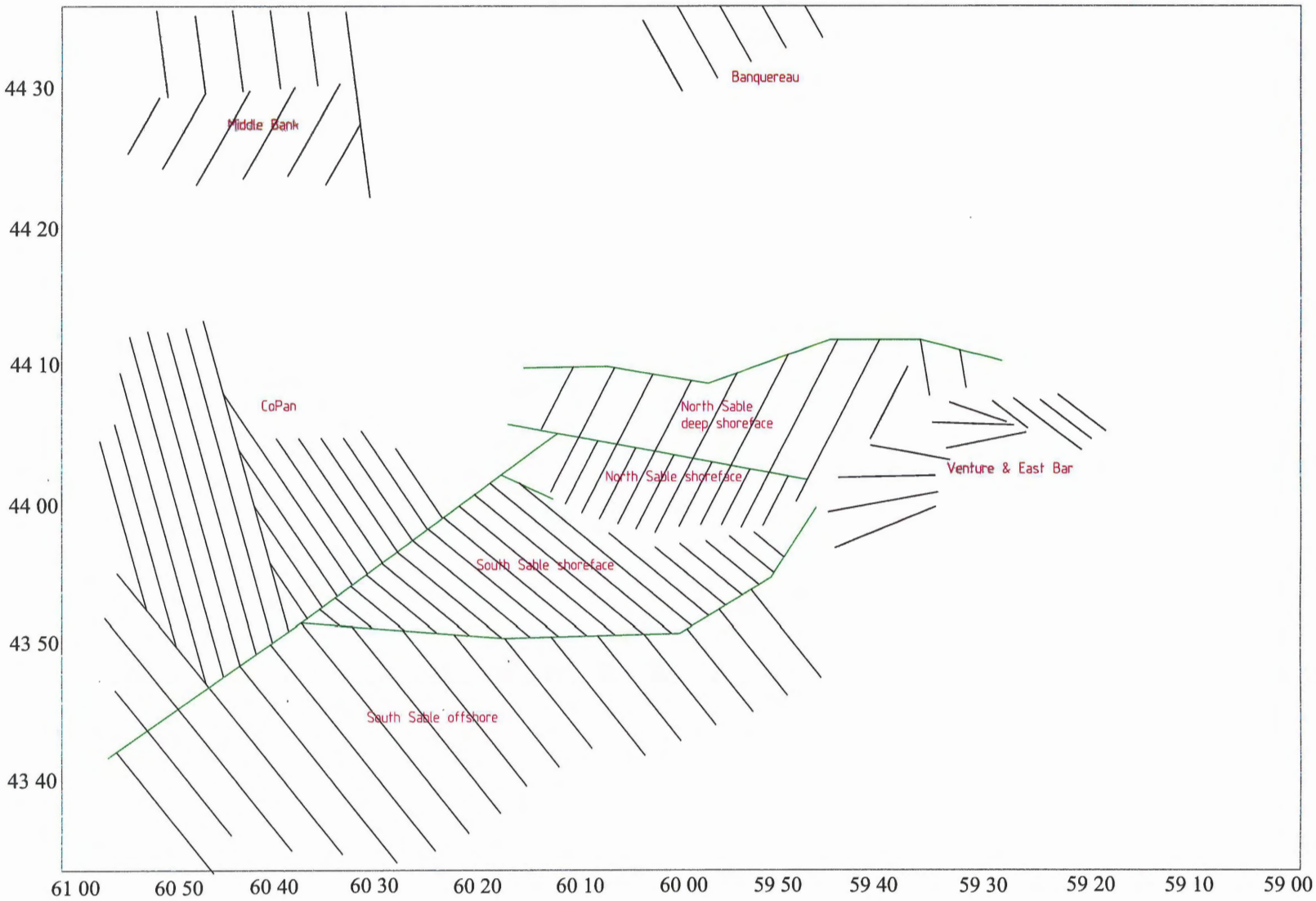

Figure 3.4 The division of zones created for the CHS database across eastern Sable Island Bank, southern Middle Bank, and southwestern Banqureau. The profiles lines (dark, thin) are oriented approximately perpendicular to the most dominant sand ridge crest lines. Sable Island is located in the small space between the South Sable shoreface (directly south of the island) and North Sable shoreface (directly north of the island) zones, in the middle of the page (King unpublished).

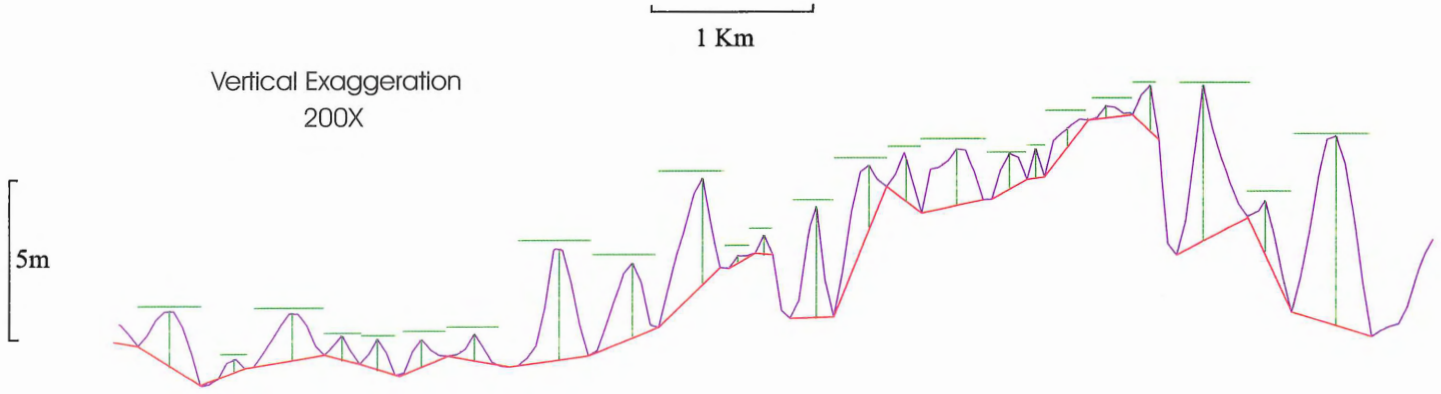

Figure 3.5. Example profile line created using the CHS bathymetry data (line five, Copan, west of Sable Island). The sand ridge is drawn in purple, the red base was drawn as a guideline for drawing the wave heights (vertical green) and the wavelengths (horizontal green). The profile line is vertically exaggerated 200X

georeferenced projections such that the UTM Eastings (for generally E-W oriented transects) or Northings (for generally N-S oriented transects) and the elevation (below sea surface) are captured in the internal CAD entity lists. The coordinates for these line entities are then extracted to a spreadsheet, corrected for a built-in elevation vertical exaggeration and a metric conversion (CAD lists in imperial units). Then wavelengths, heights and symmetry (skewness) for individual bedforms can be calculated from these data (the calculation used to measure symmetry is outlined in figure 3.6). The profile is displayed as an x, y plot where the y-component represents depth below sea level. As only one of the UTM coordinates (Easting or Northing) is preserved in this listing, the corresponding Northing (or Easting) must be recovered to re-establish its correct geographic location. This is accomplished through establishing the equation for each straight-line segment (y=mx+b) of the profile transect (for CHS data), or of the original ship's track (for seismic data). In the spreadsheet, this equation is then solved for the missing coordinate for each bedform measurement. The spreadsheet database is built up on a batch basis, either profile by profile or as a series of profiles

One shortcoming of the CHS database is that the data for the area in between the gridlines had to be interpolated to achieve the complete, bank-wide map. When ever any data is interpolated, its accuracy decreases, however, most features the CHS data is capable on resolving are such that they span a sufficient area of the gridded data, so any trends that are present will be large, and consistent enough to enable the interpolation with only a minimum of accuracy loss.

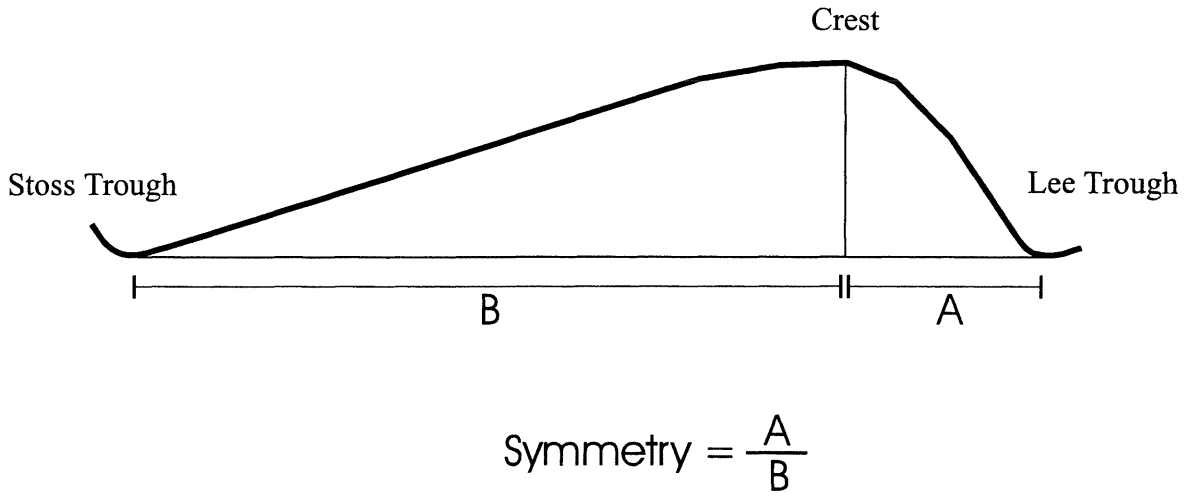

Figure 3.6. Schematic example as to how bedform symmetry was calculated. Symmetry was measured as a ratio of the distance from the ridge crest to the lee trough (A), and the distance from the ridge crest to the stoss tough (B). A ratio less than one means the bedform is skewed west (asymmetric east) and a ratio greater than one means the bedform is skewed east (asymmetric west). A symmetric bedform will have a ratio of 1. The smaller, or larger the ratio is (relative to one), the more asymmetric the bedform is. The example bedform drawn above would have a ratio less than one, as it is skewed left (west), and asymmetric to the right (east).

3.1.2 Seismic Database

For the compilation of the seismic database, data collected during BIO cruises from 1982-87, 92 and 2000 were used. King processed and digitized the raw (analogue) data as part of an ongoing study of stratigraphy and geohazards of the Sable Island Bank area. This process was completed through a number of steps, and through the use of a number of computer programs. Briefly, visible reflectors from the original seismic 'paper' data were traced on velum and scanned on a continuous scanner. Once they were in digital form, they were vectorized, aligned and scaled for differing aspect ratios using CAD software and adjusted to a datum (sea-level; 'Y=0'), while using ships navigation data (integral lateral scale adjustments to fit time-based analogue positional references on the profiles to distance-based true geographic positions). These digital profiles are thus geo-referenced and maintain all the detail of the original tracings, and can be easily manipulated to emphasize seabed features, ridge stratigraphy or other features.

The seismic morphometrics database was constructed in a similar fashion as the CHS database. The bedform heights and wavelengths were measured using vertical and horizontal lines, respectively, after being visually identified from the profile (Fig 3.7). The seismic data were however, taken a step farther than the CHS data by measuring three orders of sand ridges (first-order sand ridges, superimposed, second-order sandwaves, and further superimposed, surficial, third-order bedforms), where they could be identified. This, three-order classification of the sand ridges does not correspond directly to the various bedform sizes defined by Hoogendoorn (1989). This classification scheme is based on the vertical superposition of sand waves, where Hoogendoorn's (1989) classification is based primarily on the size the bedform. The profiles compiled in

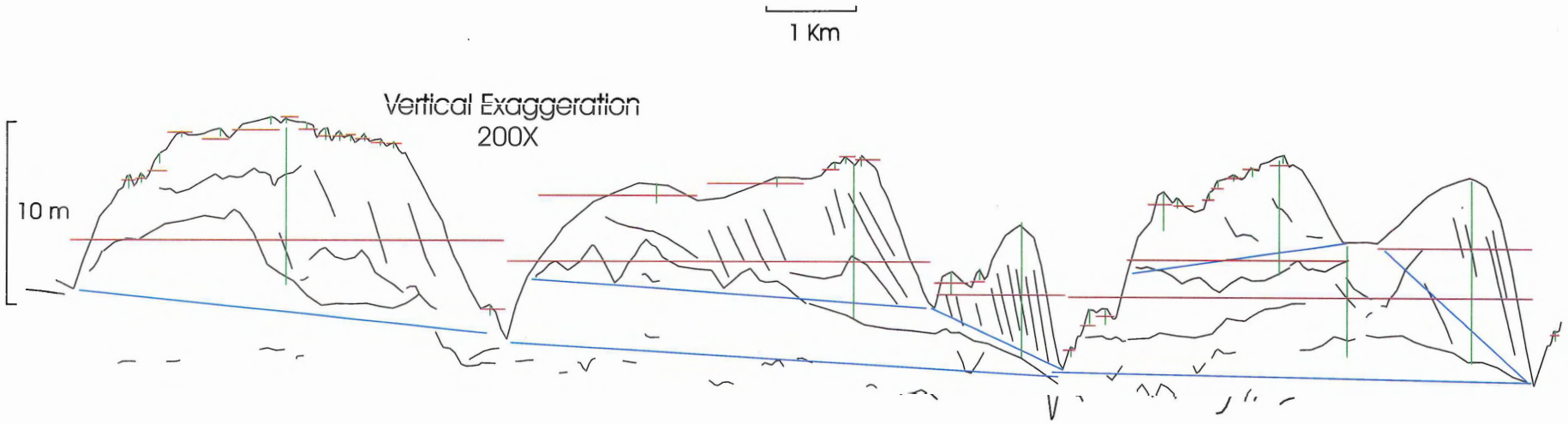

Figure 3.7. Example profile line created using the seismic data (profile line 31, from cruise 85-037). The sand ridge heights (vertical line)are displayed in green, and their wavelengths (horizontal line) are displayed with brown colored lines. The blue lines are guidelines used to help determine the boundary of the different order sand ridges. The vertical scale is exaggerated 200X. This profile also illustrates the basal reflector and master bedding planes disscused in Chapter 2.3.1 (illustrated in Figure 2.7).

this manner provide superior representation of the sand ridges and internal features together with well resolved smaller scale bedforms superimposed on the ridges (not resolved in the gridded CHS data). In an attempt to understand regional sediment dynamics, it is reasoned that these superimposed bedforms represent the most active features so knowledge of their size and distribution is necessary. The different orders were distinguished throughout the data processing by assigning each order its own drawing layer and text colour. The seismic profiles lines were georeferenced similarly to the CHS data, requiring a similar process of re-establishing the missing easting or northing map coordinate. The main difference is that the equations are much more numerous, given the non-linear nature of the ship tracks, as they are oriented in nearly all compass directions. This method of re-establishing the missing coordinate ('Profile coordinate recovery') resulted in positional accuracies better than ca. 30 m and thus well within the absolute navigational accuracy of most ship's tracks. With both eastings and northings of each measured bedform, wavelengths, heights, and symmetry could then be measured.

One shortcoming of the seismic compilation is that bedform-crestline orientation is only apparent. True orientation requires a correlation of individual features in the spreadsheet database with the bedforms mapped from CHS data (Fig. 2.5) or, where scales are appropriate, with existing sidescan data. This is possible through superimposing the database bedform ID on the bedform map thereby providing a correlation of height and wavelength with the larger bedform orientations. This is beyond the possibilities of this study because of time constraints. Nevertheless, spot observations at a wide variety of localities were conducted.

The relative precision and ultimate navigational accuracy of the CHS data set is lower in comparison with the seismic profile data set which is lower, in turn than the newer, more precise and accurate bathymetric data from multibeam sources.

3.1.3 Multibeam Bathymetry

Multibeam represents the present state-of the-art in bathymetric data collection. Survey techniques provide a rapid, accurate means of determining the morphology and nature of the sediments on the seafloor as it is capable of mapping at depths between 3 and 1000 metres below the transducer, and one ship's traverse provides bathymetric data along a swath up to seven times the water depth. Presently multibeam coverage on Sable Island Bank is limited to about 3.5 % percent of the area and this is not readily available for scientific analysis. For purposes of this project, multibeam data is utilized primarily to provide the best bathymetric control towards which the older CHS and GSCA seismic profiles can be compared.

3.2 G.I.S. Database

The spreadsheet format of the morphometrics database allowed ready incorporation of the data into a G.I.S. software package (ESRI ARC View ^{TM}) with only minor formatting adjustments. This allowed the data to be presented in a geographic sense, where trends such as size (height and/or wavelength), symmetry and water depth could easily be assessed. Although such trends were produced and used in this study, time constraints did not allow a full exploration of the obvious potential of the program.

3.3 Vibracore Data

3.3.1 Collection, location and handling

The cores used in this study were collected on BIO cruise HUDSON-2000-030A from July 13 to 21 2000. The sampling program involved detailed surficial sampling using shallow and large grab samplers, camera stations, and vibracores. Seven cores ranging in length from 42-183.5 cm, were recovered from nine attempts over three sand ridge-normal transects (Fig. 3.8, Table 3.1). Two transects, located in the Cohasset/Panuke (CoPan) hydrocarbon development area were positioned to study the ridge crest-normal surficial and internal variation at shallow (CoPan-1 transect) and relatively deeper water depths (CoPan-2 transect). Two cores were taken immediately south of Sable Island (South Sable transect) to study the mobility of the sand ridges by dating the cores using OSL. The exact positions for the core locations were chosen using seismic and multibeam bathymetric data collected and interpreted prior to coring so there positions relative to small scale (surficial) bedforms was known. Figures 3.9 and 3.10 are the Multibeam bathymetry images used to locate the core positions over the Copan and South Sable transects respectively.

Three core samples (61, 62, 63) were taken from the CoPan-1 transect. Core 61 probably reached the basal lag of this ridge. Core 62 apparently penetrated to the position of a reactivation surface (extrapolated) identified from seismic, but core 63 did not achieve sufficient penetration to reach the seismic target reflector (Fig. 3.11). Four cores were attempted along the CoPan-2 transect, (96, 97, 98, and 99) with only two of the cores (96 and 97) being successful. Core sample 98, and its second attempt, 99 were unsuccessful in penetrating an anticipated coarse sediment layer (lag) just below the

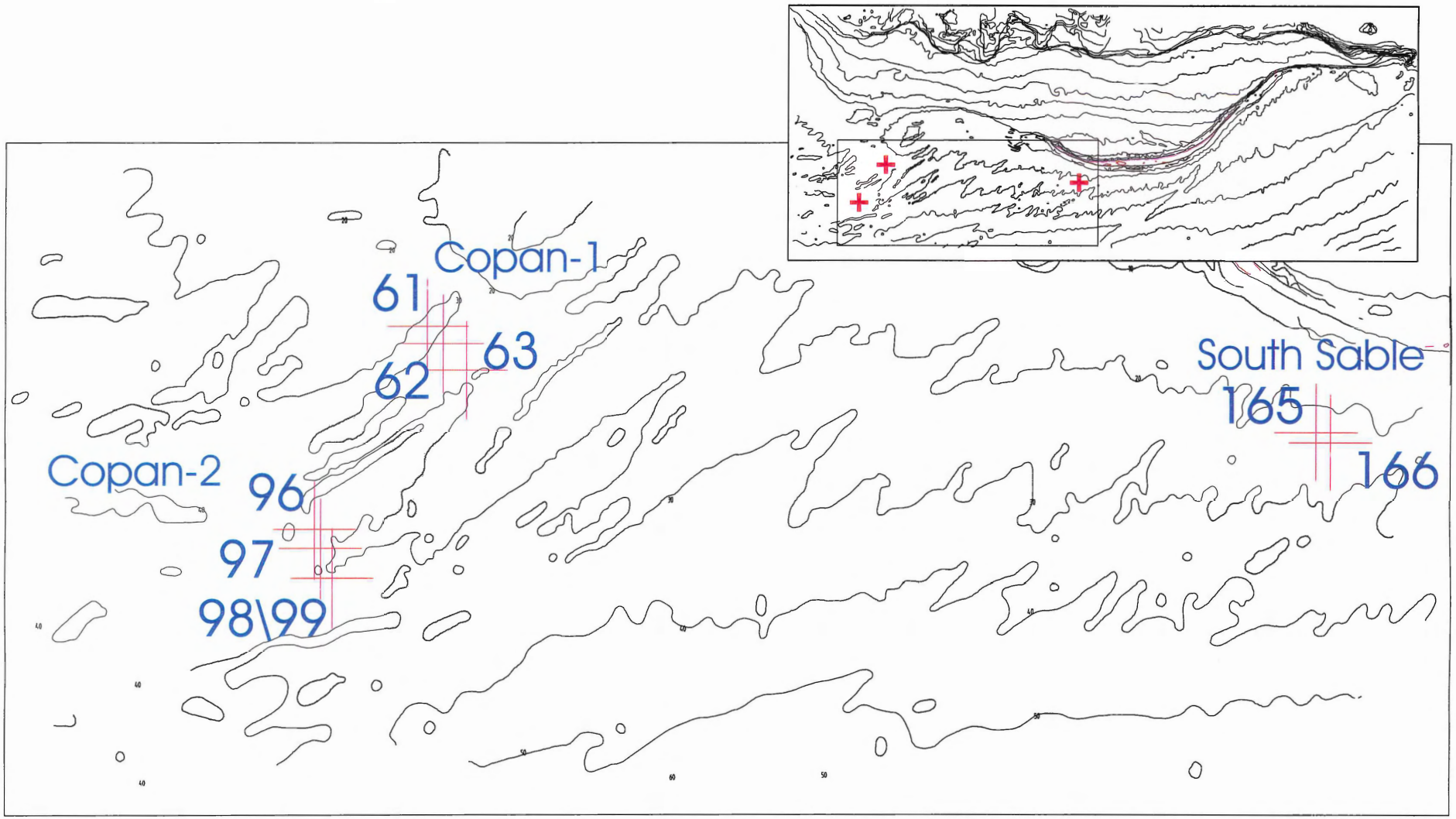

Figure 3.8. The positions across Sable Island Bank where vibracore samples were collected during B.I.O. cruise HUD-2000-30A. The geographical position (Latitude and Longitude), water depth, and length of each core are given in Table 3.1 (modified from King unpublished).

STATION NUMBER	LATITUDE	LONGITUDE	CORE LENGTH (cm)	WATER DEPTH (m)	GEOGRAPHIC LOCATION
61	43.947	-60.567	86	34	Scotian Shelf - Sable Island Bank - COPAN-1 Transect
62	43.9413	-60.559	87	29	Scotian Shelf - Sable Island Bank - COPAN-1 Transect
63	43.933	-60.547	48	26	Scotian Shelf - Sable Island Bank - COPAN-1 Transect
96	43.883	-60.630	168	38	Scotian Shelf - Sable Island Bank - COPAN-2 Transect
97	43.877	-60.627	60	33	Scotian Shelf - Sable Island Bank - COPAN-2 Transect
98	43.868	-60.621	0	38	Scotian Shelf - Sable Island Bank - COPAN-2 Transect
99	43.868	-60.621	0	38	Scotian Shelf - Sable Island Bank - COPAN-2 Transect
165	43.90	-60.095	126	24	Scotian Shelf - Sable Island Bank - South Sable Transect
166	43.899	-60.087	183.5	29	Scotian Shelf - Sable Island Bank - South Sable Transect

Table 3.1. Geographic position, location, water depth, and length of each vibracore sample taken during B.I.O. cruise HUD-2000-30A.

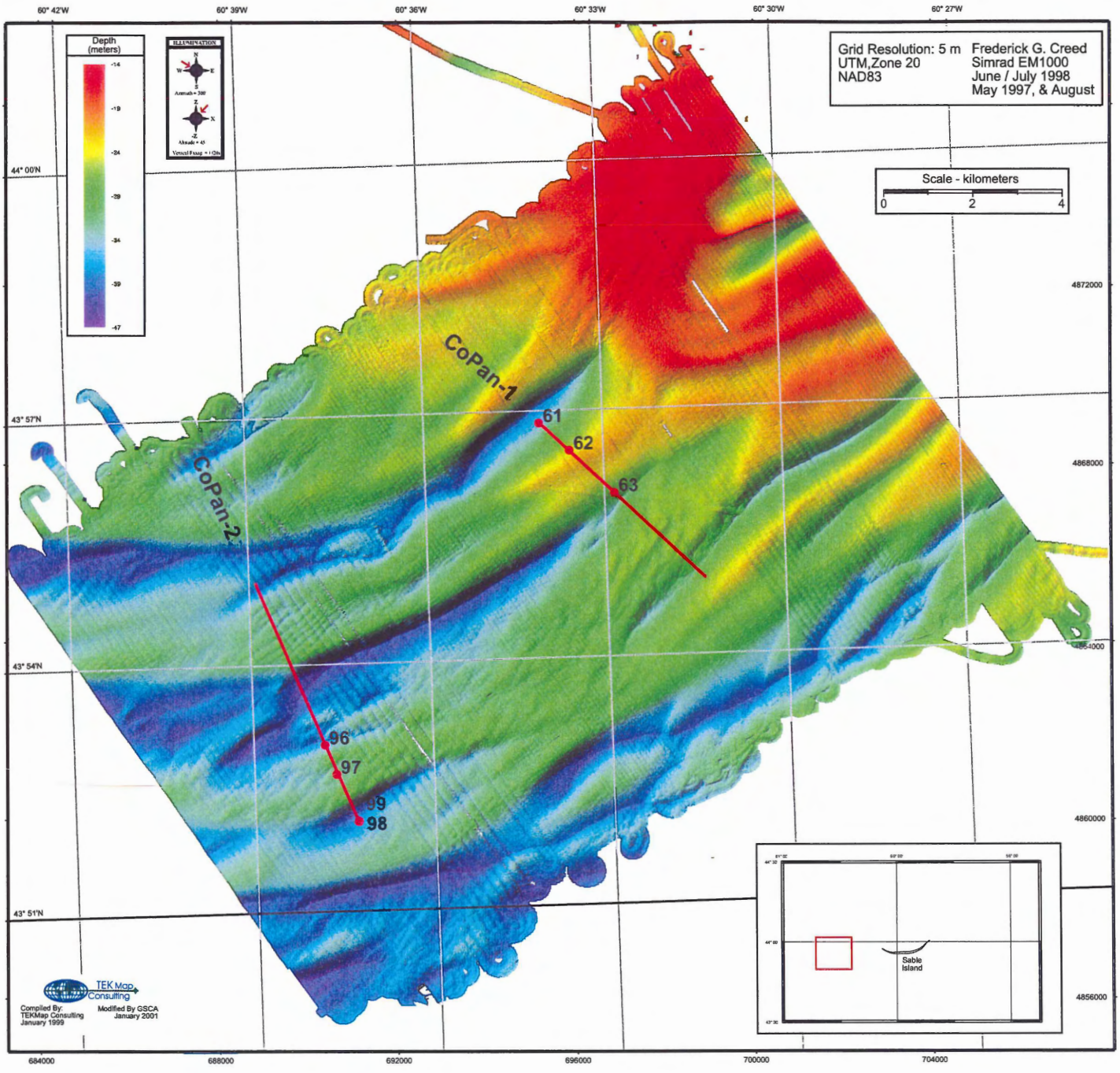

Figure 3.9. Multibeam bathymetric map where the vibracore sample locations for the Copan transects were chosen. The data was collected during B.I.O. Cruises Creed 96-501, Creed 97-090 and Creed 98-100 (Hudson 2000-30a unpublished cruise report).

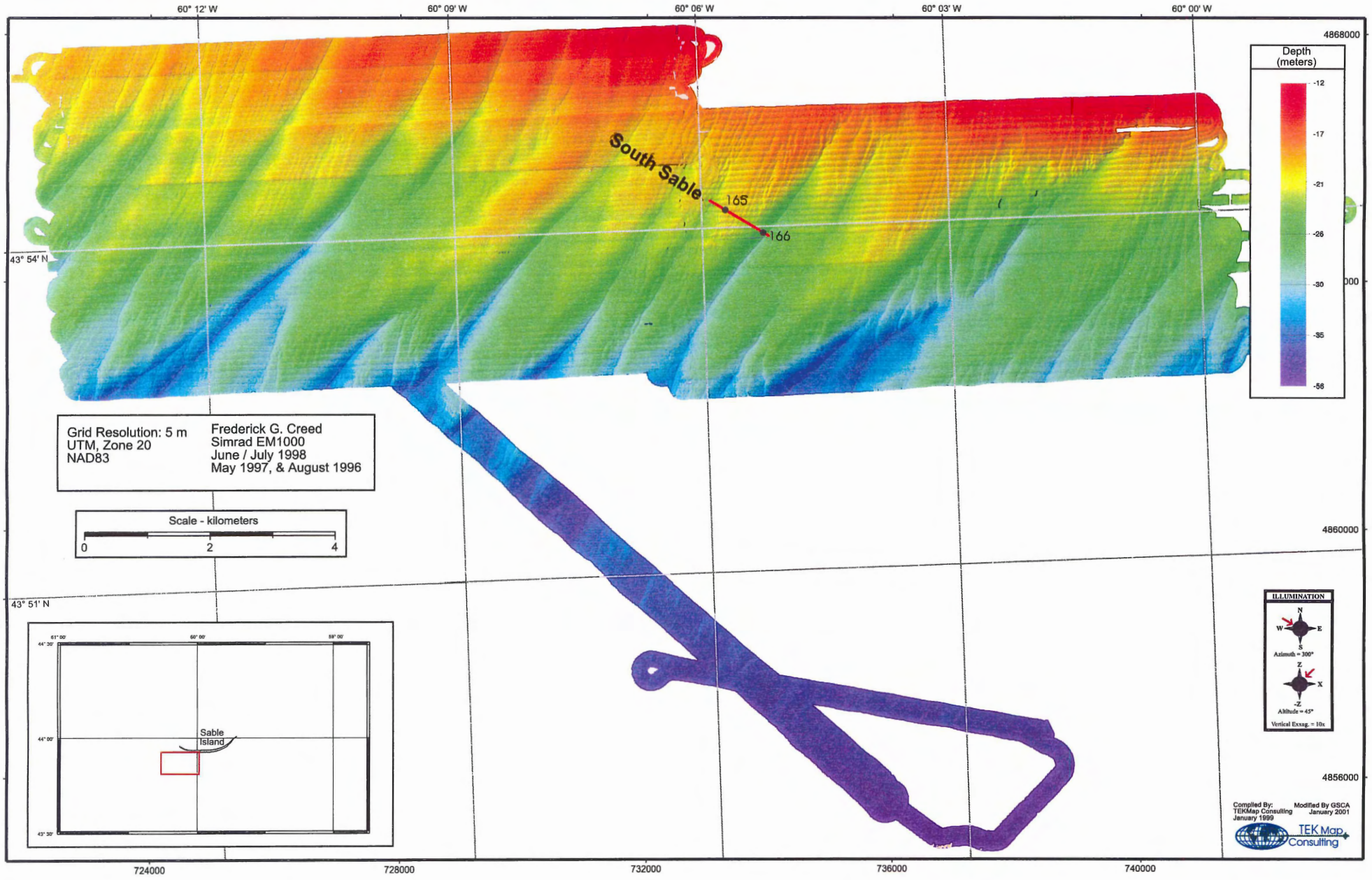

Figure 3.10. Multibeam bathymetric map showing where the vibracore sample locations for the South Sable transect were chosen. The data was collected during B.I.O. Cruises Creed 96-501, Creed 97-090 and Creed 98-100 (Hudson 2000-30a unpublished cruise report).

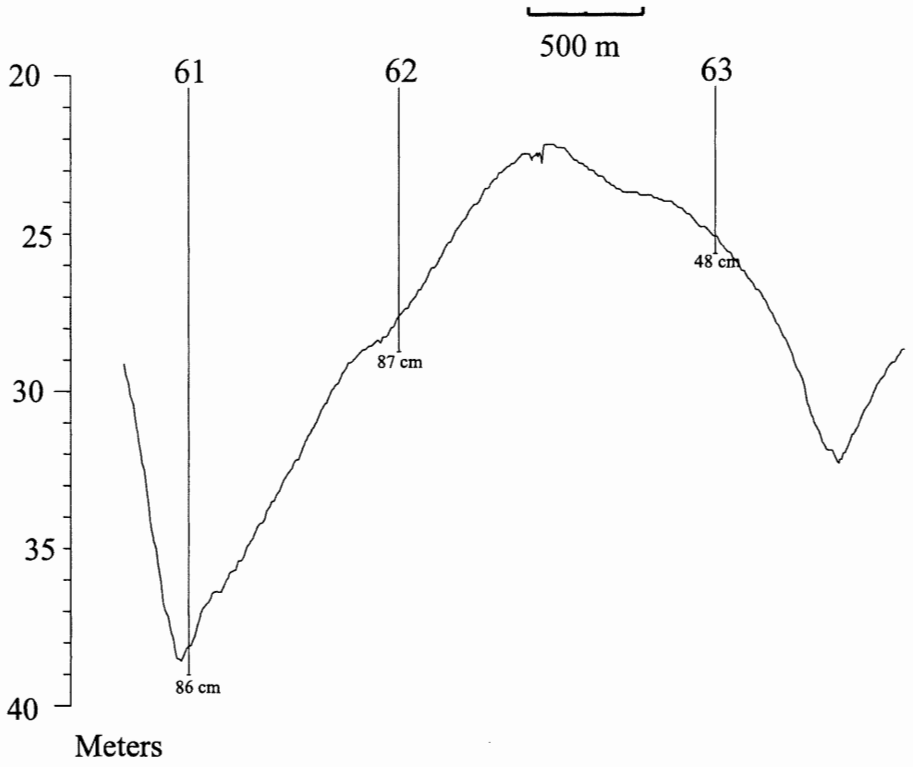

Figure 3.11. Positioning of the three vibracore samples taken over the CoPan-1 sand ridge transect. The sand ridge profile was generated using multibeam data collected on the 1996, 1997 and 1998 Creed cruises. The vertical scale is exaggerated 100X.

seabed at this location (Fig. 3.12). Two core samples were taken from the South Sable transect (165 and 166) with one (Stn. 166) reaching a depth of 183.5 cm bsf and penetrating the uppermost layer of a gravel horizon (Fig. 3.13). This horizon might represent the basal lag of this sand ridge however, no reflectors of the lag layer registered on the seismic data. During vibracoring, it is common for the cores to be disturbed due to the violent nature of the coring technique. The deformation present in most of the cores collected in this study consisted of flexing down of laminations around the edges of the core, and de-watering structures, formed as the sediments within the core liquefied and moved. The core results are discussed in more detail in chapter 4.

Plans to date the cores using OSL techniques required them to remain unexposed to light, which required extra care while handling and transporting them. They were wrapped with an opaque plastic wrap after being extracted from the vibracorer to protect them during the remainder of the cruise and while transporting them into the BIO storage refrigerator. Before being split (longitudinally along the mid-point), the cores were taken into a dark room, where the opaque wrapper was removed and the cores wrapped with duct tape. To ensure the least amount of light possible penetrated the core while being split, the cut lines were re-taped as the splitter blades passed. Protecting the cores from light also created inconvenience during the core sub-sampling, sketching and photography. The cores (working and unaltered archive halves) and OSL sub-samples will remain in cold storage at the BIO, GSCA core repository. All additional sub-sample remnants have been returned for indefinite storage at the BIO repository. The core and sub-sample analysis, and some results have also been submitted for inclusion in the

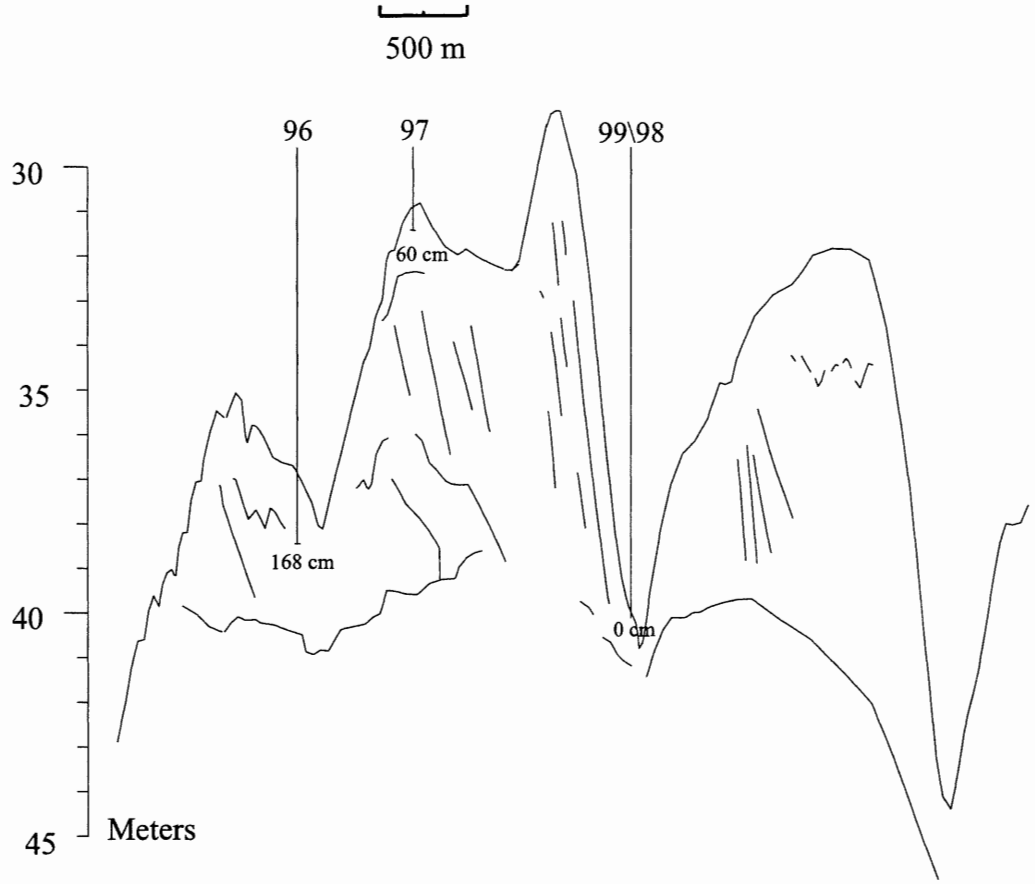

Figure 3.12. Positioning of the two successful (96 and 97) and the two unsuccessful (99 and 98) vibrocore samples taken over the CoPan-2 sand ridge transect. The sand ridge profile was generated using seismic data collected during B.I.O. cruise HUD-2000-30A.. The vertical scale is exaggerated 100X.

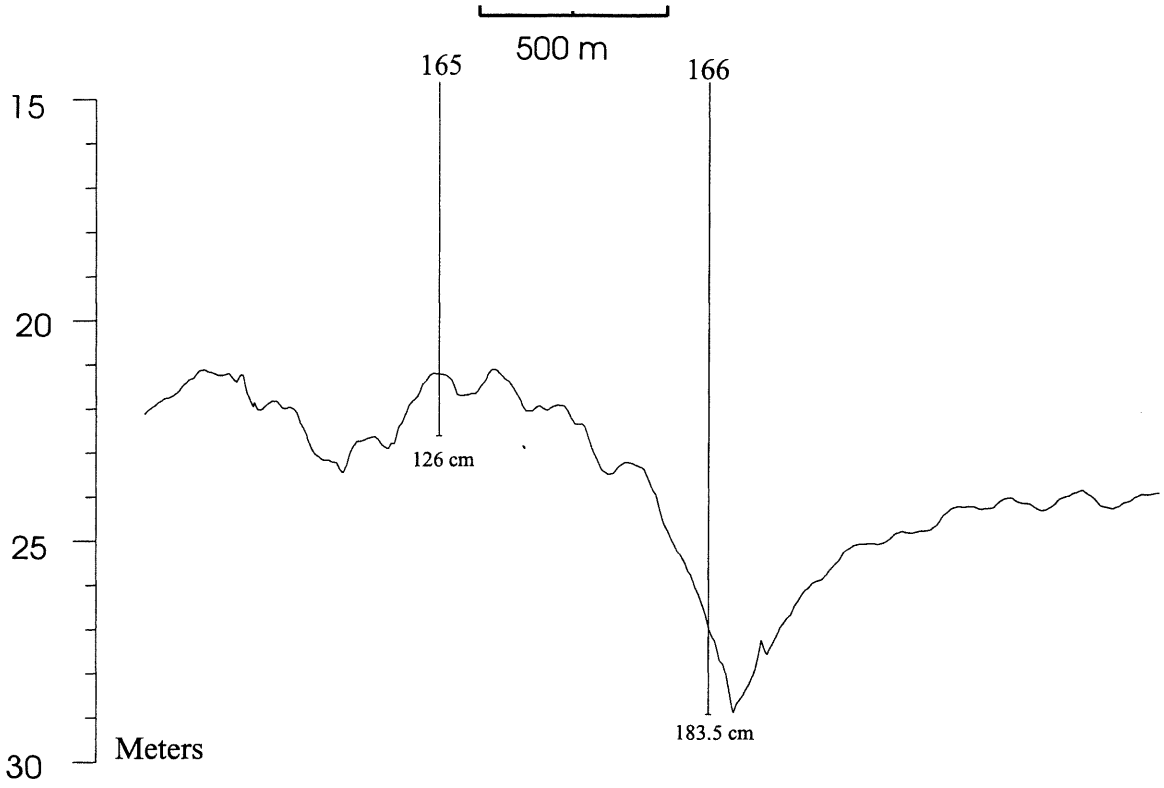

Figure 3.13. Positioning of the two vibracore samples taken over the South Sable sand ridge transect. The sand ridge profile was generated using multibeam bathymetric data collected during B.I.O. cruise HUD-2000-30A. The vertical scale is exaggerated 100X.

GSCA database. These database holdings are available at http://agc.bio.ns.ca/ED/GSC/ed-f-menu.cgi.

3.3.2 Core analysis techniques

The working halves of the cores were sub-sampled for OSL and grainsize analysis in the BIO dark room and the archive halves were used for sketching and photographing. When it was certain that a sufficient number of OSL subsamples had been obtained (for present analysis as well as for future studies), the cores were exposed to light and prepared for resin peels. Resin peels are a common sedimentologic field technique here adapted to cores. The core is draped with two layers of cheesecloth and an epoxy resin and hardener mixture is poured on top. The mixture penetrates the sediment differentially according to permeability, hardens, and when removed, reveals greatly enhanced sedimentary structure. Although peeling core samples is not standard practice, as it is very destructive to the sample, both the Dalhousie University, and BIO x-ray machines were out of service at the time, and as the sandy cores began to dry they developed fractures which would have reduced the quality of data that could be obtained through x-ray analysis. The peel technique was very successful, with results far superior to x-ray, revealing well-defined sedimentary structures that were faint or not visible prior to peeling. These were then digitally photographed and are presented alongside the core photographs in figures 4-12 to 4-18.

The subsamples taken for grainsize analysis averaged 43.44 grams and composed of sand with little or no silt, which made dry sieving the preferred method of analysis. The subsamples were dried at 40 ^{o}C for 24 hrs and sieved at half phi intervals from

-1ϕ (2mm) to 4ϕ (60um). Each grain size interval from every sample was weighed to an accuracy of 3 decimal places, and has an error of +/- 0.005 g. Grainsize distribution results (weight percent) are presented graphically alongside the core photographs (Figures 4-12 to 4-18)

Chapter 4: Results

4.1 Morphometrics Database

4.1.1 CHS Bathymetry Data

Using the CHS bathymetry data, 997 bedforms were identified and measured over 108 profile lines across eastern Sable Island Bank. The geographic coordinates of the profile lines were georeferenced, allowing the locations of each measured bedform to be plotted on a regional map. Figure 4.1 shows the locations and distribution of the ridge crests of each bedform measured using the CHS bathymetry data. Table 4.1 is a summary of the bedform sizes from the data and the water depth they occur in.

CHS bathymetry data

	Average	Max.	Min.
Wavelength (m)	1349.52	12644.00	131.00
Height (m)	1.84	16.00	0.20
Water depth (m)	37.77	118.70	2.80

Table 4.1. Summary table of bedform height, wavelength and water depth results from the CHS bathymetry database.

The wavelengths of sand ridges measured from the CHS bathymetry data vary from 12,644 m to 131 m, but the majority of the ridges are between 1300 m and 1500 m (Fig. 4.2). The heights of the sand ridges vary from 16 to 0.20 m high, but the majority of ridges are close to one meter (Fig. 4.3). Using the bedform size boundaries defined by Amos and King (1984), a plot of the measured bedform wavelength vs. height place almost all the bedforms into the sand ridge category (Fig. 4.4), with little distribution outside the zone.

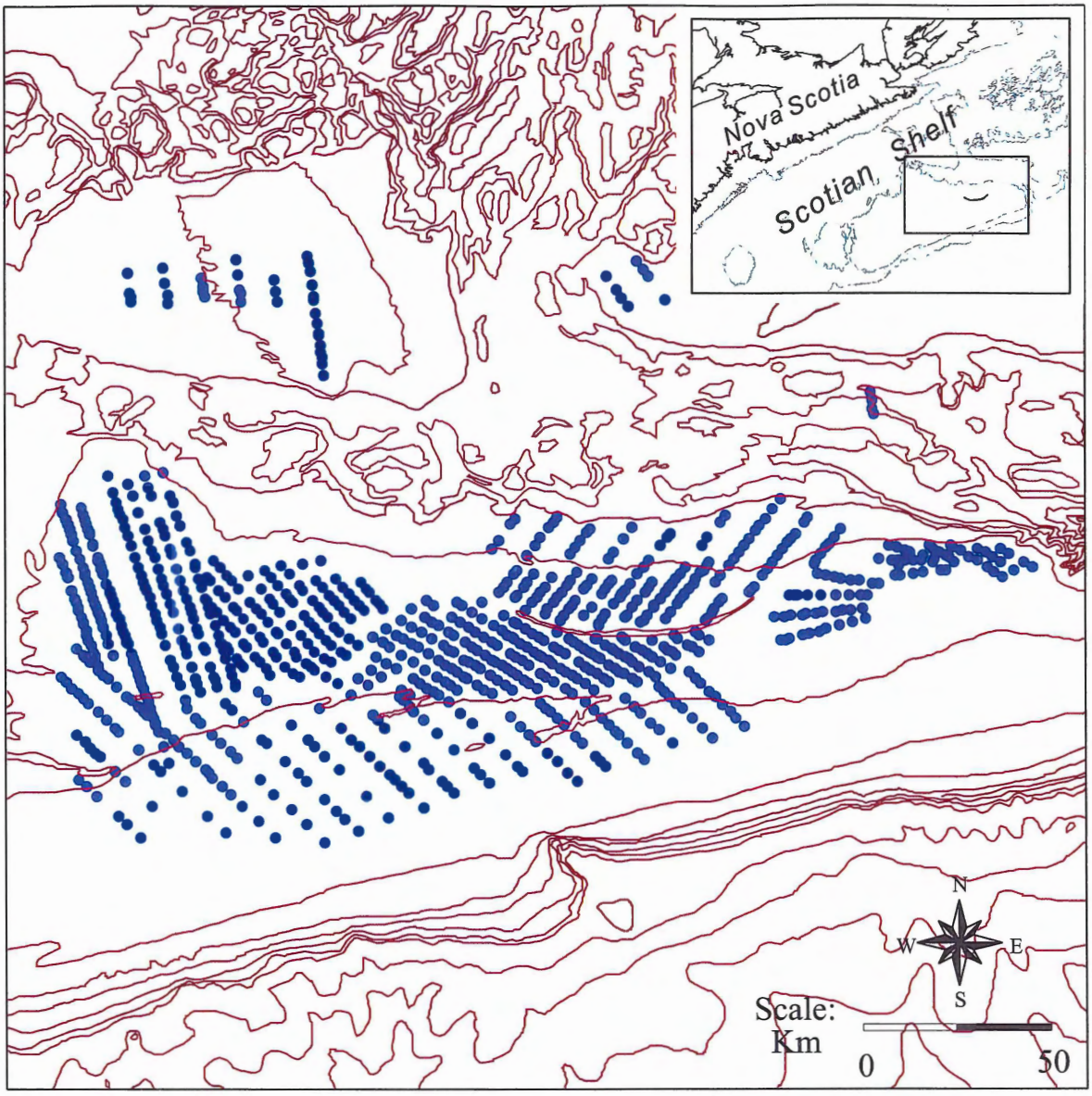

Figure 4.1. Geographic locations of the measured bedforms from the CHS Bathymetry data. Each point on the map identifies the location of a ridge crest.

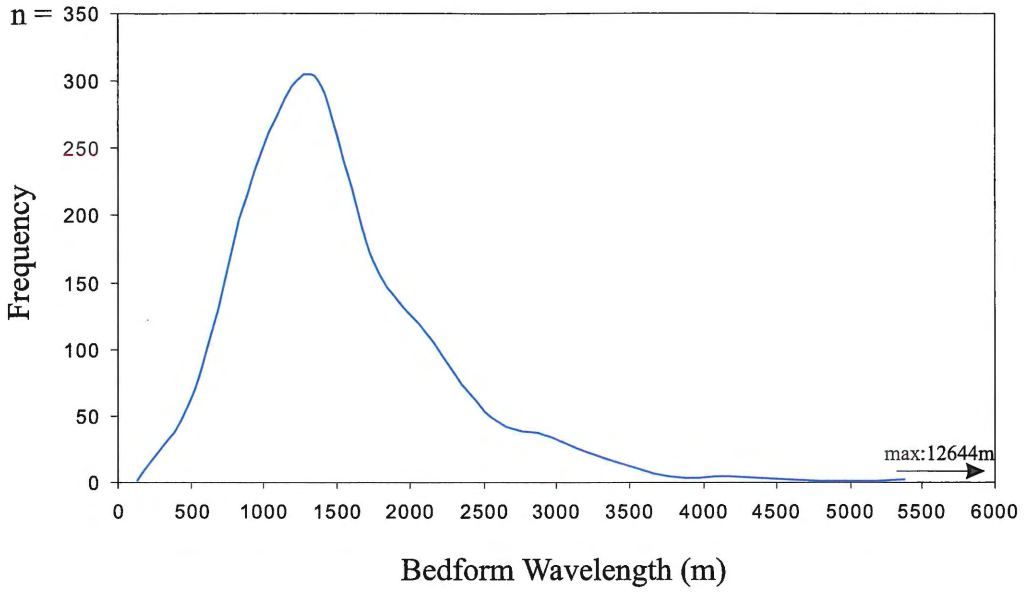

Figure 4.2. Plot of the wavelength distribution of the measured bedforms. The most common bedform sizes are between 1000 and 1750 m long.

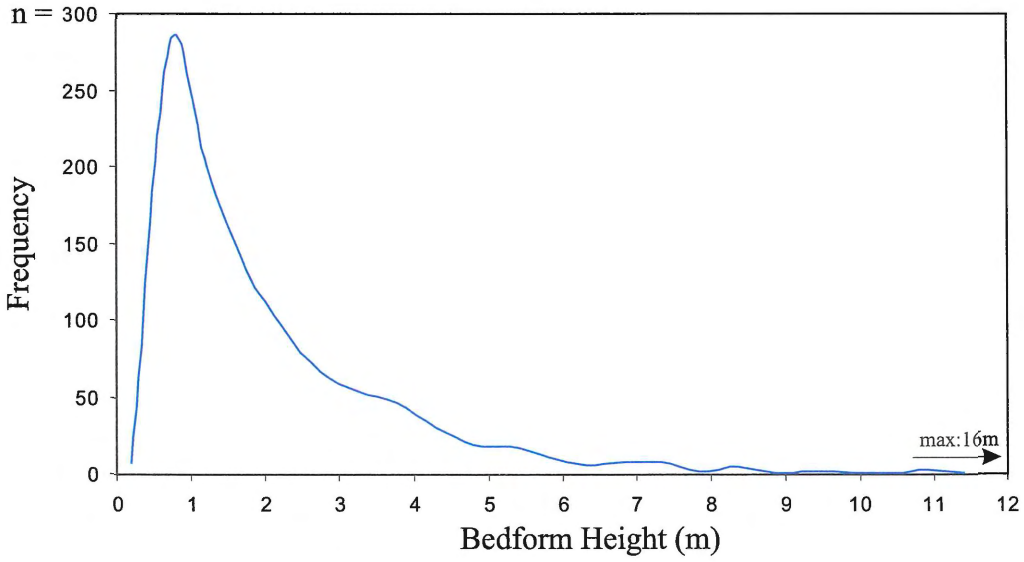

Figure 4.3. Histogram of the height distribution of the measured bedforms. The most common bedform height is close to one meter high.

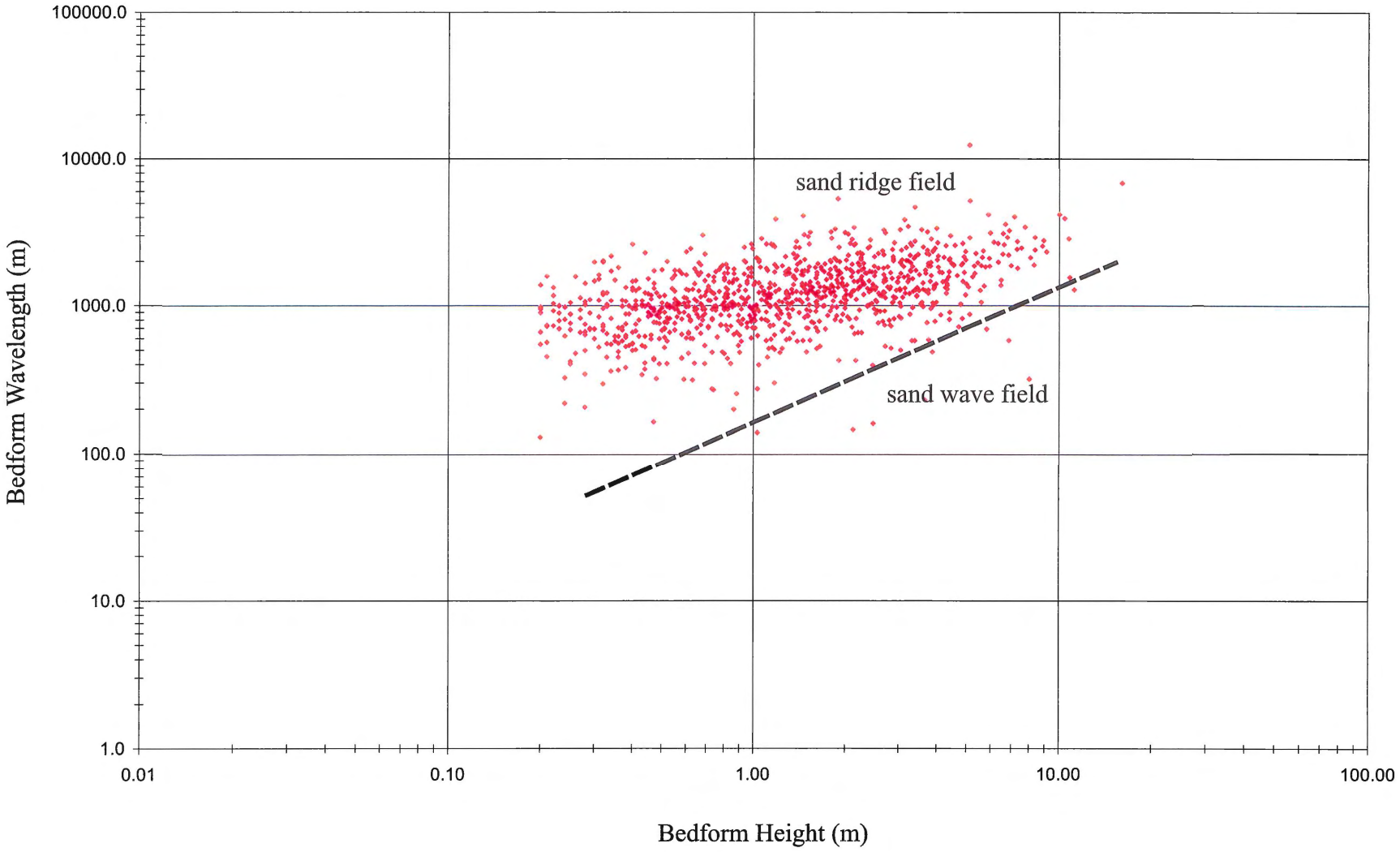

Figure 4.4. Bedform wavelength vs. height from the CHS data. Using the bedform zone boundaries defined by Amos and King (1984), almost all of the bedforms measured fall into the sand ridge field. Although ridge heights less than 0.20 m were measured, it is unlikely that bedforms of that size were resolved by CHS bathymetry. Any heights less than 0.20 m were therefore considered to be artefacts created during the data processing, and were omitted from the database. The sharp cut off of data points at < 0.20 m is caused by the removal of these values.

The symmetry of the sand ridges is plotted in Figure 4.5. The curve is centred over a symmetry of one, which shows there is no preferred asymmetry to the bedforms measured, as the majority are close to being symmetric, and an equal number of bedforms are asymmetric to the east as there are to the west.

4.1.2 Seismic Data

Using the GSCA seismic data, 5873 bedforms were identified from 172 profile lines across eastern Sable Island Bank compiled from 10 different cruises. As with the CHS bathymetry data, the geographic coordinates of the profile lines were georeferenced, allowing the locations of each measured bedform to be plotted on a regional map. Figure 4.6 shows the locations and distribution of the ridge crests of each bedform measured from the seismic data. Table 4.2 is a summary of the bedform sizes from the data and the water depth in which they occur.

Seismic data

	Average	Max.	Min.
Wavelength (m)	620.00	33898.54	28.21
Height (m)	1.04	32.68	0.10
Water depth (m)	47.22	175.30	8.65

Table 4.2. Summary table of bedform height, wavelength and water depth results from the Seismic database.

The wavelengths of sand ridges measured from the seismic data vary from 33,898 m to 28.21 m, but the majority of the ridges are close to 500 m long (Fig. 4.7). The heights of the sand ridges vary from 32.68 m to 0.10 m high, but the majority of ridges range in height from 0.75 to 1 m (Fig. 4.8). The plot of measured wavelengths vs. height

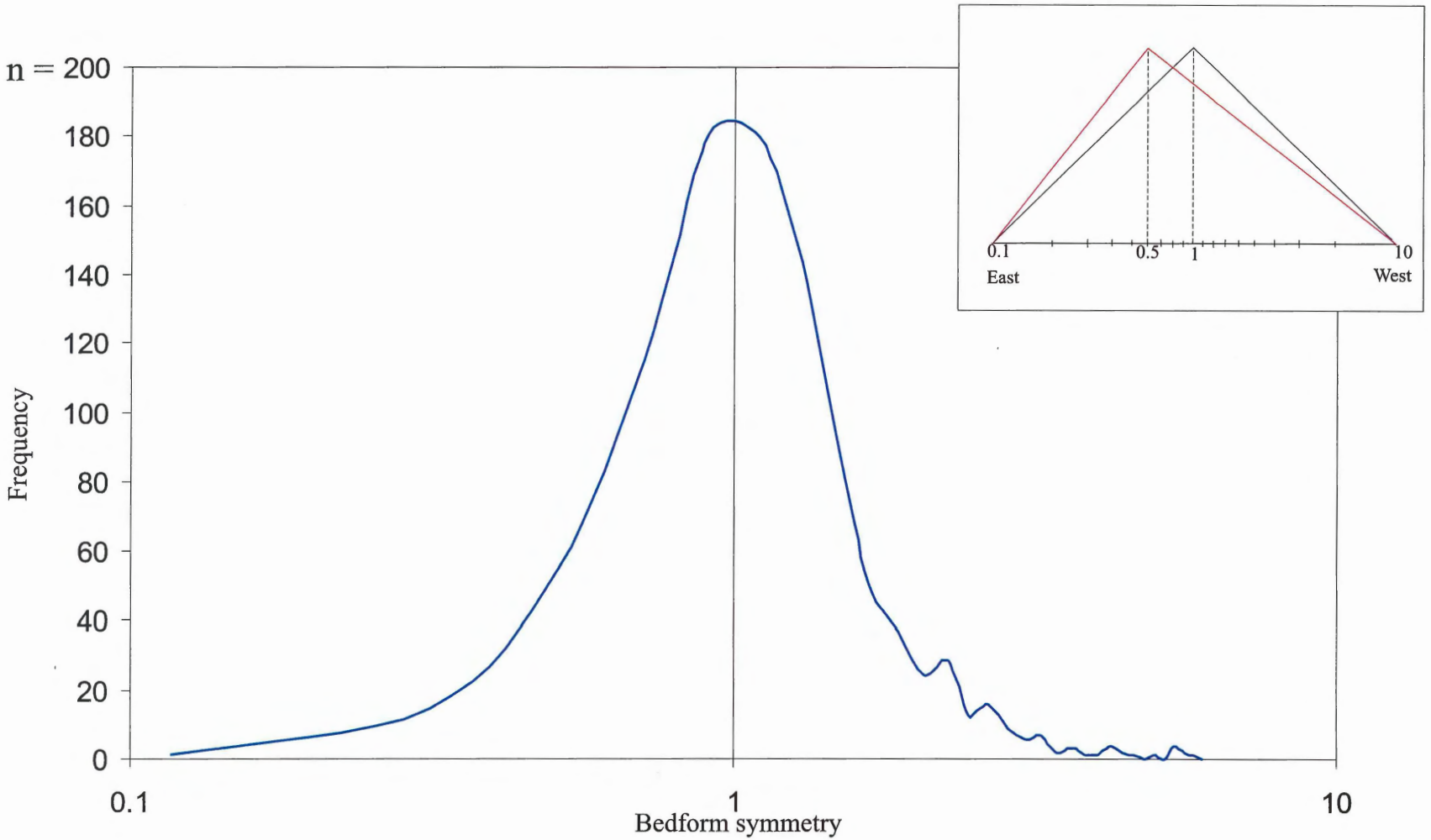

Figure 4.5. Bedform symmetry measurements from the CHS database. A bedform with a symmetry less than one is positively skewed (asymmetric to the east), where as a symmetry greater than one is negatively skewed (asymmetric to the west). The inset (top right) is a schematic illustration of a bedform that has a symmetry value of 0.5, and is therefore asymmetric east.

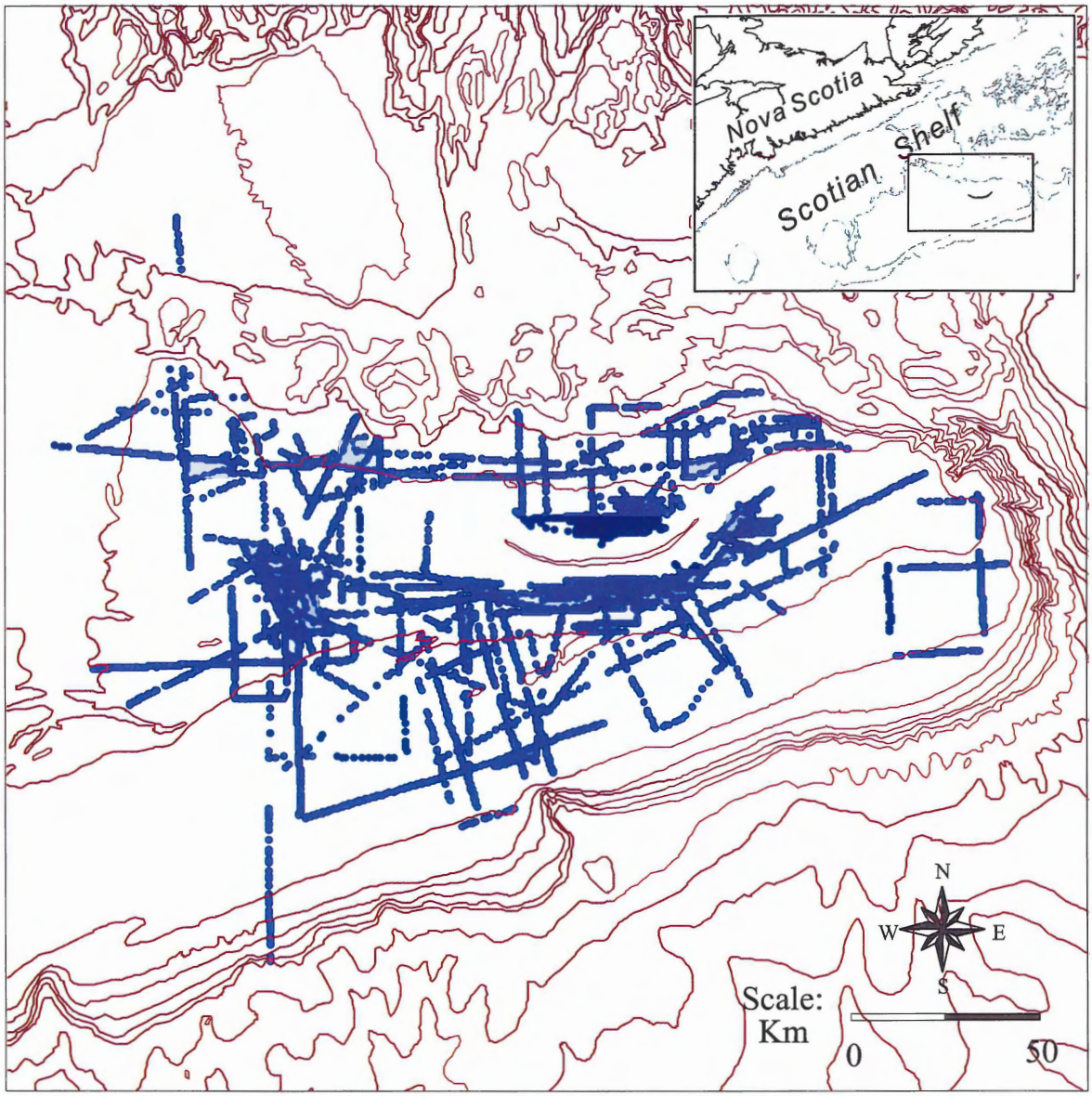

Figure 4.6. Geographic locations of the measured bedforms from the seismic data. Each point on the map identifies the location of a ridge crest.

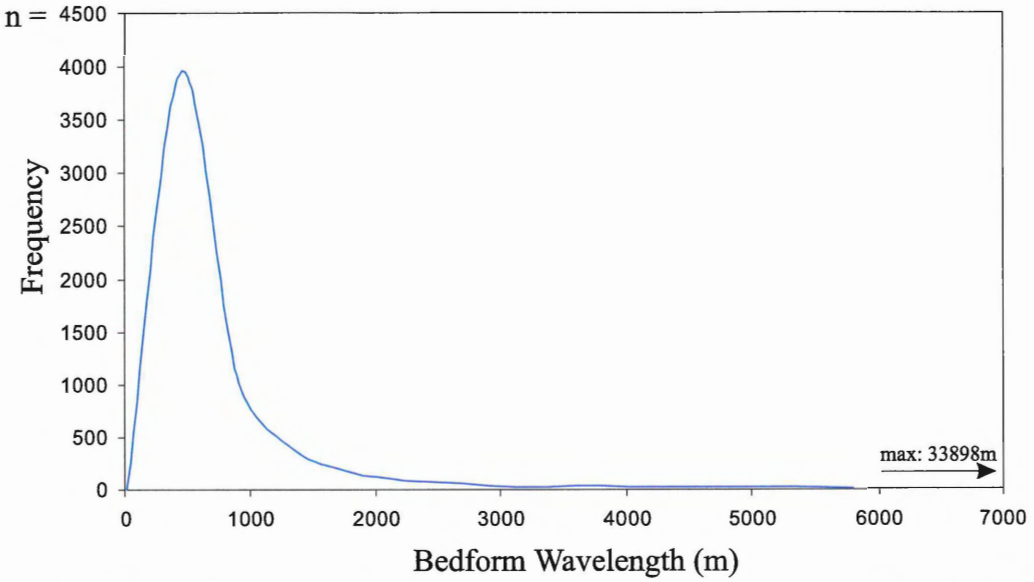

Figure 4.7. Histogram of the wavelength distribution of the measured bedforms. The most bedforms are close to 500 m long.

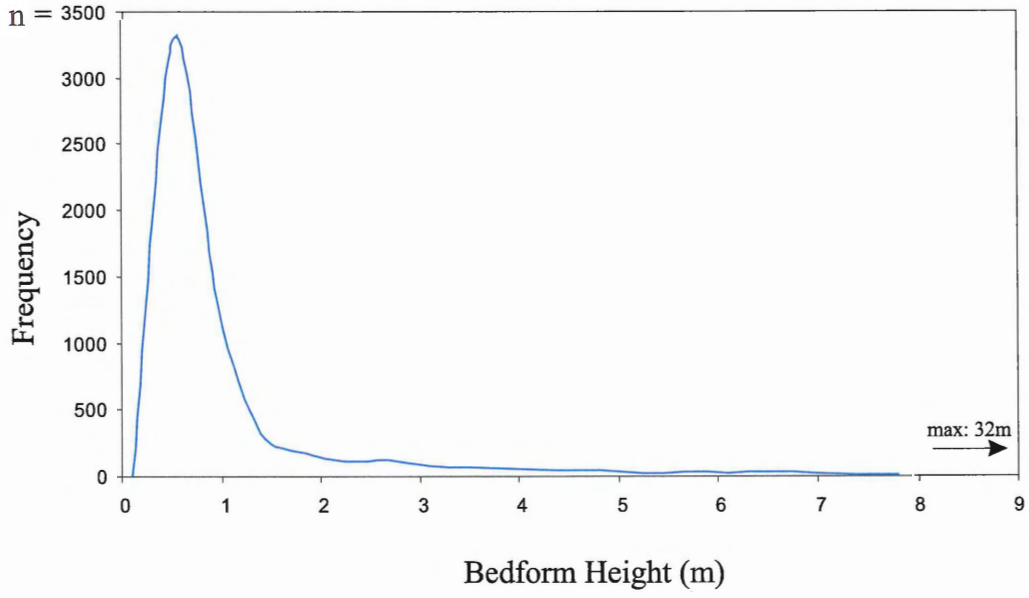

Figure 4.8. Histogram of the height distribution of the bedforms measured from the seismic data. Most of the bedforms are between 0.5 - 1.0 m high.

place almost all the bedforms measured into the sand ridge category (Fig. 4.9), with little distribution outside the zone. The symmetry of the sand ridges is plotted in Figure 4.10. The graph shows that the majority of sand ridges are slightly asymmetrically skewed to the east (symmetry value of 0.7).

4.1.3 Summary Comparison of CHS bathymetry and Seismic Results

Both CHS bathymetry and seismic data cover a significant portion of eastern Sable Island Bank. The CHS bathymetry data is more uniformly distributed over the study area but it is has fewer measured bedforms than the seismics, which has a less organized distribution of a larger number of measured bedforms (Fig. 4.1 and 4.6). The CHS bathymetry data, which can be collected using smaller ships that draw less water, has measured bedforms much closer to Sable Island than the seismic data, which needs deeper water to tow the seismic gear behind the ship.

The size range of both the wavelength and height of the bedforms in the CHS bathymetry and seismic data also differ. The average bedform size measured from CHS bathymetry data is larger than that of the seismic data, and the range between the max and min wavelength and height is smaller than that of the seismic data (Table 4.1 and 4.2). The most frequent wavelength and height measured from the CHS bathymetry data is 1341 m and 0.70 m respectively (Fig. 4.2 and 4.3), while the most frequent wavelength and height measured from the seismic data is 453 m and 0.52 m respectively (Fig. 4.7 and 4.8). These differences are caused by the differences in resolution, and style of data being collected between the two of data sets. The seismic data has a smaller resolution than CHS bathymetry, enabling smaller bedforms that would be missed by CHS

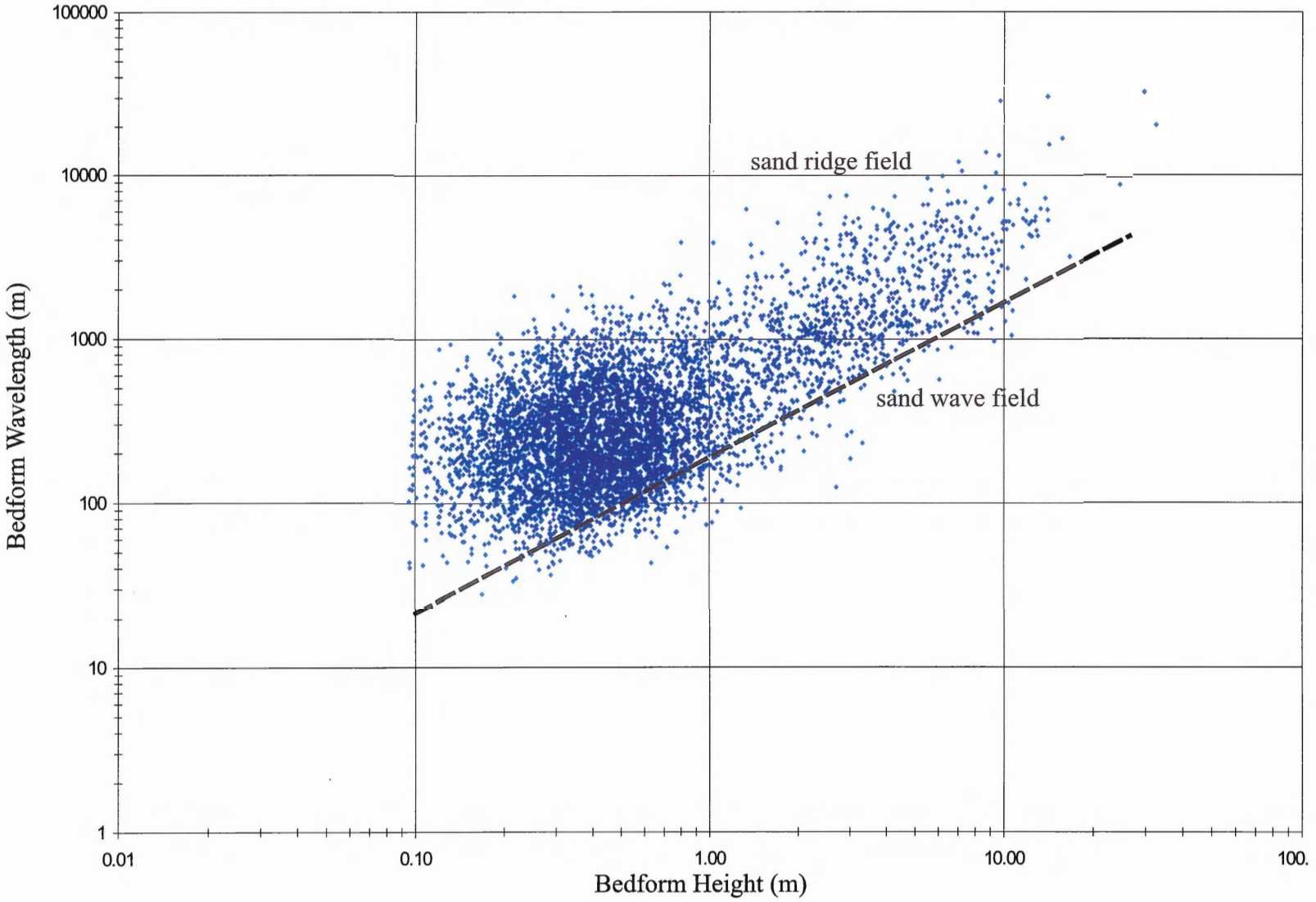

Figure 4.9. Bedform wavelength vs. height from the seismic data. Using the bedform zone boundaries defined by Amos and King (1984), almost all of the bedforms measured fall into the sand ridge field. Although ridge heights less than 0.10 m were measured, it is unlikley that bedforms of that size were resolved by seismics. Any heights less than 0.10 m were therefore considered to be artifacts created during the data processing, and were omitted from the database. The sharp cut off of data points at < 0.10 m is caused by the removal of these values.

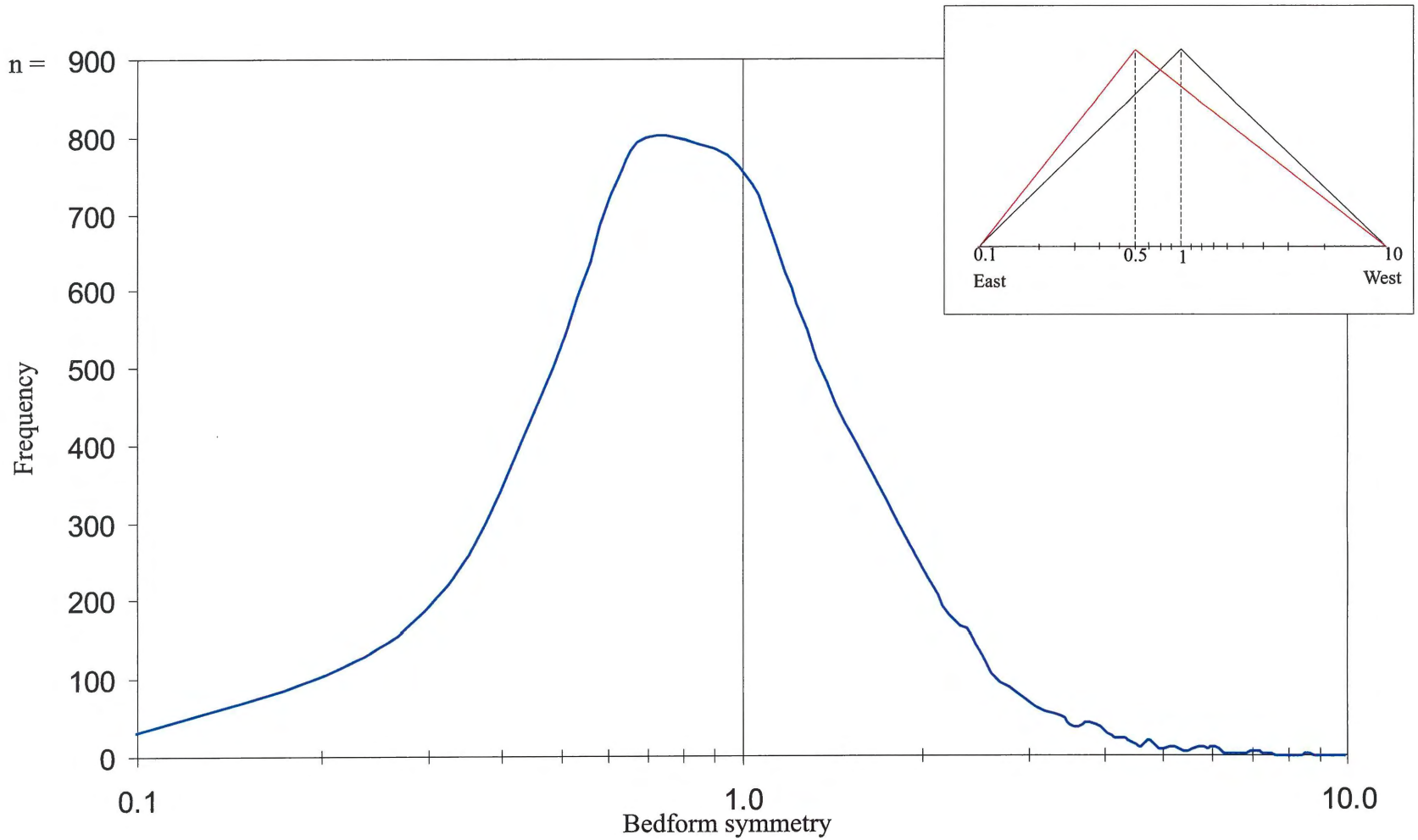

Figure 4.10. Bedform symmetry measurements from the seismic data. A bedform with a symmetry less than one is positively skewed (asymmetric to the east), where as a symmetry greater than one is negatively skewed (asymmetric to the west). The inset (top right) is a schematic illustration of a bedform that has a symmetry value of 0.5, and is therefore asymmetric east.

bathymetry to be resolved. The CHS bathymetry data would not only miss smaller bedforms, but may also combine a of smaller bedforms as being only one. Using the internal reflectors resolved by the seismic data as a guide, the bedforms could be measured more accurately, and larger sand ridges with bedforms superimposed on top of them could also be measured. This accounts for the larger scale wavelengths and heights in the seismic data compared to the CHS bathymetry data, where larger ridges weren't resolved past the surface most bedforms. Figure 4.11 is a plot of wavelengths vs. heights for both CHS bathymetry and seismic data (composite of Fig. 4.4 and 4.9). The plot shows that the bulk of the measured bedforms from the CHS bathymetry data are larger than the bulk of the bedforms measured from the seismic data. The majority of the seismic bedforms fall between wavelengths of 100 m to 1000 m and heights of 0.2 m to 0.7 m. Most of these bedforms are superimposed, surface bedforms and would be the same bedforms as those identified using the bathymetry data. (as opposed to the larger, deeper sand ridges with superimposed bedforms, that bathymetry data wouldn't pickup). This helps to illustrate that the accuracy of the two sampling techniques (CHS and seismic) is different, giving different sized bedforms. Seismic data is also able to resolve smaller bedforms, as well as larger, buried ones, giving a larger range of data points.

4.1.4 Regional Summary

The seismic data is more accurate, and complete than the CHS bathymetry database, so for plotting the bedform trends across Sable Island Bank, only the seismic data are used.

The bulk of the ridges (height 0.2 - 0.7 m; wavelength 100 – 600 m) are distributed across the study area. Most noticeably, the majority of the sand ridges on the

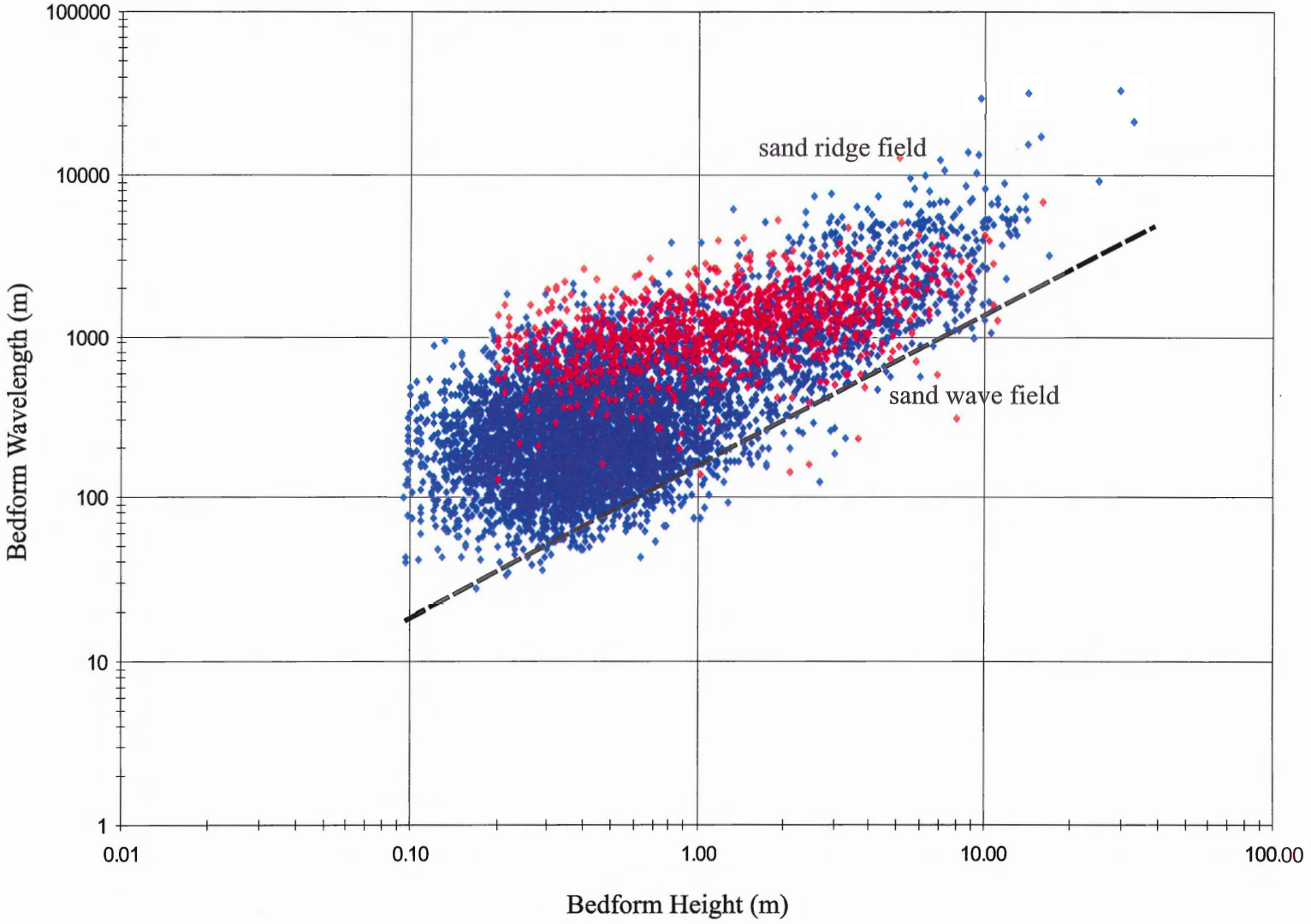

Figure 4.11. Comparison plot (wavelengths and heights) of seismic (blue) and CHS bathymetry (red) data.

eastern side of the study area and on the northern side of Sable Island are within this range. Sand ridges of this size are also present on the southern side of Sable Island, but they are mostly superimposed on larger sand ridges. The distribution of sand ridges with heights larger then 1m and wavelengths larger than 1000m are noticeably reduced east of the Harcourt-Cameron ridge on the eastern and northern side of Sable Island, and are most abundant in the southern and west side. With increasing sand ridge size, the number of ridges across the entire bank is reduced, but there are far more present on the western than on the eastern and northern sides of the island. Ridges with sizes greater then 10 m high and 5000 m long are almost exclusively on the western side of Sable Island, with the exception of a few on the north and eastern side, and the Harcourt-Cameron Ridge.

The majority of the sand ridges across the bank are symmetric, or close to symmetric, and are spread evenly through the full range of ridge sizes across the ridge field. Apart from the majority of the ridges being symmetric, little organization, and no preferred orientation is noticeable. Interchanging between positive, negative, or close to symmetric occurs in a random fashion along the same ridgeline, or parallel group of ridges. The degree of to which they are skewed also has little preferred geographic location, or ridge size. Longer and higher sand ridges have the same amount of symmetry variability as the smaller ones, and are randomly situated throughout the study area.

4.2 Vibracore Analysis

4.2.1 Core Descriptions and Initial Interpretation

Photographs of the seven cores collected, the resin peel photographs, grainsize analysis results, and a sketch highlighting the dominant features of the core are presented in figures 4.12 to 418. During the processing of the cores, the archived halves were photographed while the working halves were resin peeled. When the cores were originally split, not all the cores split evenly, leaving more sand at the top or bottom of one half of the core than the other. This causes small discrepancies in core length when the cores and peels are presented next to each other in the figures. The missing sections of the resin peels in the figures are from sub-samples taken for grainsize analysis of the cores (this study) and for OSL dating (GSCA study). The darker patches on the sides of some of the missing sections are shadows, which were cast from the flash of the camera as the peels were being photographed, by objects used to fill the spaces created as sediment was removed during sub-sampling, to prevent any further damage to the cores.

Core 2000-30A-61

Vibracore 2000-30A-61, from the Copan-1 transect, west of Sable Island (Fig 3.1, 3.2), was cored from the stoss-side trough of a sand ridge in 34 m of water, and has a length of 86 cm (Table 3.1, Fig. 3.2, 3.4). Two sand units are present in the core (Fig. 4.12), which are separated by a sharp horizon at a depth of approximately 60 cm. The top 26 cm of the lower unit was recovered, which is present from the bottom of the core (86 cm), to approximately 60 cm, and contains structureless, medium sand (1.5 – 2 ϕ). The exact depth of the unit horizon is difficult to pinpoint due to the deformation during

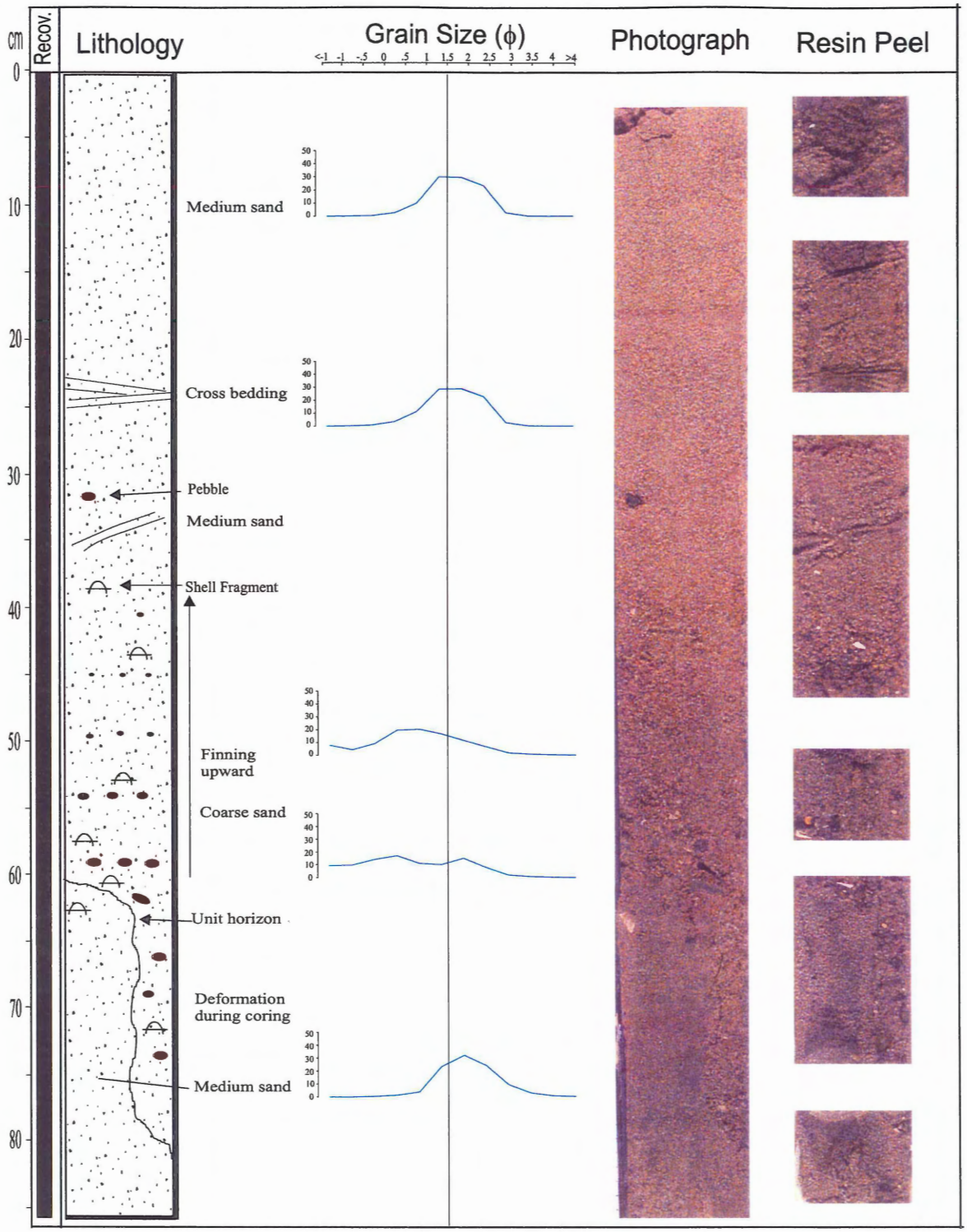

Figure 4.12. Vibracore 2000-30A-61. Cored from the bottom, stoss side of the Copan-1 transect sand ridge. The column on the left side is a sketch of the core, illustrating the lithology and dominant features. The plots in the center are grain size results for the corresponding depths. The two columns on the right side of the page are photographs of the core (left) and the resin peel (right). The white patches in the resin peel photographs are where sub-samples were extracted for the grain size anaysis. The core depths are of the far left side of the figure. Figures 4-13 to 4-18 follow the same layout.

coring. The unit horizon between the bottom and upper sand body in core 2000-30A-61 has most likely been deformed during coring, with the lower unit being sucked up, and the upper unit sucked down. The upper unit in the core is present from approximately 60 cm to the top of the core. The base of the unit consists of a coarse sand (0.5 – 1 ϕ) and shell lag in a medium sand (1.5 – 2 ϕ) matrix, which fines upward from 60 cm to 40 cm, were medium sand prevails. The unit is mostly structureless over its entire length, with the exception of dipping parallel laminae at 35 cm and cross beds at 25 cm (Fig. 4.12).

The lower stoss side of the sand ridges typically have coarse sand or a gravel lag at the seabed, as it is the erosional side of the sand ridge. This is not the case for this core where medium sand is present at the surface. It is unlikely that the sand ridge has migrated a significant amount since the multibeam image used to choose the core locations (Fig. 3.2) was compiled (1997-1998), for the sand wave to have migrated close to a full wavelength to have sampled the depositional (lee) side of the sand ridge. The fining upward sequence within the upper unit is most likely the result of a waning storm deposit, followed by megaripple migration, forming the minor structures (cross beds) in the core. It is possible that an occasional mobile layer in excess of 50 cm has migrated across the trough of the sand ridge over the past two or three years and is sitting on top of the stoss lag layer, which is what was cored. Multibeam data was collected over the area during B.I.O. cruise HUD 2000-30A but has not been analysed, causing speculation as to why the stoss lag wasn't cored until the new data is available

Core 2000-30A-62

Core 2000-30A-62 (Fig. 4.13) was collected from the middle-stoss side of the same sand ridge where core 2000-30A-61 was collected. The water depth at this location was 29 m, and the length of core recovered was 87 cm (Table 3.1, Fig. 3.2, 3.4). The sharp color change at 21 cm in Figure 4.13 is a processing artefact formed during the manipulation of the digital images. Two units are present in the core. The top 37 cm of the lower unit was recovered, from the base of the core (87 cm), to 50 cm. The recovered section of this unit consists of medium sand (1.5 ϕ) with very faint laminae at 55 – 65 cm. The unit boundary (50 cm) is sharp, and defined by the thin lag horizon of very coarse sand, small clasts and shell fragments, making up the bottom five centimetres of the upper sand unit. The horizon has also been warped downward during coring. The upper unit fines upward from 50 cm (lag horizon) to 40 cm, where medium sand (1 – 1.5 ϕ) dominates, and continues to the top of the core. Dipping laminae are present from the base of the unit to 20 cm from where the sediment has been disturbed from bioturbation or during coring and handling (Fig. 4.13).

The lower unit present in the core could represent the body of the sand ridge, over top of which the mobile zone migrates. The dipping laminae and the fining upward sequence within the upper unit most likely represents a single depositional event, such as passing of megaripple during a storm, or the migration of a sand ribbon across the stoss side of the ridge.

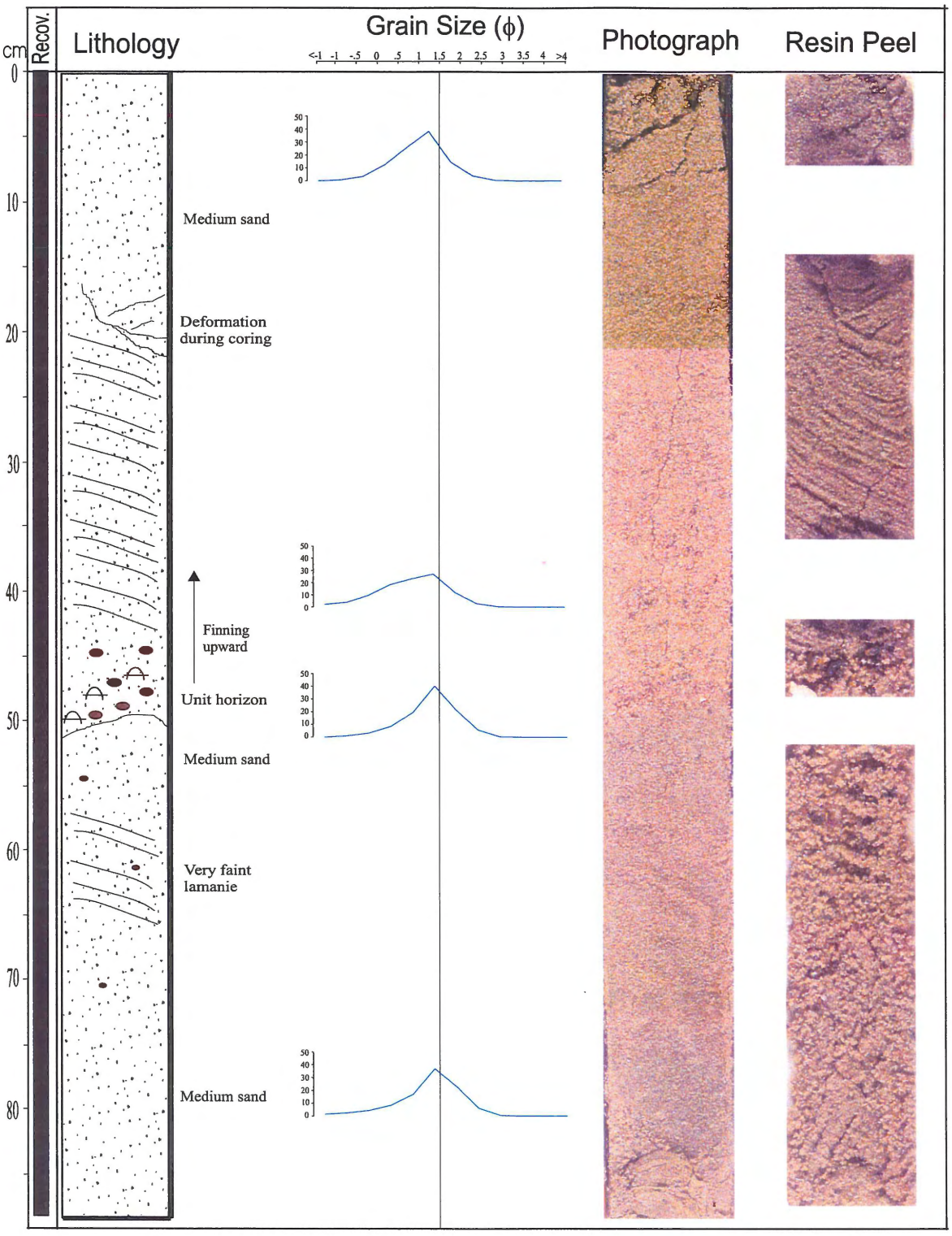

Figure 4.13. Vibracore 2000-30A-62. Cored from the middle, stoss side of the Copan-1 transect sand ridge.

Core 2000-30A-63

Vibracore 2000-30A-63 was collected along the Copan-1 in 26 m of water, on the middle -lee side of the same sand ridge as cores 2000-30A-61 and 2000-30A-62. The total length of core recovered was 48 cm (Table 3.1, Fig 3.2, 3.4). One unit is present throughout the entire core (Fig. 4.14). The grainsize changes from 1-1.5 ϕ (medium sand) at the bottom of the core (41 cm) to 1-2 ϕ (medium sand) near the top (12 cm). Parallel laminations are present throughout to core. The laminae have been extensively disturbed throughout the core, especially between 10 and 25 cm. Sediment movement within the core appears to have occurred down the left side of the photographs, where sediment was transported down from shallower depths (Fig. 4.14)

The parallel laminae present throughout the core suggest deposition under a relatively high flow regime such as sheet flow, or the unit may be the upper portion of a larger, unresolved bedform, deposited over the sand ridge. The shallow penetration of the core, and the lack of unit variability make it hard to differentiate between the two.

Core 2000-30A-96

This core was collected from the trough of a sand ridge in 38 m of water at the Copan-2 transect, and 168 cm of core was recovered (Table 3.1, Fig 3.2, 3.5). Three units are present in the core (Fig. 4.15). The lower most unit in the core makes up the bottom five centimetres (168 cm to 163 cm). The unit is fine grained (2-2.5 ϕ), and the contact with the unit above it was deformed during coring. The middle unit is 43 cm long, present from 163 cm to 120 cm where the dipping lamiae become parallel. The lower five centimetres of the unit is a coarse sand, shell rich lag layer, containing clasts as

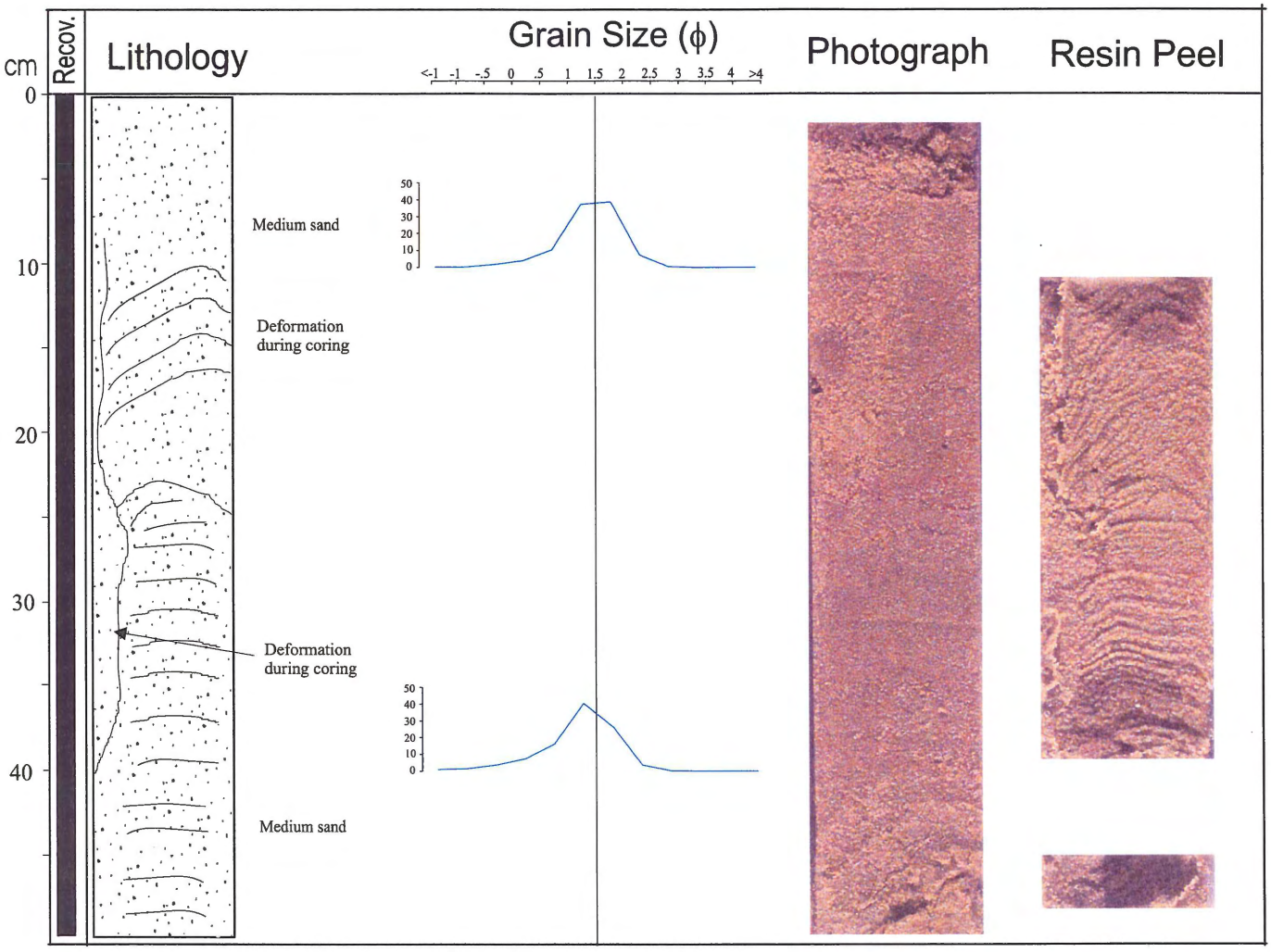

Figure 4.14. Vibracore 2000-30A-63. Cored from the middle, lee side of the Copan-1 transect sand ridge.

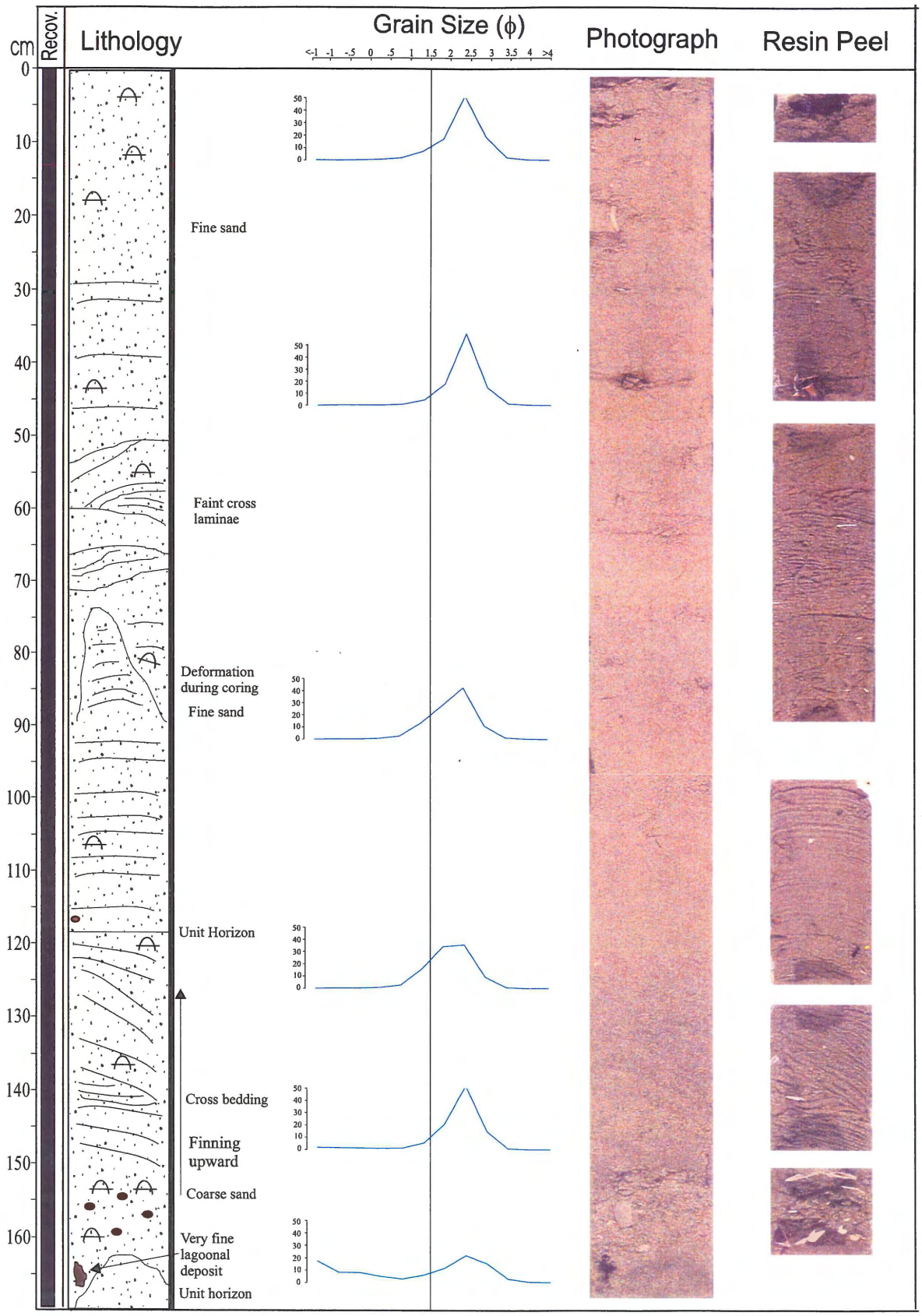

Figure 4.15. Vibracore 2000-30A-96. Cored from the bottom, lee side of the Copan-2 transect sand ridge.

big as 3 mm, shell fragments as big a 3 cm, and an allochthonous fragment of a dark organic material. Above the coarse lag layer, fine sand (2-2.5 ϕ) prevails. Dipping, parallel laminations are present in this portion on the unit, as well as cross beds at 140 – 143 cm. The third, and top most unit in the core is 120 cm thick, and is composed of fine sand (2-22.5 ϕ). Parallel laminations are present throughout the layer and are distinct from 120 to 60 cm and faint from 60 to 30 cm. Ripples and cross bedding are present from 50 to 65 cm and the structures from 65 to 70 cm could be either hummocky structures or deformation from coring. The top 30 cm of the core is structureless, and may also have been deformed during coring, or by bioturbation. Shell fragments are present throughout the length of the core, including a 2.5 cm diameter, elongated shell, lying perpendicular to the core length at 45 cm (Fig. 4.15).

The base of the lag layer at the core bottom corresponds with the base of the second order bedform seen in the seismic profile (Fig. 3.5). The lag layer is an erosional unconformity, followed by the deposition from megaripples, (cross beds, dipping laminae) and episodes of higher flow regimes (parallel laminae). The transition from lower to higher flow regime is marked at 120 cm in the core where the dipping laminae grade into parallel. The flow regime is temporarily reduced near 65 cm with the formation of ripples but returns shortly after, continuing the formation of parallel lamina. The deformation structure at 90 cm could be a result of de-watering during the deposition of the upper unit, as sheet flow moved a large amount of sediments over top of the unit or more likely was caused during coring. Bioturbation could also be the cause of the disturbed laminae at the top of the core.

Core 2000-30A-97

Positioned on the ridge crest in 33 m of water, the length of core recovered was 60 cm (Table 3.1, Fig 3.2, Fig. 3.5). The sharp color contrast at 48 cm (Fig. 4.16) is a processing artefact formed during the manipulation of the digital images. One unit is present throughout the core. The unit is composed of medium sand (1 – 2 ϕ) and parallel laminations are present throughout. Faint cross bedding is present at 45 cm. The core has also under gone a fair amount of deformation (Fig 4.16).

This core is situated on the top of the ridge (Fig 3.5), in the depositional part of the sand ridge/ribbon structure (Fig 3.2). The internal structures suggest high current regime (parallel laminae formed from sheet flow). Dewatering due to bed loading of the upper sediments could cause the deformation at 25 cm and 35 cm.

Two vibracore samples were collected from the South Sable transect, south of Sable Island (Fig 3.1, 3.3).

Core 2000-30A-165

Vibracore 2000-30A-165 was collected from the top -stoss side of a sand ridge, in 24 m of water. The length of core recovered is 126 cm (Table 3.1, Fig. 3.3, 3.6). Three units are present throughout the core (Fig. 4.17). 18 cm of the bottom most unit was recovered, which is composed of medium sand (1 – 2 ϕ) and contains parallel laminae through its entire length. A strip of sediment 63 cm long in the center was most likely liquefied during coring, and cuts across the parallel laminae. The contact between the lower and middle units is faint geologically, but can be seen by the difference in the sediment color. The middle unit is 13 cm thick, medium grained, and has parallel

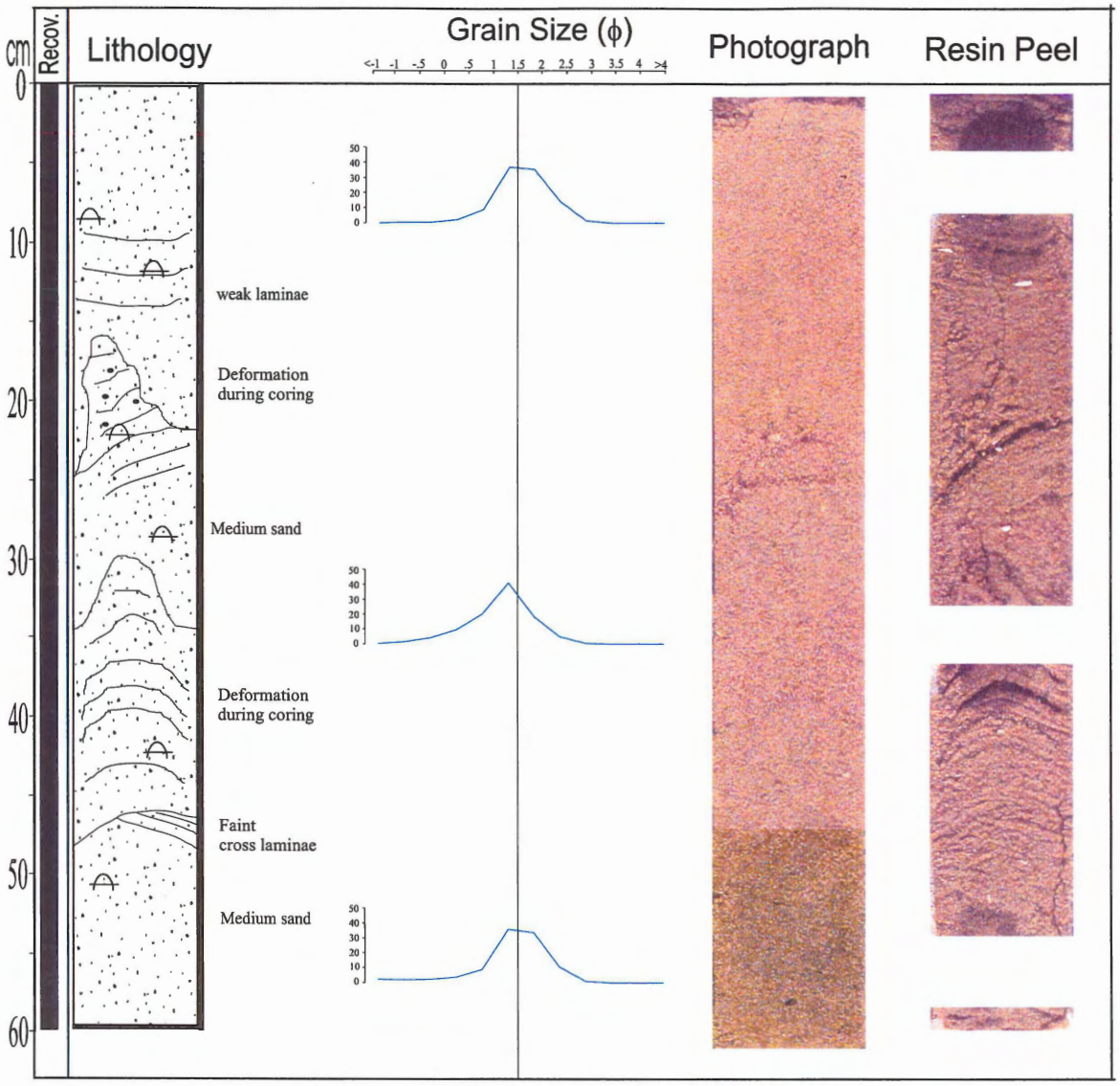

Figure 4.16. Vibracore 2000-30A-97. Cored from the top of the Copan-2 transect sand ridge.

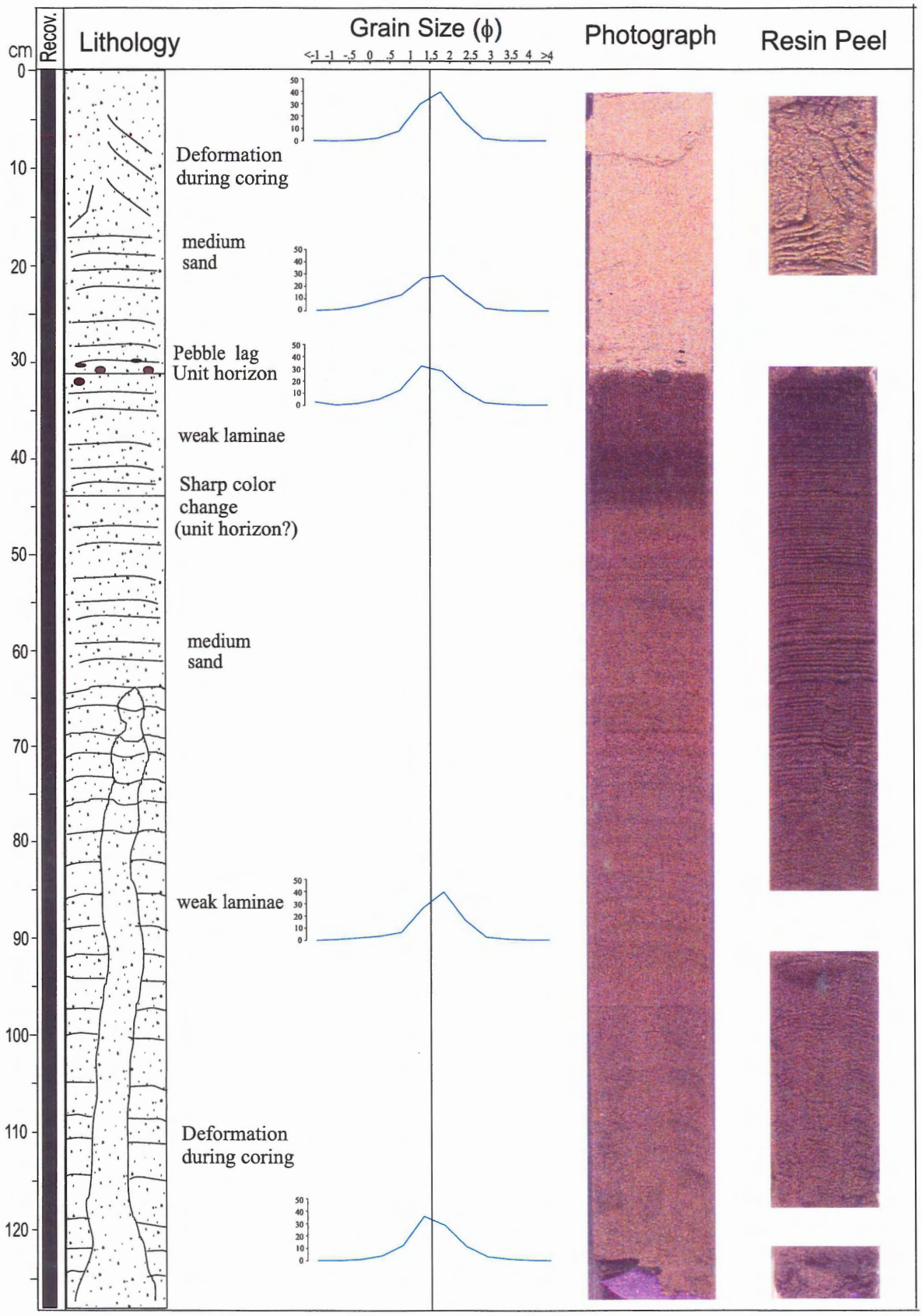

Figure 4.17. Vibracore 2000-30A-165, Cored from the top of the South Sable transect sand ridge.

laminations throughout its thickness. Individual grains in both units are coated with a dark stain, causing the dark color of the beds. The contact between the middle and upper unit is sharp, and characterized by a pebble lag and color change. The clasts range in size from –2 - -3 ϕ (4-10 mm), in a medium sand (1 – 1.5 ϕ) matrix, and are only present for 2 cm above the contact. Above the lag layer, the unit is medium sand (1.5 – 2 ϕ). Parallel laminations also occur from 31 to 15 cm, where they become very deformed due to coring (Fig. 4.17).

The lower two units have parallel laminae throughout the entire section which representing a long period of largely unchanging flow regime. It's not certain what is causing the dark staining of the grains (iron, oil, or organic related), or whether it was insitu or source related. A paleo-lagoonal horizon (to be discussed further in chapter 5) has been identified in 25 m of water, 5 km east of the core position, which could be related to the staining in some way. The upper unit corresponds to the depositional part of the sand ridge/ribbon structure, where the parallel laminations were formed in a high flow regime. The laminations at the top of the core are most likely deformed, by either bioturbation or during coring.

Core 2000-30A-166

Vibracore 2000-30A-166 was collected from the lee-trough of the sand ridge, in 29 m of water, and is 183.5 cm long (Table 3.1, Fig. 3.3, 3.6). Three units are present in the core (Fig. 4.18). 41.5 cm of the bottom most unit was recovered, and consists of fine sand (2 – 2.5 ϕ), weak laminae, and cross bedding. A 5 cm thick, dark organic deposit is also present between 155 and 160 cm. The horizon between the lower and middle unit is

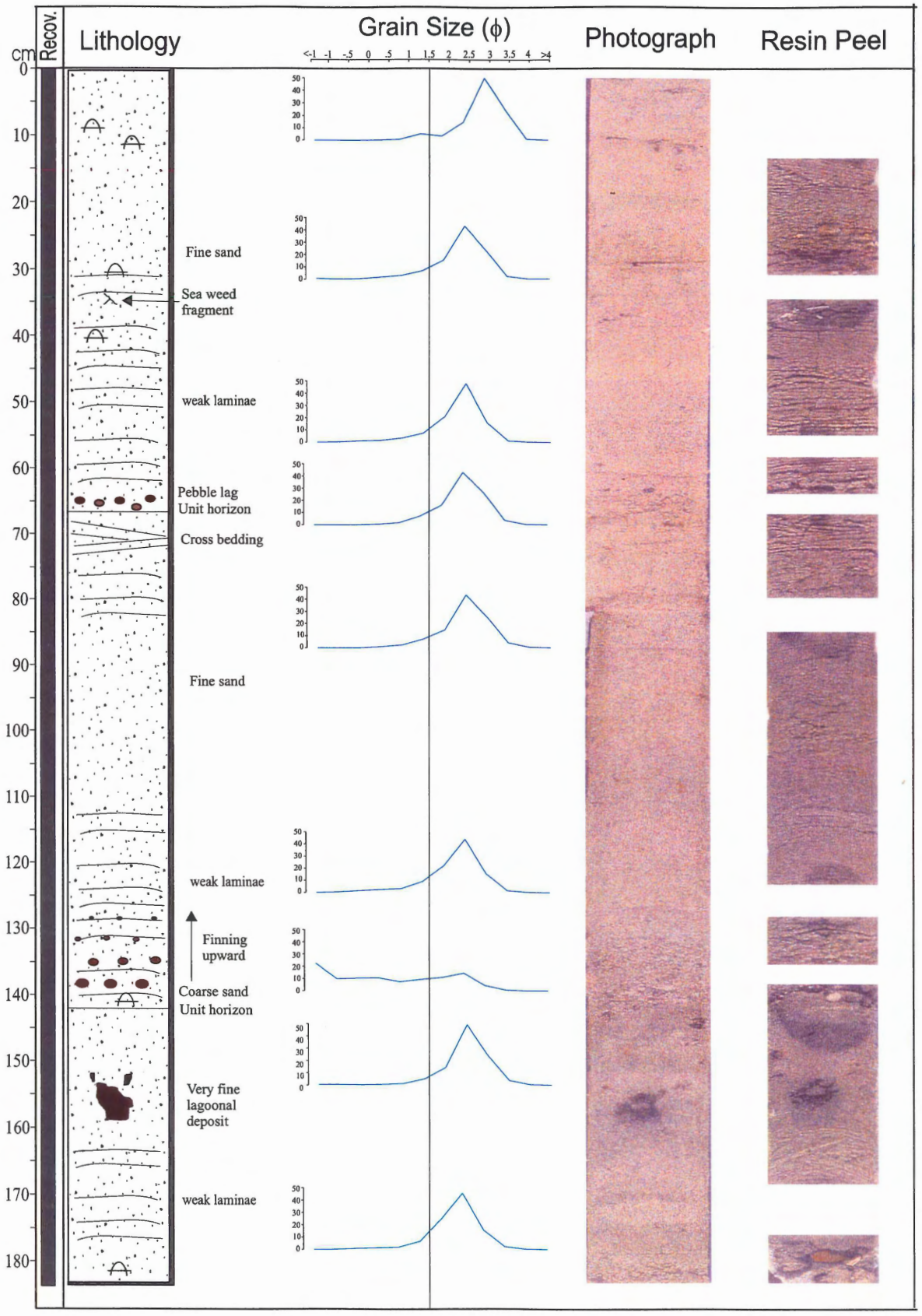

Figure 4.18. Vibracore 2000-30A-166, Cored from thebottom, lee side of the South Sable transect sand ridge.

defined by a coarse sand, pebble lag (<1 ϕ) in a fine sand (2.5 ϕ) matrix. The middle unit is 76 cm thick (142 – 66 cm) and consisted of a fining upward sequence of coarse (<-1 - -1 ϕ) to fine (2.5 ϕ) sand from a core depth of 142 to 130 cm. The remainder of the unit consists of fine sand. Weak laminae are present in the lower 29 cm as well as in the upper 16 cm of the unit, in between which is structureless. Cross beds are present at the top 5 cm of the unit. The upper unit is 66 cm thick and consists of fine to very fine sand (2.5 – 3 ϕ) and is separated from the middle unit by a thin pebble lag horizon, which has pebble size clasts (-2 - -4 ϕ) within the fine sand. Parallel laminae are present from the base of the unit (66 cm) to 30 cm, from where the unit is structureless to the top. A concentration of shell fragments, as well as a small piece of seaweed are present between 30 – 40 cm, where the transition from parallel laminations to structureless sand occurs (Fig. 4.18).

This core shows two cycles of rapid depositional events (cycle 1: 142-66 cm; cycle 2: 66-0 cm). At the base of the cycle, an erosional lag layer develops, followed by fining upward, high current regime flow; forming parallel laminae, waning (cross bed formation during lower flow regimes) and eventually stopping. The cyclic events are most likely storm related, and the unit thickness closely corresponds to the thickness of the "master bedding planes" defined by Hoogendoorn (1989) (Chapter 2). The fragment of organic material isolated at the bottom of the core is allochthonous, and is discussed further in chapter 5.

4.2.2 Summary

The consistent feature occurring in all the cores is the thick units with parallel laminae bound by a basal lag and fining upward sequences at the base, and angled laminae, cross bedding and deformation at the top. The sequence suggests deposition during tempestite conditions, as initial erosion of the underlying unit creates a lag layer, followed by sheet flow deposition (parallel laminae), during higher flow regimes, and an associated waning, and lower flow regime bedforms such as megaripples (cross-bedding, and high angled laminae). The same features are present in the cores taken from the stoss and lee sides of the sand ridge, suggesting similar depositional environments.

Chapter 5: Discussion and Conclusions

5.1 Introduction

The current understanding of the shoreface-attached sand ridges on Sable Island Bank has traditionally been associated with transverse sediment flow. Past morphologic studies on the ridge field has revealed internal structures attributed to eastward migration, but attempts to determine the rate of migration have been largely unsuccessful. The results from this study have found that the majority of the measured bedforms, and internal structures from the cores are similar to those formed under longitudinal flow conditions. Longitudinal bedforms could have been formed by down well water, washing off Sable Island during storms, and eroding the surface of the seabed (discussed in more detail below).

5.2 Discussion of Results

5.2.1 Symmetry

If transverse migration was the dominant process moving sand from west to east, parallel to Sable Island's shoreface as previously thought, one would expect the majority of the bedforms to be asymmetric in the same direction they are moving. This however, is not seen in the data collected during this study. The morphometric database shows that the measured bedforms exhibit very little preferred symmetry (only slightly east), with an equal number of bedforms skewed west as there are skewed east. The sand ridges that are skewed either negative (asymmetric west) or positive (asymmetric east) could be the

product of preferential erosion, where, through longitudinal flow one side of the ridge trough was eroded more than the other.

5.2.3 Internal Structures

The dominant features of the cores collected in this study are storm deposits, consisting of thick parallel laminae, basal lag horizons with flow waning structures near the top. This depositional sequence is typical of sheet flows, moving longitudinally through the sand ribbon and sand ridges fields.

The degree to which the sand ridges are influenced by down welling water during storms depends on how far they are from the shoreface of Sable Island. The position of the Copan transects sand ridges, west of Sable Island are no longer attached to the present day shoreface. The ridges in this area were most likely formed when sea level was lower, and the paleo-shoreface of Sable Island extended farther west from its present location. At its current location, the dominant process now acting on the ridges are storm, and tidal currents, which are from the west and northwest (perpendicular to the ridge crest lines), making the ridges more composite, as transverse flow has most likely become the dominant sediment transport process, moving bedforms over top of the paleo-bedforms, formed through longitudinal migration when the shoreface was closer to the area. This is evident in the ridge cross section (Fig 3.5), where seismic data show complex internal structures. In the cores from the Copan transects, parallel laminae deposited by sheet flows remain the dominant features, especially near the bottom of the cores however, lower flow regime bedforms (cross-bed, high angled laminae) are present, and more

abundant at the top of the cores, which are characteristic depositional features of megaripples, formed under transverse flow.

The South Sable transect is in the middle of the main ridge field, directly south of Sable Island. The multibeam bathymetry image of the area (Fig 3.10) shows an extensive tributary network of sand ribbons that flow obliquely across the ridges and gradually taper off, and phase into the sand ridges. The vibracore samples from the South Sable transect (2000-30A-165 and 2000-30A-166) were taken near the end of this tributary network (Fig. 3.10). Core 2000-30A-165 has two very different types of sediment with in it. The top unit is most likely a sand ribbon, transporting and depositing younger sediments from shallow water, to deeper water father from the island. The cross section of the ridge transect (Fig. 3.13) shows a series of smaller bedforms on top of the larger sand ridge (a series of sand ribbons), one of which was penetrated by the core. The lower two units in the core have been thoroughly stained, with almost every individual quartz grain having a stain coating on it (seen through a microscope). It is unlikely that a unit of sand of this thickness (>1m) could have been stained, and transported, while remaining as homogenous as these units are now. The units therefore must be older, and remain in the same place as when it was originally stained.

Core 2000-30A-166 was taken less than 700m east of core 2000-30A-165 and on the trough of the same sand wave. The two cores, however, are very different in appearance. Core 2000-30A-166 has no (or very little) stained grains and its internal structures are typical of a high energy, erosional environment. If transverse migration were the dominant process in which sand is moved across this ridge, one would expect to fine sediment similar to that found at the ridge crest, with internal structures typical of

lower flow regimes in the trough. This does not seem to be the case here. The structures present in the cores suggest that there is very little movement of the body of the sand ridge (seen by the homogeneous stained units) other than the sand ribbons moving over top of it. The trough however, has undergone significant changes, and appears to be in an active environment.

Through longitudinal processes, sediment moving through the sand ribbons would be dropped off in the troughs of the larger ridges, where it could either be deposited, or transported further. The sediments originally deposited where the ridge troughs are now would have been eroded to their current depths, as this is the path that sand is moving away from the island. The body of the ridges were able to remain relatively intact because the sand collected in the troughs as it moved farther away from the island, and thus, for the most part, passing by without eroding through the crests.

5.3 Longitudinal Flow

5.3.1 Schematic Model

Figure 5.1 is a schematic representation of how longitudinal flow might take place south of Sable Island. During storms, water is pushed up against Sable Island, and has nowhere to go except down, forming currents similar to those in a riptide. As the water flows over the sea floor it picks up sediments and transports it away from Sable Island. The sand is transported thought the network of sand ribbons, moving as sheet flows away from the island and eventually, into the troughs of the larger sand ridges. The sand ribbons are formed perpendicular to the shoreface of Sable Island, as that is the flow direction of the down welling water, however, the sand ridges are oriented at angles from

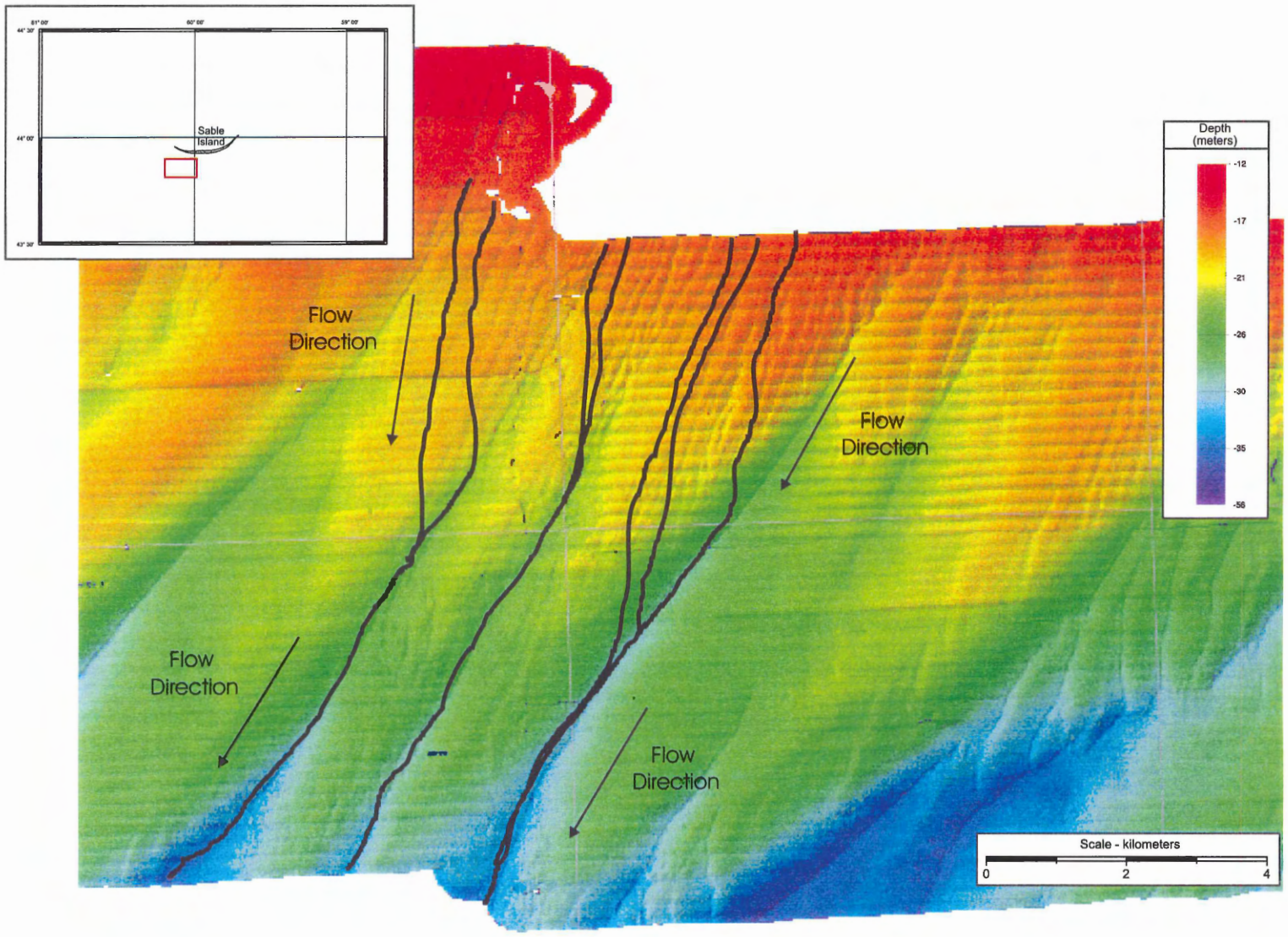

Figure 5.1. Schematic interpretation showing the proposed migration direction of longitudinally transported sediments. Sediment is transported via sand ribbons over the ridge crests and into the trough. From the trough it is transported farther away for Sable Island. (Modified from Hudson 2000-30A unpublished cruise report).

30-75° to the shoreface. Due to the different orientations, the sand ribbons flow at an oblique angle to the sand ridge crest lines, across their crests and down the lee sides into the troughs. The sand is either deposited in the troughs, or transported further away from the island (Fig. 5.1).

Hoogendoorn and Dalrymple (1989) identified internal dipping beds that they called master bedding plains (Chapter 2), which they thought were deposited during storm events, that moved larger amounts of sand (through transverse flow) and deposited them on the lee sides of the ridges. Through longitudinal flow, the master bedding plans can be explained in a similar manner, but instead of the sediments moving directly over the sand ridges (perpendicular the their crests) the sediment moves across the sand ridges at oblique angles before being deposited on the lee side (Fig. 5.1). Past estimates of migration rates determined using the master bedding plans, with the understanding that they formed under transverse flow conditions therefore would have been faster than it really is. For transverse flow, the sediment travels a smaller distance to cross the sand ridge (perpendicular to the wave crest) where as in longitudinal flow, the sediments travel at oblique angles to the ridge crests, covering a larger distance, and therefore taking a longer time before reaching the lee side of the wave. It is also unsure how much sand is deposited on the lee sides of the sand ridges and how much sediment continues to migrate through the troughs, and farther away from Sable Island. If a large amount of the flow is sediment bypass (continuing to migrate through the troughs without being deposited), the migration estimates based on transverse flow would be even farther off of the actual rate.

To date, no study has been done (to my knowledge) to determine the amount of water or sediments moving through the troughs of the sand ridges.

5.3.2 Supporting Evidence

There are some geographic and topographic features present across the bank that can also have been formed through longitudinal processes, rather than transverses processes.

5.3.2.1 Paleo-lagoonal deposit

A paleo-lagoonal deposit has been recognized in a pit on the main ridge field south of Sable Island, 5 km east of core 2000-30A-166 (E. King personal communication 2001) and dated to be 4900 +/- 80 years B.P. (GSCA Unpublished). The pit is approximately 2 m deep, situated on the lee side of a sand ridge in 25 m of water (Fig 5.2). Presently, the outcrop is elevated approximately 5 m from a sand ridge trough to its immediate east. It is questionable whether or not transverse processes could erode a 5 m deep trough, when transverse migration is more of a building up rather than a cutting down process. Longitudinal ridges are erosional bedforms, cutting down in the troughs, and building up the crests. It is more likely that longitudinal processes are at work, eroding the sediments that the down welling currents flow across, creating a trough while preserving the sediments that are in between, creating a ridge crest (similar to the process described above for the south sable cores). This horizon, or another one like it could be the source of the staining found on the sediments in core 2000-30A-165, as well as the allochthonous fragments found in cores 2000-30A-166, and 2000-30A-97.

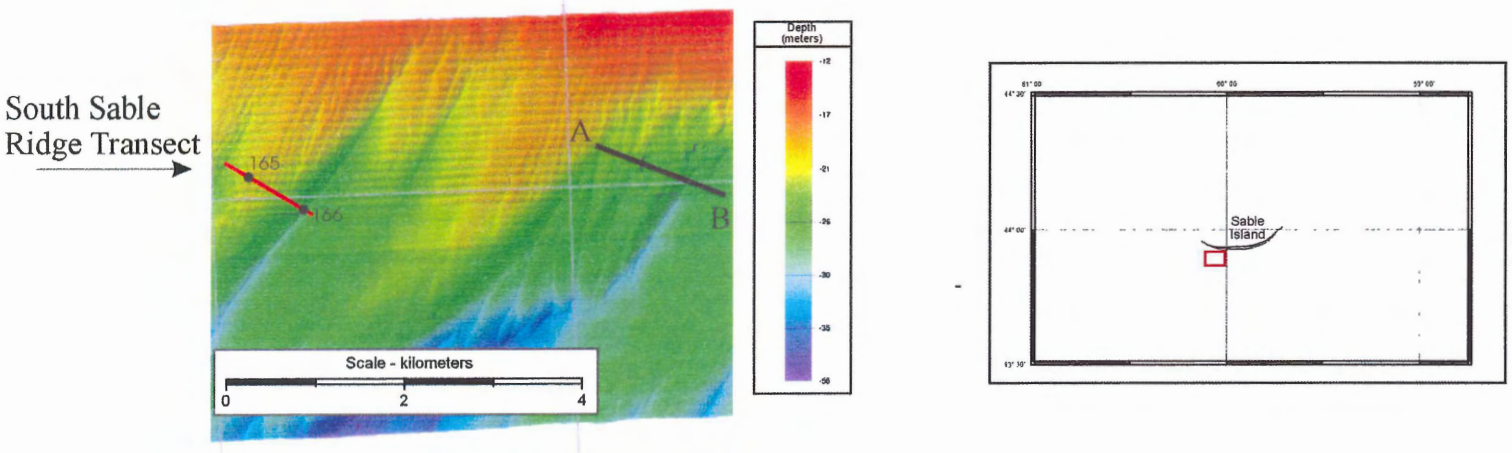

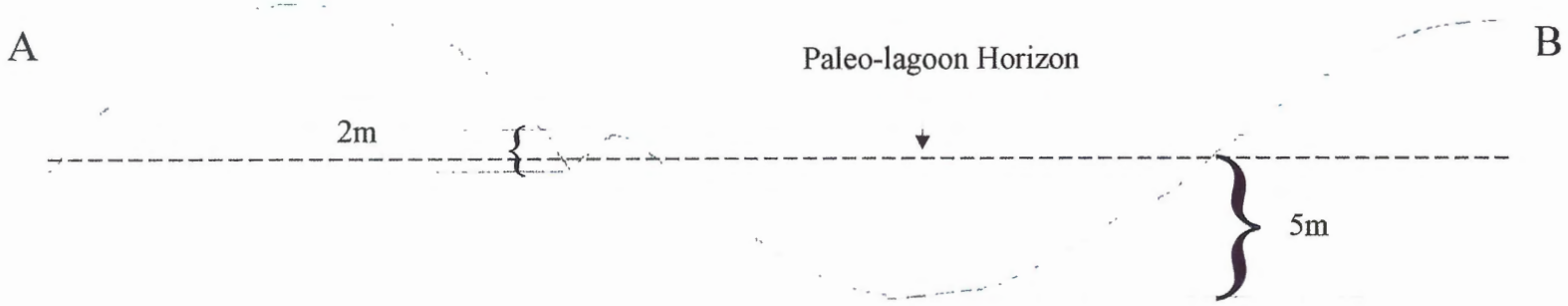

(Not drawn to scale)

Figure 5.2. Schematic illustration of the paleo-lagoon horizon south of Sable Island, and its positions relative to the sand ridge crest and trough.

5.3.2.2 Ridge Geometry

The physical geometry of the sand ridges also leads to some scepticism as to their forming and migrating through transverse flow. The ridges are far too linear, and parallel to each other to have been moving perpendicular to their crests. One would think that the ridges would migrate at different rates depending on the energy of the currents acting on them, which would very from higher, closer to the shore to lower, farther away from the shoreface in the deeper water. Some of the ridges are angled, or curved in such a way that the shallow-water ends of the ridges are farther east than their deep-water ends (Fig. 2.4). It could be argued that therefore the shallow water, higher energy portions of the ridges are migrating faster than their deep-water counterparts, however, the curvature of the sand ridges is also perpendicular to the paleo-shoreface as it has transgressed to its current position (King personal communication 2001). Through longitudinal flow, the sand ridges would have formed perpendicular to the shoreface, and as the shoreface transgressed and its orientation changed, the orientation of the sand ridges followed because the down welling currents that form the ridges are flowing perpendicular to the shoreface.

Internal structures termed the 'basal reflector' have also been identified through seismic records that are the base of the present sand ridges, and the top of an older, now buried sand ridge (Fig. 2.7). The basal reflectors are almost all either flat, convex-up (hill shaped), or tilted towards the east (west side higher than the east). This pattern is very consistent in seismic data collected throughout the entire sand ridge field (King personal communication 2001). If the ridges were migrating transversely, basal reflectors under some of the ridges should be concave-down (hole-shaped), because if the basal reflectors

were the surface of older ridges, they would have to be both crest shaped, and trough shaped. The current ridge field should therefore be resting over both crests and troughs of the paleo-ridges. If longitudinal flow was the process, very little east-west movement would occur, and because the ridges are formed through trough erosion, the basal reflectors would be the old bedding planed from when the sediments were originally deposits, and therefore, be closer to horizontal, and consistent throughout the ridge field.

The Harcourt-Cameron ridge (Fig. 2.6) is over 70 km long, extending from East Bar in water depths of 14 – 16 m, southwest, to water depths as deep as 80 m. The ridge is very linear, and its basal reflector has the same orientations through its entity. It is unlikely that a ridge of this magnitude would remain congruent in a transversely migrating environment over the history of the sand ridge system.

5.3 Conclusions

The results from this study have found that the majority of the measured bedforms, and internal structures from the cores are similar to those formed under longitudinal flow conditions.

The bedforms measured in this study fall almost exclusively within the sand ridge/ribbon size field, with an average wavelength and height of 620m and 1.04m respectively. The bedforms have little preferred symmetry, with the majority being very close to symmetric, or slightly asymmetric east.

The consistent feature occurring in all the cores are thick units of parallel laminae (deposited by high current regime sheet flow) bound by an erosional basal lag and fining upward sequences from the base, and angled laminae and cross bedding (waning energy,

megaripples). Using the multibeam image of south sable, a speculative sediment flow pattern can be constructed. The sand ribbons channel sand away from Sable Island, across the sand ridges at high angles to their crest and deposits it in the lee trough, where it is transported further towards the shelf slope.

Horizontal beds or horizons such as the homogeneous, stained units in core 2000-30A-165 and the paleo-lagoon horizon found to its east have been preserved in the crests of the sand ridges, but have been significantly eroded in the troughs. In the case for the stained unit, there is no trace of the stained grains in the bottom of the stoss side of the ridge. It might be more likely that the erosional processes of longitudinal migration eroded the units, carrying the sediments away form the ridges, instead of moving them east.

The geometry of the ridges (shape, orientation, internal structures) is consistent throughout the ridge field, and is the same among the smaller sand ridges as the larger one (Harcourt-Cameron Ridge). It is unlikely that these physical features of the ridges could stay so similar and congruent over time in such a dynamic environment.

Recommendations for Further Work

Part of this study was compiling seismic data from past cruises into a database so that bank wide trends in sand ridges could be easily displayed, and updated. Further work would involve the continued compilation of the database with new and old data to try and achieve a more complete coverage over Sable Island Bank. It is also unknown how much sand and water flows through the sand ridge troughs, and how much of the sediments are deposited, or continue to migrate off the shelf. Studies placing seabed instrumentation directly into the sand ridge troughs may be able to determine this. Continued, repetitive surveys need to be done to determine what migration processes are acting on what part of the ridges.

References

Amos, C.L., and Asprey, K.W. 1982. Report on C.S.S. Dawson Cruise 82-040, Sable Island Bank, Internal Report. Geological Survey of Canada, Atlantic Geoscience Center, Bedford Institute of Oceanography, Dartmouth, N.S., pp.112.

Amos, C.L., King, E.L. 1984. Bedforms of the Canadian Eastern Seaboard: A comparison with Global Occurrences. Marine Geology, **25**: 167-208.

Amos, C.L., Bowen, A.J., Huntley, D.A., and Lewis, C.F.M. 1988. Ripple generation under the combined influences of waves and currents on the Canadian continental shelf. Continental Shelf Research, **8**: 1129-1153.

Amos, C.L., and Nadeau, O.C. 1988. Surficial sediments of the outer banks, Scotian Shelf, Canada. Canadian Journal of Earth Sciences, **25**: 1923-1944.

Amos, C.L. and Miller, A.A.L. 1990. The Quaternary stratigraphy of southwest Sable Island Bank, eastern Canada. Geological Society of America Bulletin, **102**: 915-934.

Amos, C.L., Bowen, A.J., Huntley, D.A., Judges, J.T., and Li, M.Z. 1999. Ripple Migration and Sand Transport Under Quasi-Orthogonal Combined Flows on the Scotian Shelf. Journal of Coastal Research, **15**: 1-14.

Anonymous. 1984. Sable Island. Principal Station Data. Environment Canada, Atmospheric Environment Service, Toronto, Ontario. pp 46.

Atmospheric Dynamics Corporation. 1979. Climatological Conditions at Sable Island. Report prepared for Petro-Canada Inc. pp 36.

Boczar-Karakiewicz, B and Bona, J.L. 1986. Wave-dominated shelves: a model of sand-ridge formation by progressive infragravity waves. *In* Shelf Sands and Sandstones. *Edited by* R.J. Knight and J.R. Mclean. Canadian Society of Petroleum Geologists, Memoir 11. pp. 163-180.

Boczar-Karakiewicz, B, Drapeau, G., and Bona, J.L. 1987. Sand ridges on Sable Island Bank, Scotian Shelf. *In* Coastal Sediments '87 volume 2. *Edited by* N.C. Kraus. Proceeding, American Society of Civil Engineers. pp. 2157-2169

Boyd, R., Scott, D.B., and Douma, M. 1988. Glacial tunnel valleys and Quaternary history of the outer Scotian shelf. Nature, **33**: 561-564.

Cameron, H.L. 1965. The shifting sands of Sable Island. Geographical Review, **55**: 463-476.

Chakhotin, P.S., Medvedev, V.S., and Longinov, V.V. 1972. Sand ridges and waves on the shelf of tidal seas. Oceanology, **12**(3): 386-394.

Coleman, J.M., Roberts, H.H., Murray, S.P., and Salama, M. 1981. Morphology and dynamic sedimentology of the eastern Nile Delta shelf. Marine Geology, **42**: 301-326.

Dalrymple, R.W., and Hoogendoorn, E.L. 1997. Erosion and Deposition on Migrating Shoreface-attached Ridges, Sable Island, Eastern Canada. Geoscience Canada, 24: 25-36.

Davies, J.L. 1964. A morphogenic approach to world shorelines. Zeitschrift fur Geomorphologie, **8**: 127-142.

Duane, D.B., Field, M.E., Meisburger, E.P., Swift, D.J.P., and Williams, S.J. 1972. Linear Shoals on the Atlantic Inner Continental Shelf, Florida to Long Island, Chapter 2. *In* Shelf Sediment Transport: Process and Pattern. *Edited by* D.J.P Swift and O.H. Pilkey. Dowden, Hutchinson and Ross, Stroudsburg. pp. 447-498.

Evans-Hamilton Inc. 1976. Study of sand waves on Sable Island Bank, Phase II, Final Report. Prepared for Mobil Oil Canada Ltd. Halifax, N.S. pp. 67.

Evans-Hamilton Inc. 1977. Final Report of a Sable Island Data Analysis and Design Study. Report prepared for Mobil Oil Canada Ltd. pp. 114.

Fader, G.B., and King, L.H. 1981. A reconnaissance study of the surficial geology of the Grand Banks of Newfoundland. Geological Survey of Canada, Paper 81-1A: 45-46.

Field, M.E., Nelson, C.H., Cacchione, D.A., and Drake, D.E. 1981. Sand waves on an epicontinental shelf: Northern Bering Sea. Marine Geology, **2**:233-258.

Figueiredo, A.G. Jr., Sanders, J.E., and Swift, D.J.P. 1982. Storm-graded layers on inner continental shelves: examples from southern Brazil and the Atlantic coast of the Central United States. Sedimentary Geology, **31**: 171-190.

Forrester, W.D. 1983. Canadian Tidal Manual. Department of Fisheries and Oceans, Canadian Hydrographic Service, Ottawa, Ontario, pp. 138

Geonautics Limited. 1982. Analysis of bedforms from Georges Bank, the adjacent Canadian Shelf and global occurrences. Submitted to Geological Survey of Canada under D.S.S. Contract Number 083C.23420-2-R635.

Hoogendoorn, E.L., and Dalrymple, R.W. 1986. Morphology, lateral migration, and internal structures of shoreface-connected ridges, Sable Island Bank, Nova Scotia, Canada. Geology, **14**:400-403.

Hoogendoorn, E. L. 1989. Sedimentology and Dynamics of Shoreface–Attached Ridges, Sable Island Bank, Nova Scotia. Unpublished PhD Theses. Queen's - University, Kinston Ontario. pp. 483

Huthanace, J.M. 1982. On the mechanism forming linear sand banks. Estuarine, Coastal and Shelf Science, **14**: 79-99.

Ingersoll, R.W., and Ryan, B.A. 1997. Repetitive Surveys to Assess Sand Ridge Movement Offshore Sable Island. Proceedings Oceans 97, 1377-1393.

King, L.H. 1970. Surficial geology of the Halifax-Sable Island map area. Marine Science Paper No. 1, pp. 16.

King, L.H., MacLean, B. and Fader, G.B.J. 1974. Unconformities on the Scotian Shelf. Canadian Journal of Earth Sciences, **11**: 89-100

King, L.H. 1996. Late Wisconsinan ice retreat from the Scotian Shelf. GSA Bulletin, **108** (8): 1056-1067

King, E.L. 2000. Towards a Glacial and Post-Glacial Geologic Framework on Sable Island Bank: A Long-term History of Environmental Change. GSCA SEEMAG Workshop March 2 and 3, 2000, BIO, Dartmouth, N.S.

King, E.L. 2001. A Glacial Origin for Sable Island: Ice and Sea-Level Fluctuations from Seismic Stratigraphy on Sable Island Bank, Scotian Shelf, offshore Nova Scotia. Current Research, Geological Survey of Canada, pp. 18

Li, M.Z., Amos, C.L., and Heffler, E. 1997. Boundary layer dynamics and sediment transport under storm and non-storm conditions on the Scotian Shelf. Marine Geology, **141**: 157-181.

Li, M.Z., and Amos, C.L. 1998. Predicting ripple geometry and bed roughness under combined waves and currents in a continental shelf environment. Continental Shelf Research, **18**: 941-970.

Li, M.Z., and Amos, C.L. 1999. Field observations of bedforms and sediment transport thresholds of fine sand under combined waves and currents. Marine Geology, **158**: 147-160.

Li, M.Z., King, E.L. Chapman, B., Girouard, P., Jodrey, F., Merchant, M., Murphy, B., Szlavka, B., Wile, B., Uyesugi, M., and Camplell, A. 2001. A Geological and Geophysical Survey on Sable Island Band and Scotian Shelf: CSS Hudson 2000030A Cruise Report and Preliminary Results. Geological Survey of Canada internal report, pp.50 .

McBride, R.A., Moslow, T.F., and Figueiredo, A. 1986. Origin and occurrence of shoreface-attached sand ridges, North Atlantic Shelf, U.S.A. Society of Economic Paleontologists and Mineralogists Annual Midyear Meeting, Raleigh, North Carolina, Abstracts, **3**: 0-74.

McLaren, S.A. 1988. Quaternary seismic stratigraphy and sedimentation of the Sable Island sand body, Sable Island Bank, outer Scotian Shelf. Unpublished MSc Thesis, Center for Marine Geology, Dalhousie University, Technical Report 11, 95 pp.

Mobil Oil Canada Ltd. 1983. Venture Development Project, Environmental Impact Statement. Volume IIIa, Biophysical Assessment, pp 415.

Neu, H. J. A. 1982. 11 Year deep-water wave climate of Canadian Atlantic waters. Canadian Technical Report of Hydrography and Ocean Seismics, No 13. pp 41.

Parker, G., Lanfredi, N.W., and Swift, D.J.P. 1982. Seafloor response to flow in a southern hemisphere sand-ridge field: Argentine inner shelf. Sedimentary Geology, **33**: 195-216.

Patterson, G. 1894. Sable Island; Its History and Phenomena. Transactions of the Royal Society of Canada, Section II, pp 48.

Quinlan, G., and Beaumont, C. 1981. A comparison of observed and theoretical postglacial relative sea level in Atlantic Canada. Canadian Journal of Earth Sciences, **18**: 1146-1163.

Sankeralli, L.M. 1998. The origin of the morphology of the eastern Scotian Shelf, Atlantic Canada. Unpublished MSc Thesis, Dept. Earth and Atmospheric Sciences, University of Alberta, pp 209.

Scott, D.B., Medioli, F.S., Duffett, T.E. 1984. Holocene rise of relative sea level at Sable Island, Nova Scotia, Canada. Geology, **12**: 173-176.

Scott, D.B., Boyd, R., and Medioli, F.S. 1987. Relative sea level changed in Atlantic Canada: Observed level and sedimentological changes vs. theoretical models. *In* Sea-level fluctuations and coastal evolution. *Edited by* D. Nummedal, O.H. Pilkey, and J.D. Howard. SEMP Special Publication Number 41. p. 68.

Scott, D.B, Boyd, R., Douma, M., Medioli, R.S., Yuill, S., Leavitt, E., and Lewis, C.F.M. 1989. Sable Island Bank: Holocene relative sea-level changes and Quaternary glacial events on a continental shelf edge; *In* Late Quaternary sea-level correlation and applications. *Edited by* D.B. Scott, P.A.Pirazzoli and C.A. Honig. NATO ASI Series C, Mathematical and Physical Sciences, **256**: 150-120.

Smith, J.D. 1969. Geomorphology of a sand ridge. Journal of Geology, **77**(1): 39-55.

Stea, R.R., Piper, D.J.W., Fader, G.B.J., and Boyd, R. 1989. Wisconsinan glacial and sea-level history of Maritime Canada and the adjacent shelf: A correlation of land and sea events. GSA Bulletin, **110** (7): 821-845.

Swift, D.J.P., and Field, M.E. 1981. Evolution of a classic sand ridge field: Maryland sector, North American inner shelf. Sedimentology, **28**: 461-482.